An analysis of discretizations of the Helmholtz equation in L^2 and in negative norms (extended version)

S. Esterhazy, J.M. Melenk

Vienna University of Technology, Wiedner Hauptstraße 8-10, A-1040 Vienna

Abstract

For a model Helmholtz problem at high wavenumber k we present a wavenumber-explicit error analysis in the L^2 and H^{-1} norms for the Galerkin FEM. For the convergence in L^2, we show that the lowest order case $p = 1$ is special in that the relative error in L^2 scales at best with k whereas it does not for higher order discretizations. An alternative to the Galerkin method with better dispersion properties is the optimally blended spectral-finite element scheme of [Ainsworth & Wajid, SIAM J. Numer. Anal. (2010)]. For this method, we present an error analysis in L^2 for the lowest order case $p = 1$ in one dimension, showing that the L^2-error is improved by a factor k compared to the lowest order Galerkin FEM.

Keywords: Helmholtz equation, high order FEM, dispersion error, regularity

1. Introduction

The Helmholtz equation is a basic equation when treating wave propagation problems in a time-harmonic setting. Typical applications include acoustic and electromagnetic scattering problems as well as laser physics. A particular case of interest is that of high wavenumbers k. Then the conditions on the discretization are stringent due to the requirement to resolve the oscillatory nature of the solution. More subtle is that classical discretizations of the Helmholtz equation suffer strongly from dispersion errors. The stability and dispersive properties of discretizations of the Helmholtz equation are by now understood for both regular and unstructured meshes. For regular, translation-invariant grids we refer to [6, 14, 12, 10, 1, 3, 2]—see also the discussion in [11]. One of the outcomes of these analyses on regular grids is that high order methods are significantly less susceptible to dispersion errors ("pollution errors") than low order methods. The works [18, 19, 11, 17] rigorously establish this observation also for discretizations on unstructured meshes. A similar observation concerning the superior behavior of high order methods can be made for spectral methods as demonstrated in the k-explicit analyses in [15, 23].

The analysis of [18, 19, 11, 17] focuses on norms related to the H^1-norm such as the norm $\|\cdot\|_{\mathcal{H}}$ of (2.3). Here, we study the convergence in weaker norms, in particular in the H^{-1}-norm. Closely related to the convergence in the H^{-1}-norm is the preformance of the method for the evaluation of linear functionals. In the present note, we concentrate on some linear functionals that are generated by weighted volume integrals. While the asymptotic convergence rates are, of course, the ones to be expected from the underlying duality arguments, the novel aspect of the present paper over [18, 19, 11, 17] is that we obtain better estimates in the wavenumber k. Indeed, for the pertinent dual problems, we obtain an *a priori* bound that is by a factor k better than what a straightforward

Email addresses: esterhazy@asc.tuwien.ac.at (S. Esterhazy), melenk@tuwien.ac.at (J.M. Melenk)

application of [18, 19, 11, 17] would yield. These results are collected in Corollary 4.5 for the general case of hp-FEM and specialized to the h-FEM in Corollary 4.6.

We mentioned above that higher order Galerkin discretizations are less prone to pollution errors. A particular observation made in this paper for the L^2 and H^{-1}-convergence of the h-FEM Galerkin method is that the lowest order case $p = 1$ is rather special: The k-dependence of the error is asymptotically (as $kh \to 0$) worse by a factor k than for the cases $p \geq 2$ (cf., e.g., Remark 4.7 and, more generally, Corollary 4.6). A variety of method have been proposed in the literature to combat or at least mitigate the pollution effect, in particular for low order methods. Especially for regular, translation invariant meshes powerful tools such as Fourier techniques are available to understand and analyze discretizations and to design new schemes with good dispersion properties. The recent proposal of [4] shows in particular that a suitable combination of the Galerkin FEM and the spectral element method (SEM) can lead to new methods with significantly reduced dispersion errors. This dispersion analysis is done on regular, translation-invariant grids and suggests greatly reduced actual errors. For a 1D model problem on regular grids, we provide an actual error analysis for the lowest order discretization and show that the greatly reduced dispersion error leads to a gain in accuracy by a factor k as compared with the Galerkin FEM. Thus, the particularly poor behavior of lowest order Galerkin h-FEM (i.e., $p = 1$) mentioned above is overcome with this optimally blended scheme of [4] (cf. Section 6).

2. The Helmholtz model problem

We consider a specific model problem on a bounded Lipschitz domain $\Omega \subset \mathbb{R}^d$ with Robin boundary conditions:

$$\begin{aligned} -\Delta u - k^2 u &= f \quad \text{in} \quad \Omega, \\ \partial_n u - iku &= g \quad \text{on} \quad \partial\Omega, \end{aligned} \tag{2.1}$$

where

$$k \geq k_0 > 0.$$

The weak formulation of our model has the form:

$$\text{Find } u \in H^1(\Omega) \text{ s.t.} \quad B(u,v) = l(v) \quad \forall v \in H^1(\Omega), \tag{2.2}$$

$$B(u,v) := \int_\Omega \nabla u \cdot \nabla \bar{v} - k^2 u\bar{v} - ik\int_{\partial\Omega} u\bar{v}, \qquad l(v) := \int_\Omega f\bar{v} + \int_{\partial\Omega} g\bar{v},$$

where $f \in (H^1(\Omega))'$ and $g \in H^{-1/2}(\partial\Omega)$—additional regularity of f and g will be stipulated shortly. An important role is played by the norm

$$\|u\|_{\mathcal{H}}^2 := \|\nabla u\|_{L^2(\Omega)}^2 + k^2\|u\|_{L^2(\Omega)}^2. \tag{2.3}$$

With respect to this norm, the bilinear form $B(\cdot,\cdot)$ is continuous uniformly in $k \geq k_0 > 0$, i.e., there exists $C_c > 0$ independent of k such that

$$|B(u,v)| \leq C_c\|u\|_{\mathcal{H}}\|v\|_{\mathcal{H}} \qquad \forall u,v \in H^1(\Omega)$$

(see, e.g., [18, Cor. 3.4]). The bilinear form B also satisfies the Gårding inequality

$$\operatorname{Re} B(u,u) = \|\nabla u\|_{L^2(\Omega)}^2 - k^2\|u\|_{L^2(\Omega)}^2 = \|u\|_{\mathcal{H}}^2 - 2k^2\|u\|_{L^2(\Omega)}^2 \qquad \forall u \in H^1(\Omega). \tag{2.4}$$

The abstract conforming discretization is as follows: given a closed space $V_N \subset H^1(\Omega)$, the finite element approximation $u_N \in V_N$ is determined by the condition

$$B(u_N, v) = l(v) \qquad \forall v \in V_N. \tag{2.5}$$

With these observations in hand, [19, Thm. 3.2] formulated the following result:

Proposition 2.1 ([19, Thm. 3.2])**.** *Define the adjoint solution operator $S^*: L^2(\Omega) \to H^1(\Omega)$ by the condition*

$$B(v, S^* f) = \int_\Omega v \overline{f} \qquad \forall v \in H^1(\Omega)$$

and the adjoint approximation property η_N by

$$\eta_N^{L^2} := \sup_{0 \neq f \in L^2(\Omega)} \inf_{v \in V_N} \frac{\|S^* f - v\|_{\mathcal{H}}}{\|f\|_{L^2(\Omega)}}. \tag{2.6}$$

If the condition

$$2C_c k \eta_N^{L^2} \leq 1 \tag{2.7}$$

is fulfilled, then the Galerkin approximation $u_N \in V_N$ defined by (2.5) exists and is unique. Furthermore, the following two a priori estimates are valid:

$$\|u - u_N\|_{\mathcal{H}} \leq 2C_c \inf_{v \in V_N} \|u - v\|_{\mathcal{H}}, \tag{2.8}$$

$$\|u - u_N\|_{L^2(\Omega)} \leq C_c \eta_N^{L^2} \inf_{v \in V_N} \|u - v\|_{\mathcal{H}}. \tag{2.9}$$

Proposition 2.1 gives abstract conditions and estimates for the Galerkin error in the $\mathcal{H}$- and $L^2(\Omega)$-norm; we will make these estimates more specific in the context of the *hp*-FEM below. We will also give estimates in the $(H^1(\Omega))'$-norm and estimates for the evaluation of linear functionals. For *a priori* estimates in the $(H^1(\Omega))'$-norm and $H^{-1}(\Omega)$-norm (we set $H^{-1}(\Omega) = (H_0^1(\Omega))'$), we have the following abstract result, which we will quantify below:

Lemma 2.2. *Define*

$$\eta_N^{H^1} := \sup_{\substack{f \in H^1(\Omega) \\ f \neq 0}} \inf_{v \in V_N} \frac{\|S^* f - v\|_{\mathcal{H}}}{\|f\|_{H^1(\Omega)}}, \qquad \eta_N^{H_0^1} := \sup_{\substack{f \in H_0^1(\Omega) \\ f \neq 0}} \inf_{v \in V_N} \frac{\|S^* f - v\|_{\mathcal{H}}}{\|f\|_{H^1(\Omega)}}. \tag{2.10}$$

If the solvability condition (2.7) is satisfied, then the Galerkin error $u - u_N$ satisfies

$$\|u - u_N\|_{(H^1(\Omega))'} \leq 2C_c^2 \eta_N^{H^1} \inf_{v \in V_N} \|u - v\|_{\mathcal{H}}$$

$$\|u - u_N\|_{H^{-1}(\Omega)} \leq 2C_c^2 \eta_N^{H_0^1} \inf_{v \in V_N} \|u - v\|_{\mathcal{H}}.$$

Proof. We will just prove the estimate for $\|u - u_N\|_{(H^1(\Omega))'}$ using a duality argument and Galerkin orthogonality: For arbitrary $v \in H^1(\Omega)$ and $w_N \in V_N$ we have

$$\left|(u - u_N, v)_{L^2(\Omega)}\right| = |B(u - u_N, S^* v)| = |B(u - u_N, S^* v - w_N)| \leq C_c \|u - u_N\|_{\mathcal{H}} \|S^* v - w_N\|_{\mathcal{H}}.$$

Since w_N is arbitrary, we can conclude

$$\left|(u - u_N, v)_{L^2(\Omega)}\right| \leq C_c \|u - u_N\|_{\mathcal{H}} \|v\|_{H^1(\Omega)} \eta_N^{H^1}.$$

Dividing by $\|v\|_{H^1(\Omega)}$, taking the supremum over $v \in H^1(\Omega)$, and inserting the best approximation result (2.8) yields the claimed bound. $\square$

We will also be interested in the error in linear functionals. Specifically, we will consider linear functionals of the form

$$v \mapsto L(v) := \int_\Omega \overline{z} v \tag{2.11}$$

where the function $z \in L^2(\Omega)$ (or even smoother). The *a priori* analysis for the error $L(u - u_N)$ is done, as usual, by duality arguments:

Lemma 2.3. *Let $z \in L^2(\Omega)$ and L be given by (2.11). Assume that (2.7) holds. Then*

$$|L(u) - L(u_N)| = |L(u - u_N)| \leq C_c \left(\inf_{v \in V_N} \|u - v\|_{\mathcal{H}} \right) \left(\inf_{w \in V_N} \|S^* z - w\|_{\mathcal{H}} \right).$$

Proof. Follows from arguments very similar to those of the proof Lemma 2.2. □

3. Regularity

The above considerations show that we have to quantify the adjoint approximation properties $\eta_N^{L^2}$, $\eta_N^{H^1}$, and $\eta_N^{H^1_0}$. This leads to the study of the regularity of the solution operator and the adjoint operator. In this connection, it is worth noting that $S^* f$ is also the solution of a Helmholtz problem; in fact, $S^* f = \overline{S(\overline{f}, 0)}$, where $(f, g) \mapsto S(f, g)$ denotes the solution operator for (2.1). This shows that the regularity properties of S^* can be inferred from those of S.

3.1. Prelude: the 1D situation

Several of the regularity issues for (2.1) can be already be seen in 1D. An important motivation for us to discuss the 1D situation in some detail is that we will study numerically the 1D situation below and will therefore need the regularity assertion given here. As the 1D model problem, we consider the following situation studied already in [13, 14, 12]:

$$-u'' - k^2 u = f \quad \text{in } I = (0,1), \qquad u(0) = 0, \qquad u'(1) - \mathbf{i} k u(1) = g \in \mathbb{C}. \tag{3.1}$$

The Green's function is known explicitly, namely,

$$G(x, y) = \frac{1}{k} \begin{cases} \sin(kx) e^{\mathbf{i} k y} & , \quad 0 \leq x \leq y \leq 1 \\ \sin(ky) e^{\mathbf{i} k x} & , \quad 0 \leq y \leq x \leq 1, \end{cases} \tag{3.2}$$

so that the solution can be written as

$$u(x) = \int_0^1 G(x, y) f(y)\, dy + g \frac{\sin kx}{k(\cos k - \mathbf{i} \sin k)}. \tag{3.3}$$

For a constant $C > 0$ that is independent of $k \geq k_0 > 0$, one has the following stability estimate (see, e.g., [12, Thm. 4.4])

$$\|u\|_{\mathcal{H}} \leq C \left[\|f\|_{L^2(I)} + |g| \right]. \tag{3.4}$$

For smooth f, the solution formula (3.3) is an oscillatory integral (for large k) so that integration by parts is expected to give an additional power of k^{-1}. The following lemma asserts the validity of this expectation. Instead of working with the solution formula, we prove it using arguments that will also be used in the multidimensional case:

Lemma 3.1. *The solution u of (3.1) satisfies, for a constant C independent of $k \geq k_0$, f, and g,*

$$\|u\|_{\mathcal{H}} \leq C \left[k^{-1} \|f\|_{H^1(I)} + |g| \right]. \tag{3.5}$$

Proof. We may restrict our attention to the case $g = 0$. Define the function $u_0(x) := -k^{-2} f(x) + k^{-2} f(0) \cos kx$. Then $\|u_0\|_{\mathcal{H}} \leq C k^{-1} \|f\|_{H^1(I)}$. The difference $\delta := u - u_0$ satisfies

$$\begin{aligned} & -\delta'' - k^2 \delta = -k^{-2} f'', \\ & \delta(0) = 0, \qquad \delta'(1) - \mathbf{i} k \delta(1) = -(-k^{-2} f'(1) - k^{-1} f(0) \sin k) + \mathbf{i} k (-k^{-2} f(1) + k^{-2} f(0) \cos k). \end{aligned}$$

Applying now the stability estimate (3.4) and the Sobolev embedding theorem gives

$$\|\delta\|_{\mathcal{H}} \leq C\left[k^{-2}\|f''\|_{L^2(I)} + k^{-2}|f'(1)| + k^{-1}|f(1)| + k^{-1}|f(0)|\right] \leq C\left[k^{-2}\|f''\|_{L^2(I)} + k^{-1}\|f\|_{H^1(I)}\right].$$

Hence, we have obtained

$$\|u\|_{\mathcal{H}} \leq \|u_0\|_{\mathcal{H}} + \|\delta\|_{\mathcal{H}} \leq C\left[k^{-2}\|f\|_{H^2(I)} + k^{-1}\|f\|_{H^1(I)}\right].$$

The term $k^{-2}\|f\|_{H^2(I)}$ can be reduced to a term of the form $k^{-1}\|f\|_{H^1(I)}$ by the same interpolation arguments that are worked out in the proof of Lemma 3.4 below. □

Remark 3.2. We note that the term involving $|g|$ in (3.5) is not improved by a factor k^{-1} as compared with (3.4). Inspection of the solution formula (3.3) shows that its k-dependence is sharp. Thus, better estimates (with respect to k) can only be expected for the case of homogeneous boundary conditions. See also [12, Sec. 4.7.2]. ■

Concerning the regularity of the solution u of (3.1) we have:

Proposition 3.3. *Let $s \in \mathbb{N}_0$. Then there exist constants C, $\lambda > 0$ such that the following is true. For every $f \in H^s(I)$ and $g \in \mathbb{C}$ the solution u of (3.1) can be written as $u = u_{H^{s+2}} + u_{\mathcal{A}}$ where $u_{H^{s+2}} \in H^{s+2}(I)$ and $u_{\mathcal{A}}$ is analytic. Additionally,*

$$\begin{aligned} k^{s+2}\|u_{H^{s+2}}\|_{L^2(I)} + \|u_{H^{s+2}}\|_{H^{s+2}(I)} &\leq C\|f\|_{H^s(I)}, \\ \|u_{\mathcal{A}}\|_{\mathcal{H}} &\leq C\left[\|f\|_{L^2(I)} + |g|\right], \\ \|u_{\mathcal{A}}^{(n+2)}\|_{L^2(I)} &\leq C\lambda^n k^{-1}\max\{k,n\}^{n+2}\left[\|f\|_{L^2(I)} + |g|\right] \qquad \forall n \in \mathbb{N}_0. \end{aligned}$$

Proof. Follows by arguing as in the proof of [17, Thm. 4.5] and the appropriate modifications for the Dirichlet boundary conditions at $x = 0$ ([17, Thm. 4.5] considers (2.1) with Robin boundary conditions). □

3.2. Regularity in higher dimensions

We return to our multidimensional model problem (2.1).

3.2.1. Stability

The bilinear form B given by (2.2) is not coercive in $H^1(\Omega)$. Thus the Lax-Milgram-Lemma is not applicable to show existence and uniqueness. Nevertheless, the bilinear form B satisfies a Gårding inequality by (2.4). That is, the operator has the form "coercive + compact perturbation", which makes the Fredholm theory applicable, and solvability follows from uniqueness. This was shown in [20, Prop. 8.1.3] (see, e.g., [11, Example 2.1] for some details). That is, for every $f \in (H^1(\Omega))'$ and every $g \in H^{-1/2}(\partial\Omega)$, the variational problem (2.1) is uniquely solvable with the stability bound

$$\|u\|_{\mathcal{H}} \leq C(k)\left[\|f\|_{(H^1(\Omega))'} + \|g\|_{H^{-1/2}(\partial\Omega)}\right]$$

for a constant $C(k) > 0$, whose dependence on k is unspecified. For *convex* domains Ω, [20, Prop. 8.1.4] (for $d = 2$) and [9] (for $d = 3$) established the k-explicit stability bound

$$k^{-1}\|u\|_{H^2(\Omega)} + \|u\|_{\mathcal{H}} \leq C\left[\|f\|_{L^2(\Omega)} + \|g\|_{L^2(\partial\Omega)}\right]$$

for a $C > 0$ that is independent of k. This motivates us to introduce the stability constant $C_{sol}(k)$ as follows: For the bounded Lipschitz domain Ω (not necessarily convex) and $k > 0$ we let $C_{sol}(k) > 0$ be the least constant such that for every $f \in L^2(\Omega)$ and $g \in L^2(\partial\Omega)$ the solution u of (2.1) satisfies

$$\|u\|_{\mathcal{H}} \leq C_{sol}(k)\left[\|f\|_{L^2(\Omega)} + \|g\|_{L^2(\partial\Omega)}\right]. \tag{3.6}$$

We mention that we are particularly interested in the case that $C_{sol}(k)$ is polynomially bounded, i.e.,

$$C_{sol}(k) \le \widetilde{C}_{sol} k^{\theta} \tag{3.7}$$

for some $\widetilde{C}_{sol}$, $\theta \ge 0$ independent of k. As mentioned above, for convex Ω we have $\theta = 0$ whereas for general Lipschitz domain Ω we have $\theta = 5/2$ by [11, Thm. 2.4].

The stability bound (3.6) merely requires $f \in L^2(\Omega)$. As in the 1D situation discussed in Section 3.1, it is possible to obtain a better k-dependence by exploiting additional regularity of the data f. The following result shows this for the multi-dimensional case:

Lemma 3.4. *Let $\Omega \subset \mathbb{R}^d$, $d \in \{2,3\}$ be a bounded Lipschitz domain. Let $C_{sol}(k)$ be given by (3.6). Let $f \in H^1(\Omega)$ and $g = 0$. Then there exists $C > 0$ independent of f and k such that*

$$\|u\|_{\mathcal{H}} \le C k^{-1}(1 + C_{sol}(k))\|f\|_{H^1(\Omega)}.$$

Proof. Assume first $f \in H^2(\Omega)$. Define the function $u_0 := -k^{-2} f$. Then $\|u_0\|_{\mathcal{H}} \le C k^{-1}\|f\|_{L^2(\Omega)} + k^{-2}\|f\|_{H^1(\Omega)}$. Then the function $\delta := u - u_0$ satisfies

$$\begin{aligned} -\Delta\delta - k^2\delta &= f - (-\Delta u_0 - k^2 u_0) = +k^{-2}\Delta f \qquad \text{in } \Omega, \\ \partial_n \delta - \mathbf{i}k\delta &= 0 - (\partial_n u_0 - \mathbf{i}k u_0) \qquad \text{on } \partial\Omega. \end{aligned}$$

By the stability (3.6) and generous trace estimates we have

$$\begin{aligned} \|\delta\|_{\mathcal{H}} &\le C_{sol}(k)\left[k^{-2}\|\Delta f\|_{L^2(\Omega)} + k^{-2}\|\partial_n f\|_{L^2(\partial\Omega)} + k^{-1}\|f\|_{L^2(\partial\Omega)}\right] \\ &\le C C_{sol}(k)\left[k^{-2}\|f\|_{H^2(\Omega)} + k^{-1}\|f\|_{H^1(\Omega)}\right] \end{aligned}$$

and conclude from the triangle inequality $\|u\|_{\mathcal{H}} \le \|u_0\|_{\mathcal{H}} + \|\delta\|_{\mathcal{H}}$

$$\|u\|_{\mathcal{H}} \le C\left[k^{-2}\|f\|_{\mathcal{H}} + C_{sol}(k)(k^{-2}\|f\|_{H^2(\Omega)} + k^{-1}\|f\|_{H^1(\Omega)})\right]. \tag{3.8}$$

In order to lower the regularity requirement for f from H^2 to H^1, we employ an interpolation argument. Specifically, we will work with the "real method" of interpolation (see, e.g., [25, 24] for an introduction to these methods). Recognizing that $H^1(\Omega)$ is the interpolation space $H^1(\Omega) = (L^2(\Omega), H^2(\Omega))_{1/2,2}$ (see, e.g., [8, eqn. (14.2.5)]) we can write, for every $t > 0$, the function $f \in H^1(\Omega)$ as

$$f = (f - f_{H^2}) + f_{H^2},$$

where $f_{H^2} \in H^2(\Omega)$ and the following estimates are true:

$$\|f - f_{H^2}\|_{L^2(\Omega)} + t\|f_{H^2}\|_{H^2(\Omega)} \le C t^{1/2}\|f\|_{H^1(\Omega)}, \tag{3.9}$$

$$\|f_{H^2}\|_{H^1(\Omega)} \le C\|f\|_{H^1(\Omega)}; \tag{3.10}$$

here, the estimate (3.9) follows from the definition of the K-functional and, for example, the observation [25, Thm. 1.3.3, (c)] while (3.10) follows from [7]. Selecting $t = k^{-2}$, we arrive at

$$\|f - f_{H^2}\|_{L^2(\Omega)} \le k^{-1}\|f\|_{H^1(\Omega)}, \qquad \|f_{H^2}\|_{H^1(\Omega)} + k^{-1}\|f_{H^2}\|_{H^2(\Omega)} \le C\|f\|_{H^1(\Omega)}.$$

We write $u = u_1 + u_2$, where u_1 and u_2 solve

$$\left\{\begin{aligned} -\Delta u_1 - k^2 u_1 &= f - f_{H^2} && \text{in } \Omega, \\ \partial_n u_1 - \mathbf{i}k u_1 &= 0 && \text{on } \partial\Omega, \end{aligned}\right. \qquad \left\{\begin{aligned} -\Delta u_2 - k^2 u_2 &= f_{H^2} && \text{in } \Omega, \\ \partial_n u_2 - \mathbf{i}k u_2 &= 0 && \text{on } \partial\Omega. \end{aligned}\right.$$

We obtain from (3.6) for u_1 and from (3.8) for u_2 that

$$\begin{aligned} \|u\|_{\mathcal{H}} &\le \|u_1\|_{\mathcal{H}} + \|u_2\|_{\mathcal{H}} \\ &\le C_{sol}(k)\|f - f_{H^2}\|_{L^2(\Omega)} + C\left[k^{-2}\|f_{H^2}\|_{\mathcal{H}} + C_{sol}(k)(k^{-2}\|f_{H^2}\|_{H^2(\Omega)} + k^{-1}\|f_{H^2}\|_{H^1(\Omega)})\right] \\ &\le C(1 + C_{sol}(k))k^{-1}\|f\|_{H^1(\Omega)}, \end{aligned}$$

which allows us to conclude the proof. ∎

Remark 3.5. The improvement in the powers of k of Lemma 3.4 over (3.6) is due to a combination of additional regularity for f and the special boundary condition $g = 0$; see also Remark 3.2. Inspection of the solution formula (3.3) for the 1D situation suggests that further improvements with respect to k cannot be obtained by merely stipulating more regularity of f. In addition to regularity, some conditions on the behavior of f near $\partial\Omega$ need to be imposed. ■

3.2.2. Regularity by decomposition

A key step in the arguments of [19] and likewise in [18, 17, 11] is to decompose the solution of (2.1) into a part with finite regularity but k-independent bounds and an analytic part with k-explicit control over all derivatives. We cite from [17] the following version:

Proposition 3.6 ([17, Thm. 4.5])**.** *Let $\Omega \in \mathbb{R}^d$, $d \in \{2,3\}$ be a bounded Lipschitz domain. Assume additionally that Ω has an analytic boundary. Let $C_{sol}(k)$ be given by (3.6). Fix $s \in \mathbb{N}_0$. Then there exist constants C, $\lambda > 0$ independent of $k \geq k_0 > 0$ such that for every $f \in H^s(\Omega)$ and $g \in H^{s+1/2}(\partial\Omega)$ the solution $u = S(f,g)$ of the Helmholtz problem (2.1) can be written as $u = u_{H^{s+2}} + u_{\mathcal{A}}$, where, for all $n \in \mathbb{N}_0$,*

$$\|u_{\mathcal{A}}\|_{\mathcal{H},\Omega} \leq CC_{sol}(k)\left(\|f\|_{L^2(\Omega)} + \|g\|_{H^{1/2}(\partial\Omega)}\right), \tag{3.11}$$

$$\|\nabla^{n+2}u_{\mathcal{A}}\|_{L^2(\Omega)} \leq C\lambda^n k^{-1}C_{sol}(k)\max\{n,k\}^{n+2}\left(\|f\|_{L^2(\Omega)} + \|g\|_{H^{1/2}(\partial\Omega)}\right), \tag{3.12}$$

$$\|u_{H^{s+2}}\|_{H^{s+2}(\Omega)} + k^{s+2}\|u_{H^{s+2}}\|_{L^2(\Omega)} \leq C\left(\|f\|_{H^s(\Omega)} + \|g\|_{H^{s+1/2}(\partial\Omega)}\right). \tag{3.13}$$

As we have seen in the 1D case, it is possible to improve the estimates by one power of k for the special case of homogeneous boundary conditions and some additional regularity of the right-hand side f. This extends to the multi-dimensional case:

Theorem 3.7. *Let $\Omega \in \mathbb{R}^d$, $d \in \{2,3\}$ be a bounded Lipschitz domain. Assume additionally that Ω has an analytic boundary. Fix $s \in \mathbb{N}$. Then there exist constants C, $\lambda > 0$ independent of $k \geq k_0 > 0$ such that for every $f \in H^s(\Omega)$ the solution u of (2.1) with $g = 0$ can be written as $u = u_{H^{s+2}} + u_{\mathcal{A}}$, where, for all $n \in \mathbb{N}_0$,*

$$\|u_{\mathcal{A}}\|_{\mathcal{H},\Omega} \leq Ck^{-1}(1 + C_{sol}(k))\|f\|_{H^1(\Omega)}, \tag{3.14}$$

$$\|\nabla^{n+2}u_{\mathcal{A}}\|_{L^2(\Omega)} \leq C\lambda^n k^{-2}(1 + C_{sol}(k))\max\{n,k\}^{n+2}\|f\|_{H^1(\Omega)}, \tag{3.15}$$

$$\|u_{H^{s+2}}\|_{H^{s+2}(\Omega)} + k^{s+2}\|u_{H^{s+2}}\|_{L^2(\Omega)} \leq C\|f\|_{H^s(\Omega)}. \tag{3.16}$$

Proof. We decompose the data $f \in H^s(\Omega)$: Using the operators L_Ω and H_Ω of [19, (4.1b)], we can write f as a sum of a function $f_H \in H^s(\Omega)$ and an analytic function f_L, i.e.,

$$f = L_\Omega f + H_\Omega f =: f_L + f_H;$$

by [19, Lemma 4.2, Lemma 4.3], we have, for some C, $\eta > 0$ independent of k, the bounds

$$\|f_H\|_{H^{s_1}(\Omega)} \leq Ck^{s_1-s_2}\|f\|_{H^{s_2}(\Omega)}, \qquad 0 \leq s_1 \leq s_2 \leq s, \tag{3.17}$$

$$\|\nabla^n f_L\|_{L^2(\Omega)} \leq C(\eta k)^n\|f\|_{L^2(\Omega)} \qquad \forall n \in \mathbb{N}_0, \tag{3.18}$$

$$\|\nabla^n f_L\|_{L^2(\Omega)} \leq C(\eta k)^{n-s}\|f\|_{H^s(\Omega)} \qquad \forall n \geq s. \tag{3.19}$$

We denote by u_L and u_H the solutions to (2.1) with $g = 0$ and right-hand sides f_L and f_H, respectively. For u_H, we have $f_H \in H^s(\Omega)$ together with $\|f_H\|_{L^2(\Omega)} \leq Ck^{-1}\|f\|_{H^1(\Omega)}$ by (3.17). In view of Proposition 3.6, we may write $u_H = u_{H^{s+2}} + \widetilde{u}_{\mathcal{A}}$ with

$$\begin{aligned} k^{s+2}\|u_{H^{s+2}}\|_{L^2(\Omega)} + \|u_{H^{s+2}}\|_{H^{s+2}(\Omega)} &\leq C\|f_H\|_{H^s(\Omega)} \leq C\|f\|_{H^s(\Omega)}, \\ \|\widetilde{u}_{\mathcal{A}}\|_{\mathcal{H}} &\leq C_{sol}(k)\|f_H\|_{L^2(\Omega)}, \\ \|\nabla^n\widetilde{u}_{\mathcal{A}}\|_{L^2(\Omega)} &\leq C\lambda^n k^{-1}C_{sol}(k)\max\{k,n\}^n\|f_H\|_{L^2(\Omega)} \qquad \forall n \in \mathbb{N}_0. \end{aligned}$$

Recalling that $\|f_H\|_{L^2(\Omega)} \le Ck^{-1}\|f\|_{H^1(\Omega)}$, we see that $u_{H^{s+2}}$ and $\widetilde{u}_{\mathcal{A}}$ have the desired properties. We now turn to u_L. Since f_L and $\partial\Omega$ are analytic, the solution u_L is analytic. For bounds on the derivatives of u_L, we first note that Lemma 3.4 yields

$$\|u_L\|_{\mathcal{H}} \le Ck^{-1}(1 + C_{sol}(k))\|f_L\|_{H^1(\Omega)}. \tag{3.20}$$

For higher order derivatives of u_L, we proceed as in the proof of [19, Lemma 4.13]: Upon setting $\varepsilon := 1/k$, we observe that u_L satisfies

$$-\varepsilon^2\Delta u_L - u_L = \varepsilon^2 f_L \quad \text{in } \Omega, \qquad \varepsilon^2\partial_n u_L - \mathbf{i}\varepsilon u_L = 0 \quad \text{on } \partial\Omega,$$

with f_L satisfying the estimates above. Hence, the equation satisfied by u_L has the same structure as in the proof of [19, Lemma 4.13], which makes [16, Prop. 5.4.5, Rem. 5.4.6] applicable. The result is then

$$\|\nabla^{n+2}u_L\|_{L^2(\Omega)} \le CK^{n+2}\max\{n,k\}^{n+2}\left[k^{-2}\|f_L\|_{L^2(\Omega)} + k^{-1}\|u_L\|_{\mathcal{H}}\right]$$

for a $K > 0$ independent of k and n. Inserting now the estimate (3.20) for u_L yields

$$\|\nabla^{n+2}u_L\|_{L^2(\Omega)} \le CK^{n+2}\max\{n,k\}^{n+2}k^{-2}\left\{\|f_L\|_{L^2(\Omega)} + (1 + C_{sol}(k))\|f\|_{H^1(\Omega)}\right\}.$$

Using $\|f_L\|_{L^2(\Omega)} \le C\|f\|_{L^2(\Omega)}$ and setting $u_{\mathcal{A}} := \widetilde{u}_{\mathcal{A}} + u_L$ finishes the proof. □

4. Convergence analysis

4.1. hp-convergence analysis

We perform our convergence analysis for spaces V_N that have approximation properties typical of the $H^1(\Omega)$-conforming spaces of piecewise polynomials of degree p. Specifically, we stipulate the following Assumption 4.1, which formalizes the approximation properties of the *hp*-FEM spaces defined in [18, Sec. 5] and formulated explicitly in [19, Prop. 5.3]; essentially, those spaces are spaces of piecewise (mapped) polynomials of degree p on a mesh $\mathcal{T}$ whose elements have diameter h.

Assumption 4.1. *The space V_N depends on two discretization parameters h and p and has the following two properties:*

1. *Let $\gamma > 0$ be given. Then there exist constants C, $\sigma > 0$ independent of k and the discretization parameters h, p such that if u is analytic on Ω with*

$$\|\nabla^n u\|_{L^2(\Omega)} \le C_u\gamma^n\max\{n,k\}^n \qquad \forall n \in \mathbb{N}_0$$

   then

$$\inf_{v\in V_N}\|u - v\|_{\mathcal{H}} \le CC_u\left(1 + \frac{kh}{p}\right)\left(\left(\frac{h}{h+\sigma}\right)^p + k\left(\frac{kh}{\sigma p}\right)^p\right).$$

2. *Let $s \in \mathbb{N}_0$ be given. Then there exists a constant C independent of k and the discretization parameters h, p such that if $u \in H^{s+1}(\Omega)$, then*

$$\inf_{v\in V_N}\|u - v\|_{\mathcal{H}} \le C\left(1 + \frac{kh}{p}\right)\left(\frac{h}{p}\right)^s\|u\|_{H^{s+1}(\Omega)}, \qquad p \ge s+1.$$

A further assumption on the parameters h and p is that

$$\frac{kh}{p} \le \overline{C}$$

for a fixed constant $\overline{C} > 0$. This implies that the factors $(1 + kh/p)$ in the above estimates can be dropped.

It will be convenient to introduce the following shorthand:

$$\varepsilon(h,p,k) := \left(\frac{h}{h+\sigma}\right)^p + k\left(\frac{kh}{\sigma p}\right)^p \tag{4.1}$$

The approximation properties of Assumption 4.1 together with the regularity assertions of Proposition 3.6 and Theorem 3.7 allow us to estimate the quantities $\eta_N^{L^2}$ as well as $\eta_N^{H^1}$ and $\eta_N^{H_0^1}$ of (2.10):

Theorem 4.2. *Let $\Omega \subset \mathbb{R}^d$, $d \in \{2,3\}$ be a bounded Lipschitz domain with an analytic boundary. Assume the approximation space V_N to have the properties stated in Assumption 4.1. Then for constants C, $\sigma > 0$ independent of h, k, and p:*

$$\eta_N^{L^2} \leq C\left[\frac{h}{p} + C_{sol}(k)k^{-1}\left\{\left(\frac{h}{h+\sigma}\right)^p + k\left(\frac{kh}{\sigma p}\right)^p\right\}\right], \tag{4.2}$$

$$\eta_N^{H_0^1} \leq \eta_N^{H^1} \leq C\left[\left(\frac{h}{p}\right)^{\min\{2,p\}} + (1+C_{sol}(k))k^{-2}\left\{\left(\frac{h}{h+\sigma}\right)^p + k\left(\frac{kh}{\sigma p}\right)^p\right\}\right]. \tag{4.3}$$

Proof. The estimate (4.2) has already been shown in [19, Prop. 5.3]; it follows from the approximation properties of V_N in combination with the regularity assertion Proposition 3.6. The first bound in (4.3) follows directly from the definition. For the second estimate in (4.3), let $f \in H^1(\Omega)$ be arbitrary. Then $u := S^* f = \overline{S(\overline{f},0)}$ can, according to Theorem 3.7 with $s = 1$, be written as

$$u = u_{H^3} + u_{\mathcal{A}},$$

where the contributions u_{H^3} and $u_{\mathcal{A}}$ have the regularity properties stated there. Therefore, we get from Assumption 4.1

$$\begin{aligned}
\inf_{v\in V_N} \|u_{H^3} - v\|_{\mathcal{H}} &\leq C\left(\frac{h}{p}\right)^{\min\{2,p\}} \|f\|_{H^1(\Omega)},\\
\inf_{v\in V_N} \|u_{\mathcal{A}} - v\|_{\mathcal{H}} &\leq Ck^{-2}(1+C_{sol}(k))\|f\|_{H^1(\Omega)}\left[\left(\frac{h}{h+\sigma}\right)^p + k\left(\frac{hk}{\sigma p}\right)^p\right].
\end{aligned}$$

The result now follows. □

Remark 4.3. As mentioned above, for our model problem (2.1), the constant $C_{sol}(k)$ satisfies the polynomial bound (3.7) with $\theta = 5/2$. Hence, the crucial condition (2.7) is satisfied if, for a sufficiently small c_1 and a sufficiently large c_2, the following two conditions are satisfied:

$$\frac{kh}{p} \leq c_1 \qquad \text{and} \qquad p \geq c_2 \log k. \tag{4.4}$$

■

Next, we formulate a best approximation result for data $(f,g) \in H^s(\Omega) \times H^{s+1/2}(\partial\Omega)$, which is proved very similarly to Theorem 4.2.

Theorem 4.4. *Let $\Omega \subset \mathbb{R}^d$, $d \in \{2,3\}$ be a bounded Lipschitz domain with an analytic boundary. Let the approximation space V_N satisfy Assumption 4.1. For the solution u of (2.1) we have:*

(i) If $s \in \mathbb{N}_0$ and $f \in H^s(\Omega)$ and $g \in H^{s+1/2}(\partial\Omega)$, then

$$\begin{aligned}
\inf_{v\in V_N} \|u - v\|_{\mathcal{H}} \leq{}& C\left(\frac{h}{p}\right)^{\min\{s+1,p\}} \left[\|f\|_{H^s(\Omega)} + \|g\|_{H^{s+1/2}(\partial\Omega)}\right]\\
&+ C_{sol}(k)k^{-1}\left\{\left(\frac{h}{h+\sigma}\right)^p + k\left(\frac{kh}{\sigma p}\right)^p\right\}\left[\|f\|_{L^2(\Omega)} + \|g\|_{H^{1/2}(\partial\Omega)}\right].
\end{aligned}$$

(ii) If $s \in \mathbb{N}$ and $f \in H^s(\Omega)$ and $g = 0$, then

$$\begin{aligned} \inf_{v \in V_N} \|u - v\|_{\mathcal{H}} &\leq C \left(\frac{h}{p}\right)^{\min\{s+1,p\}} \|f\|_{H^s(\Omega)} \\ &\quad + (1 + C_{sol}(k))k^{-2} \left\{ \left(\frac{h}{h+\sigma}\right)^p + k \left(\frac{kh}{\sigma p}\right)^p \right\} \|f\|_{H^1(\Omega)}. \end{aligned}$$

Proof. (i) follows from Proposition 3.6 and the approximation properties of V_N. The estimate in (ii) is shown similarly, but we are able to exploit the improved k-dependence of Theorem 3.7. □

We are now in position to formulate some *a priori* error estimates. For simplicity of notation, we employ the abbreviation $\varepsilon(h, p, k)$ of (4.1):

Corollary 4.5. *Assume the hypotheses of Theorem 4.4. Assume in addition that h and p are such that condition (2.7) is satisfied.*

(i) If $s \in \mathbb{N}_0$, $f \in H^s(\Omega)$ and $g \in H^{s+1/2}(\partial\Omega)$, then with $C_{f,g} := \|f\|_{H^s(\Omega)} + \|g\|_{H^{s+1/2}(\partial\Omega)}$

$$\begin{aligned} \|u - u_N\|_{\mathcal{H}} &\leq C C_{f,g} \left\{ \left(\frac{h}{p}\right)^{\min\{s+1,p\}} + k^{-1} C_{sol}(k) \varepsilon(h,p,k) \right\}, \\ \|u - u_N\|_{L^2(\Omega)} &\leq C \left\{ \left(\frac{h}{p}\right) + k^{-1} C_{sol}(k) \varepsilon(h,p,k) \right\} \|u - u_N\|_{\mathcal{H}}, \\ \|u - u_N\|_{H^{-1}(\Omega)} &\leq C \left\{ \left(\frac{h}{p}\right)^{\min\{2,p\}} + k^{-2}(1 + C_{sol}(k)) \varepsilon(h,p,k) \right\} \|u - u_N\|_{\mathcal{H}}. \end{aligned}$$

Furthermore, if the function z in (2.11) is in $H^{s'}(\Omega)$ ($s' \in \mathbb{N}$) then

$$|L(u) - L(u_N)| \leq C \left\{ \left(\frac{h}{p}\right)^{\min\{s'+1,p\}} + k^{-2}(1 + C_{sol}(k)) \varepsilon(h,p,k) \right\} \|u - u_N\|_{\mathcal{H}}.$$

(ii) If $s \in \mathbb{N}$ and $f \in H^s(\Omega)$ and $g = 0$, then with $C_f := \|f\|_{H^s(\Omega)}$

$$\begin{aligned} \|u - u_N\|_{\mathcal{H}} &\leq C C_f \left\{ \left(\frac{h}{p}\right)^{\min\{s+1,p\}} + k^{-2}(1 + C_{sol}(k)) \varepsilon(h,p,k) \right\}, \\ \|u - u_N\|_{L^2(\Omega)} &\leq C \left\{ \left(\frac{h}{p}\right) + k^{-1} C_{sol}(k) \varepsilon(h,p,k) \right\} \|u - u_N\|_{\mathcal{H}}, \\ \|u - u_N\|_{H^{-1}(\Omega)} &\leq C \left\{ \left(\frac{h}{p}\right)^{\min\{2,p\}} + k^{-2}(1 + C_{sol}(k)) \varepsilon(h,p,k) \right\} \|u - u_N\|_{\mathcal{H}}. \end{aligned}$$

Furthermore, if the function z in (2.11) is in $H^{s'}(\Omega)$ ($s' \in \mathbb{N}$) then

$$|L(u) - L(u_N)| \leq C \left\{ \left(\frac{h}{p}\right)^{\min\{s'+1,p\}} + k^{-2}(1 + C_{sol}(k)) \varepsilon(h,p,k) \right\} \|u - u_N\|_{\mathcal{H}}.$$

Proof. Follows by combining the above results. □

4.2. h-FEM

The above considerations are formulated in a general hp-setting. We will now present some numerical examples for the h-FEM since it features a more pronounced k-dependence. For example, we can simplify

$$\varepsilon(h,p,k) = \left(\frac{h}{h+\sigma}\right)^p + k\left(\frac{kh}{\sigma p}\right)^p \leq C_p k^{p+1} h^p.$$

The next corollary follows from Corollary 4.5 by fixing p. Additionally, we assume explicitly the condition (3.7) in order to make the k-dependence more visible:

Corollary 4.6 (h-FEM)**.** *Assume the hypotheses of Corollary 4.5 and (3.7). Fix $p \in \mathbb{N}$. Then:*

(i) If $s \in \mathbb{N}_0$, $f \in H^s(\Omega)$, and $g \in H^{s+1/2}(\partial\Omega)$, then with $C_{f,g} = \|f\|_{H^s(\Omega)} + \|g\|_{H^{s+1/2}(\partial\Omega)}$

$$\begin{aligned}
\|u - u_N\|_{\mathcal{H}} &\leq CC_{f,g}\left[h^{\min\{s+1,p\}} + k^\theta (kh)^p\right], \\
\|u - u_N\|_{L^2(\Omega)} &\leq CC_{f,g}\left[h^{\min\{s+1,p\}} + k^\theta (kh)^p\right] h\left[1 + k^{\theta+1}(kh)^{p-1}\right], \\
\|u - u_N\|_{H^{-1}(\Omega)} &\leq CC_{f,g}\left[h^{\min\{s+1,p\}} + k^\theta (kh)^p\right] \begin{cases} h^2(1 + k^{\theta+1}(kh)^{p-2}) & \text{if } p \geq 2 \\ hk^\theta & \text{if } p = 1. \end{cases}
\end{aligned}$$

If the function z in (2.11) is in $H^{s'}(\Omega)$ ($s' \in \mathbb{N}$), then

$$|L(u) - L(u_N)| \leq CC_{f,g}\left[h^{\min\{s+1,p\}} + k^\theta (kh)^p\right]\left[h^{\min\{s'+1,p\}} + k^{\theta-1}(kh)^p\right].$$

(ii) If $s \in \mathbb{N}$ and $f \in H^s(\Omega)$ and $g = 0$, then with $C_f = \|f\|_{H^s(\Omega)}$

$$\begin{aligned}
\|u - u_N\|_{\mathcal{H}} &\leq CC_f\left[h^{\min\{s+1,p\}} + k^{\theta-1} (kh)^p\right], \\
\|u - u_N\|_{L^2(\Omega)} &\leq CC_f\left[h^{\min\{s+1,p\}} + k^{\theta-1} (kh)^p\right] h\left[1 + k^{\theta+1}(kh)^{p-1}\right], \\
\|u - u_N\|_{H^{-1}(\Omega)} &\leq CC_{f,g}\left[h^{\min\{s+1,p\}} + k^{\theta-1} (kh)^p\right] \begin{cases} h^2(1 + k^{\theta+1}(kh)^{p-2}) & \text{if } p \geq 2 \\ hk^\theta & \text{if } p = 1. \end{cases}
\end{aligned}$$

If the function z in (2.11) is in $H^{s'}(\Omega)$ ($s' \in \mathbb{N}$), then

$$|L(u) - L(u_N)| \leq CC_{f,g}\left[h^{\min\{s+1,p\}} + k^{\theta-1}(kh)^p\right]\left[h^{\min\{s'+1,p\}} + k^{\theta-1}(kh)^p\right].$$

Remark 4.7. A different way of phrasing the $L^2(\Omega)$-convergence result is as follows: If Ω has an analytic boundary and we assume that the exact solution $u \in H^{m+1}(\Omega)$ of (2.1) satisfies

$$|u|_{H^j(\Omega)} \sim k^j, \qquad j = 0, \ldots, m+1,$$

and the solvability condition (2.7) is satisfied, then for $p \geq m$

$$\|u - u_N\|_{L^2(\Omega)} \leq C_m \Big(\frac{hk}{p}\Big)^{m+1} \Big\{1 + C_{sol}(k)\Big[\frac{1}{k}\left(\frac{h}{h+\sigma}\right)^{p-1} + k\Big(\frac{hk}{\sigma p}\Big)^{p-1}\Big]\Big\}. \tag{4.5}$$

This follows by combining the estimate for $\eta_N^{L^2}$ with the *a priori* bound $\inf_{v\in V_N} \|u - v\|_{\mathcal{H}} \leq Ch^m \|u\|_{H^{m+1}(\Omega)} \leq Ck(kh/p)^m$ (cf. Assumption 4.1). The estimate (4.5) illustrates again the special nature of the case $p = 1$ when it comes to the k-dependence. ■

5. Numerical Examples

5.1. 1D examples

We show several numerical examples for the simple 1D model problem (3.1). Without proof we mention that the convergence results of Corollary 4.6 are valid in this case as well (in spite of the fact that Dirichlet boundary conditions are imposed on parts of the boundary) with the special choice $\theta = 0$; in particular, the different k-dependence for the cases $g \neq 0$ and $g = 0$ applies.

Example 5.1. We consider the smooth 1D example of (2.1) with $f \equiv 1$ and $g = 0$. With $\theta = 0$, Corollary 4.6 gives

$$\|u - u_N\|_{\mathcal{H}} \leq C\left(h^p + k^{-1}(kh)^p\right) \leq Ck^{p-1}h^p.$$

In Fig. 1, we plot the relative error in the $H^1(I)$-seminorm. A closed form solution for u is available, (6.6), and shows $\|u'\|_{L^2(I)} \sim k^{-1}$. Hence, the relative error in the $H^1(I)$-seminorm (even in the $\|\cdot\|_{\mathcal{H}}$-norm) is expected to behave like $O((kh)^p)$, i.e., order p in the number N_λ of degrees of freedom per wavelength. This is visible in Fig. 1, where the relative error in the $H^1(I)$-seminorm is plotted versus N_λ. Fig 2 shows the relative error in the $L^2(I)$-norm versus N_λ. From the closed form solution (6.6) we infer $\|u\|_{L^2(I)} \sim k^{-2}$. Hence, Corollary 4.6 yields

$$\frac{\|u - u_N\|_{L^2(I)}}{\|u\|_{L^2(I)}} \leq C\frac{1}{k^{-2}}\{h^p + k^{-1}(kh)^p\}h\{1 + k(kh)^{p-1}\} \leq C(kh)^{p+1}(1 + k(kh)^{p-1}).$$

This formula shows that, in its k-dependence, the asymptotic behavior of the case $p = 1$ is different from the case $p > 1$; this is again visible in Fig. 2, where we plot the relative error in $L^2(I)$ versus N_λ.

We finally turn to the convergence behavior for the linear functional given by $z \equiv 1$ in (2.11). From (6.6) we get $|L(u)| \sim k^{-2}$ so that we expect by Cor. 4.6

$$\frac{|L(u) - L(u_N)|}{|L(u)|} \leq C\frac{1}{k^{-2}}k^{p-1}h^p k^{p-1}h^p \leq C(kh)^{2p},$$

which is again visible in Fig. 3. ■

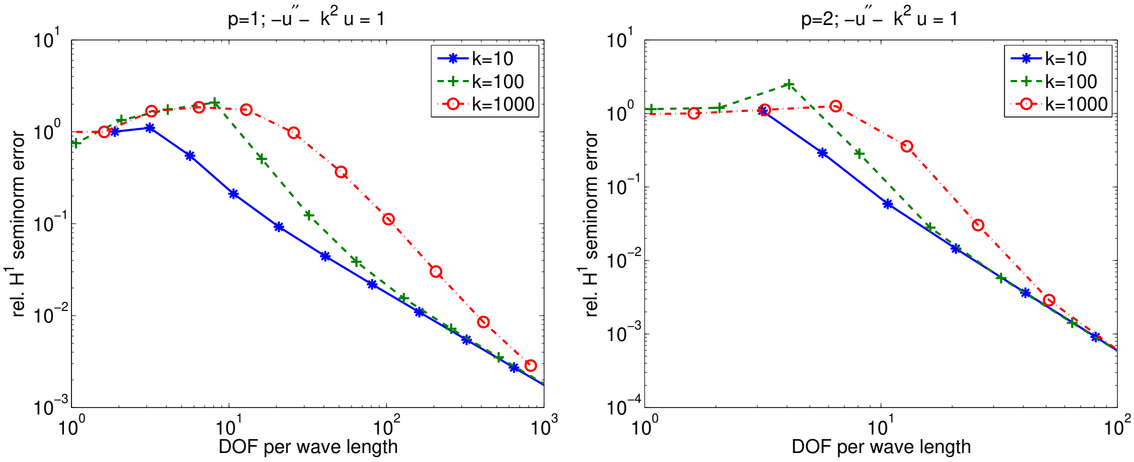

Figure 1: h-FEM for smooth f; relative error in H^1-seminorm, $p = 1$, 2 (see Example 5.1).

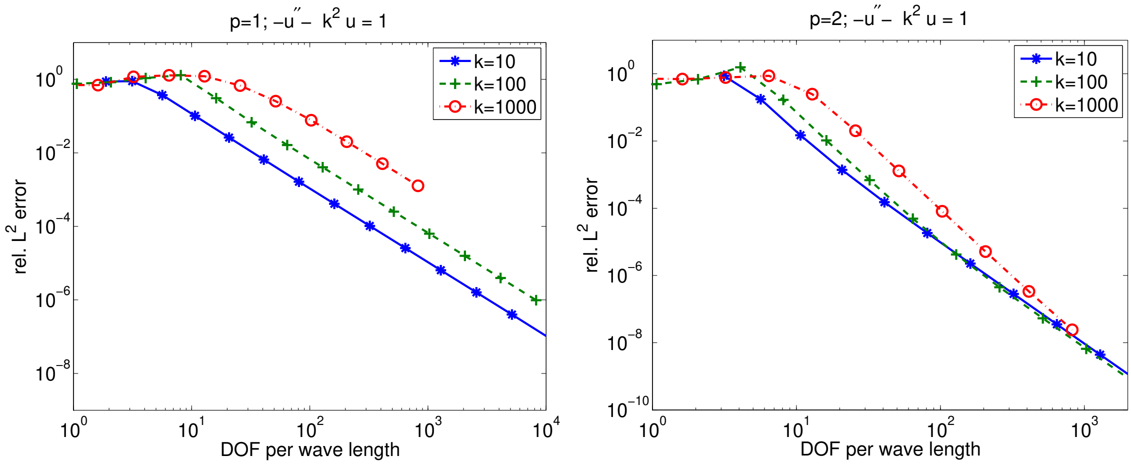

Figure 2: h-FEM for smooth f, relative error in L^2, $p = 1$, 2 (see Example 5.1).

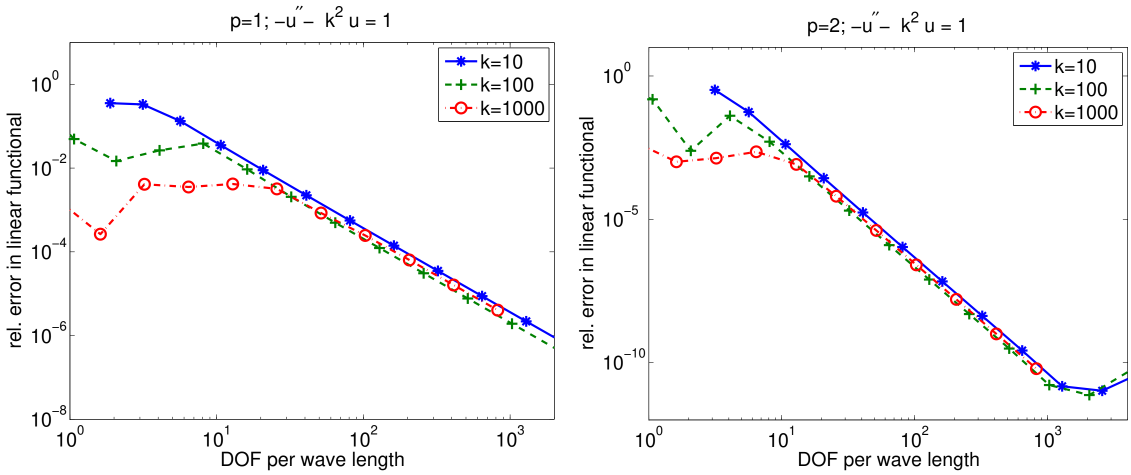

Figure 3: h-FEM for smooth f; error in smooth linear functional, $p = 1$, 2 (see Example 5.1).

Example 5.2. We consider (3.1) with $f(x) = x^\alpha$ and $g = 0$. We take the specific choices $\alpha = -1/2$ and $\alpha = 1/2$. Figs. 4, 5 present H^1-seminorm error as well as the k-scaled $L^2(I)$-norm error for $\alpha = -1/2$ and $p \in \{1, 2\}$ (Fig. 4) and for $\alpha = 1/2$ and $p \in \{2, 3\}$ (Fig. 5).

For $\alpha = -1/2$, the right-hand side f is in $H^s(I)$ for every $s < 0$ and for $\alpha = 1/2$, the right-hand side f is in $H^s(I)$ for every $s < 1$. Hence, we expect Cor. 4.6 to be applicable with $s = 0$ and $s = 1$, respectively. We first consider the case $\alpha = -1/2$ (corresponding to $s = 0$). Then, only case (i) is applicable in Cor. 4.6, yielding

$$\|u - u_N\|_{\mathcal{H}} \quad \leq \quad C\left(h^{\min\{s+1,p\}} + k^p h^p\right) \leq C\left(h + (kh)^p\right) = Ch\left(1 + k^p h^{p-1}\right),$$

where we inserted $s = 0$. We note the pronounced difference between the cases $p = 1$ and $p = 2$, which is also visible in Fig. 4. For $\alpha = 1/2$, a similar situation arises. Applying case (ii) of Cor. 4.6 with $s = 1$, we expect the behavior

$$\|u - u_N\|_{\mathcal{H}} \quad \leq \quad C\left(h^{\min\{s+1,p\}} + k^{p-1} h^p\right) \leq C\left(h^2 + k^{p-1} h^p\right) = Ch^2\left(1 + k^{p-1} h^{p-2}\right),$$

which is again visible in Fig. 5.

The absolute error in the linear functional of (2.11) with $z = 1$ is presented in Fig. 6. The top row corresponds to $\alpha = -1/2$ in conjunction with $p = 1$ and $p = 2$ whereas the bottom row depicts the case $\alpha = 1/2$ with $p = 2$ and $p = 3$. The first two cases ($p = 1$ for $\alpha = -1/2$ and $p = 2$ for $\alpha = 1/2$) are covered by Cor. 4.6. An improved estimate $O(h^{\min\{s+3/2,p\}+p})$ can be shown by exploiting the fact that the solution has a singularity at one point only; we refer to Lemma B.5 for details. This improved bound is visible in the numerics in Fig. 6 for the case $\alpha = -1/2$ in conjunction with $p = 2$ and the the case $\alpha = 1/2$ together with $p = 3$. ∎

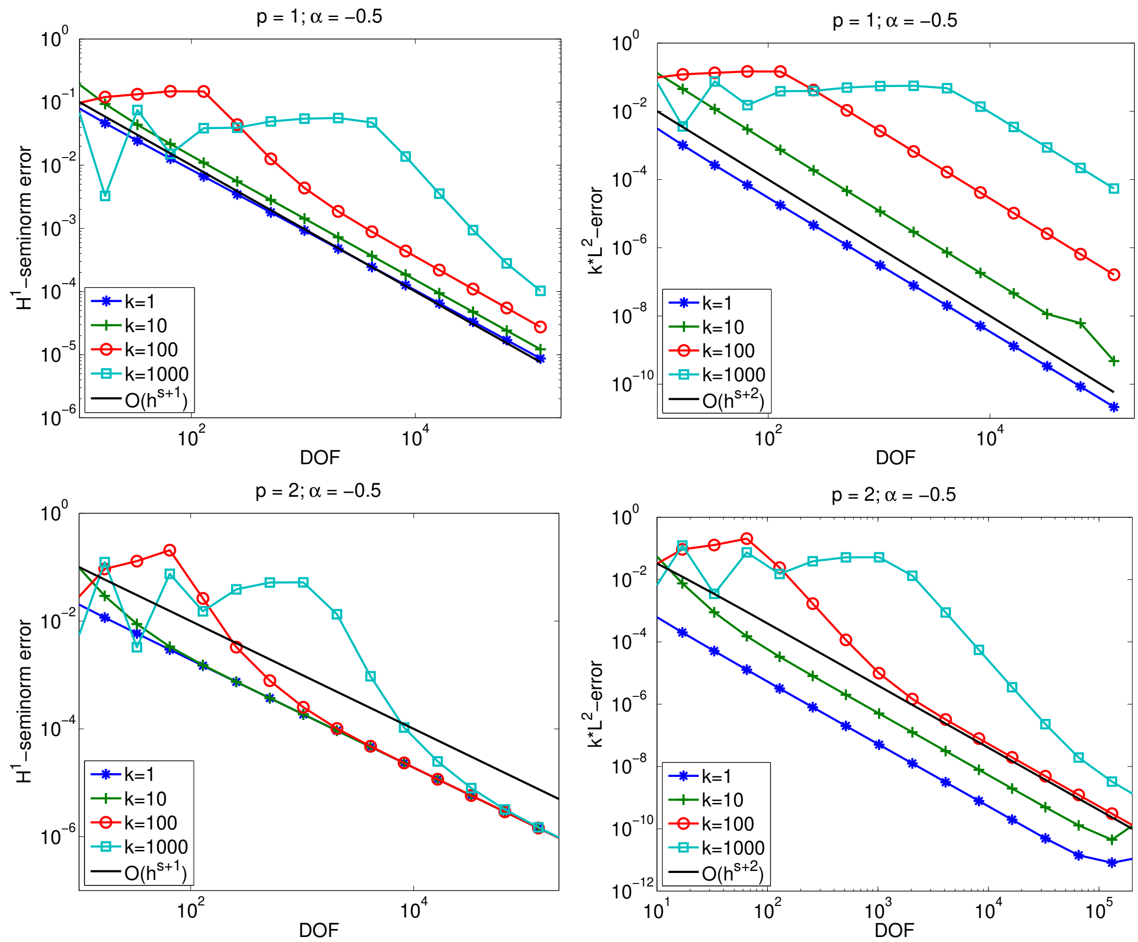

Figure 4: h-FEM for $\alpha = -1/2$: $p = 1$ (top row) and $p = 2$ (bottom row) (see Example 5.2).

5.2. 2D examples

The following three two-dimensional examples consider

$$\begin{aligned} -\Delta u - |\mathbf{k}|^2 u &= 0 \quad \text{in} \quad \Omega, \\ \partial_n u - \mathbf{i}|\mathbf{k}| u &= g \quad \text{on} \quad \partial\Omega, \end{aligned}$$

where g is chosen such that the exact solution u is given by $u(\mathbf{x}) = e^{i\mathbf{x}\cdot\mathbf{k}} = e^{\mathbf{i}(k_1 x + k_2 y)}$ with $k_1 = -k_2 = k/\sqrt{2}$ and k ranges from 4 to 80. The first geometry studied in Example 5.3 is convex so

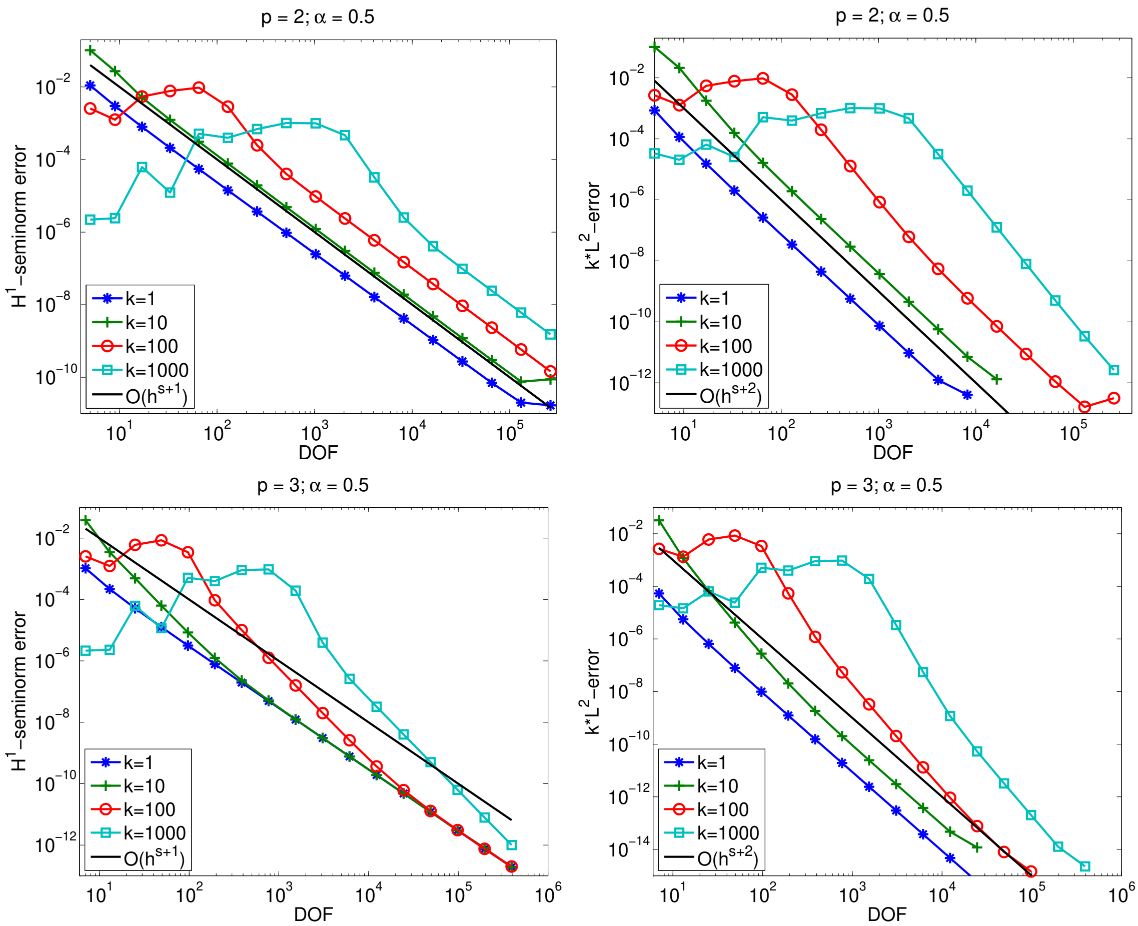

Figure 5: h-FEM for $\alpha = +1/2$: $p = 2$ (top row) and $p = 3$ (bottom row) (see Example 5.2).

that the stability bound (3.7) is true with $\theta = 0$; the geometries in Examples 5.4, 5.5 are non-convex so that only the bound with $\theta = 5/2$ is available. The estimate (3.7) with $\theta = 5/2$ is likely to be pessmistic. Indeed, the numerical results for all three geometries are very similar, and we do not observe a stronger pollution effect in Examples 5.4, 5.5 than in Example 5.3. All three examples are computed with the hp-FEM software package NETGEN/NGSOLVE by J. Schöberl [22, 21]. The curved geometry is resolved using high order approximations as provided by NETGEN/NGSOLVE.

Example 5.3. The domain consists of the square $[-1, 1]^2$ with two semicircular caps attached, i.e., $\overline{\Omega} = [-1, 1]^2 \cup \{(x, y)|(x \pm 1)^2 + y^2 \leq 1\}$ (see Fig. 7, (a)), and $k \in \{4, 20, 80\}$. For fixed $p = 1, 2$ we present in Fig. 8 the absolute error in L^2 as well as in the H^1-seminorm versus the number of degrees of freedom per wavelength. We observe the same marked difference between the cases $p = 1$ and $p = 2$ that we have seen already in 1D and which is explained by Corollary 4.6. The convergence when evaluating a linear functional of the form (2.11) given by $z \equiv 1$ is presented in Fig. 9. ■

Example 5.4. The geometry is the non-convex domain depicted in Fig. 7, (b). Its boundary consists of pieces of circular arcs with radii 1, 2, and 0.5. The domain is a subset of $[-2, 0.5] \times [-0.5, 2]$ and thus $\operatorname{diam} \Omega \leq 3.6$. The h-FEM (error in L^2 and H^1-seminorm as well as the error in a smooth linear functional) with $k = \{4, 20, 80\}$ and $p = 1, 2$ is presented in Figs. 10, 11. ■

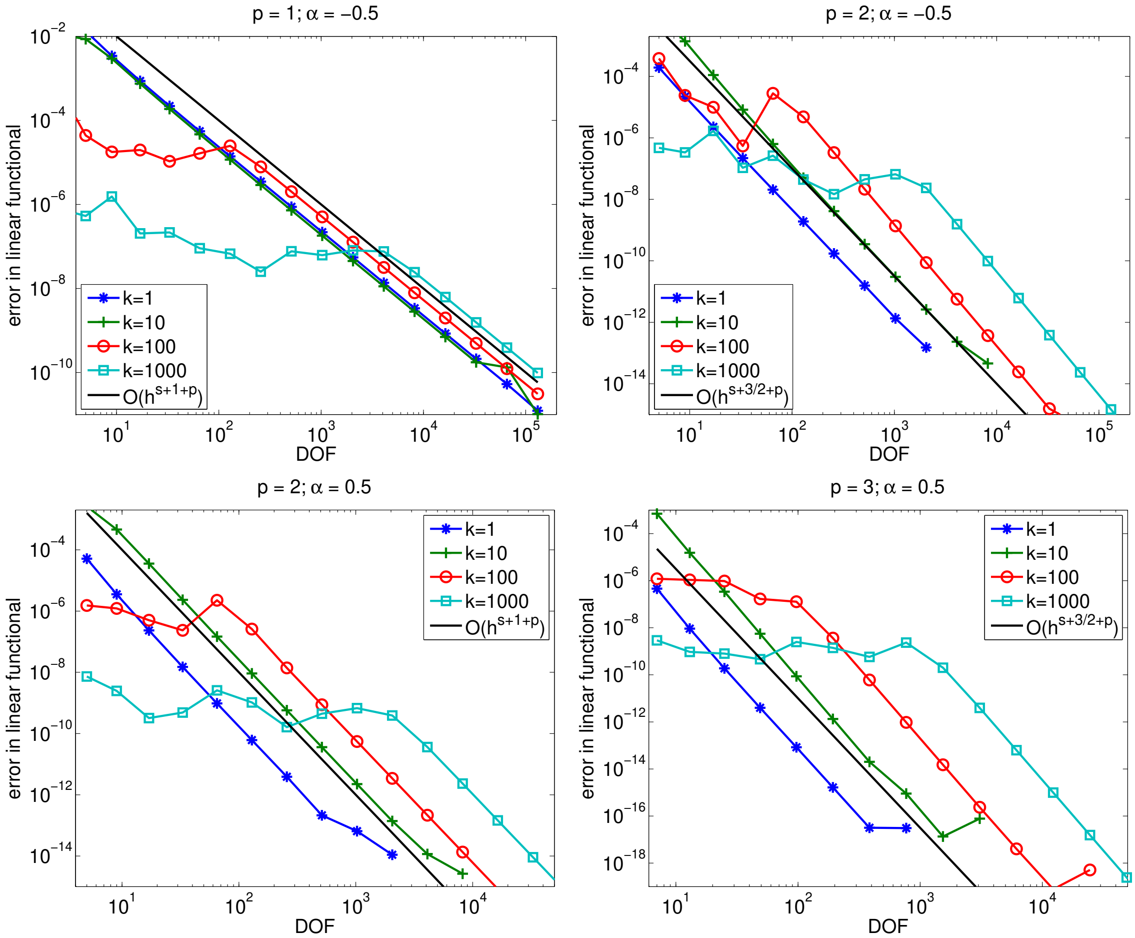

Figure 6: Error in smooth linear functions: top row: the case $\alpha = -1/2$ with $p = 1$ (left) and $p = 2$ (right). Bottom row: the case $\alpha = 1/2$ with $p = 2$ (left) and $p = 3$ (right) (see Example 5.2).

Example 5.5. The geometry is the non-simply connected domain shown in Fig. 7, (c). It is the geometry of Example 5.3 with a circle of radius 1/2 removed. The numerical results (L^2 and H^1-seminorm convergence as well as convergence of the linear functional given by $z = 1$) for $k = \{8, 20, 80\}$ and $p = 1$, 2 are shown in Figs. 12, 13. ∎

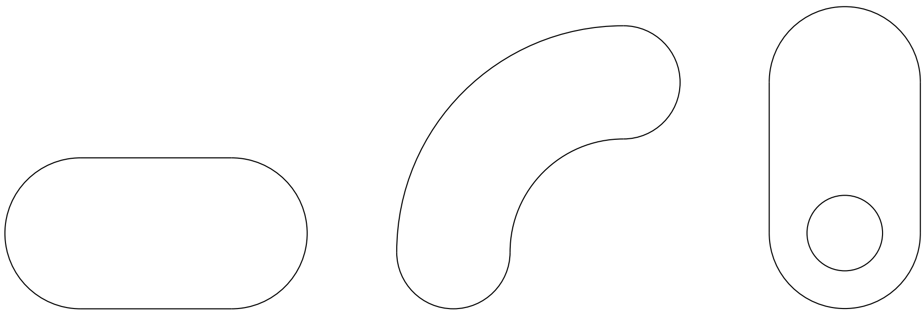

(a) Example 5.3 (b) Example 5.4 (c) Example 5.5

Figure 7: Domain geometries for Examples 5.3, 5.4, 5.5

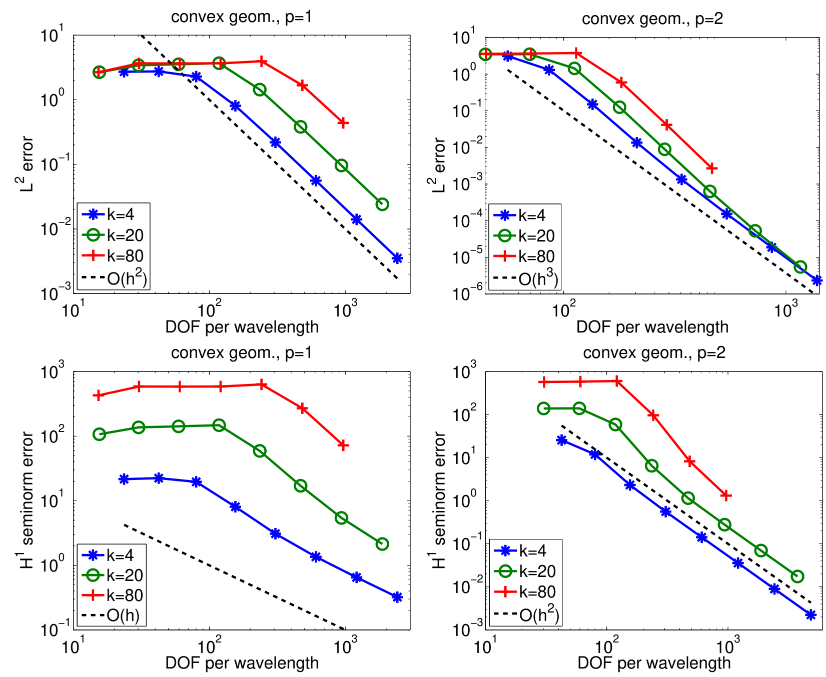

Figure 8: (cf. Example 5.3) h-FEM with $p = 1$ (left) and $p = 2$ (right) for convex domain. Top: L^2-error. Bottom: H^1-seminorm error.

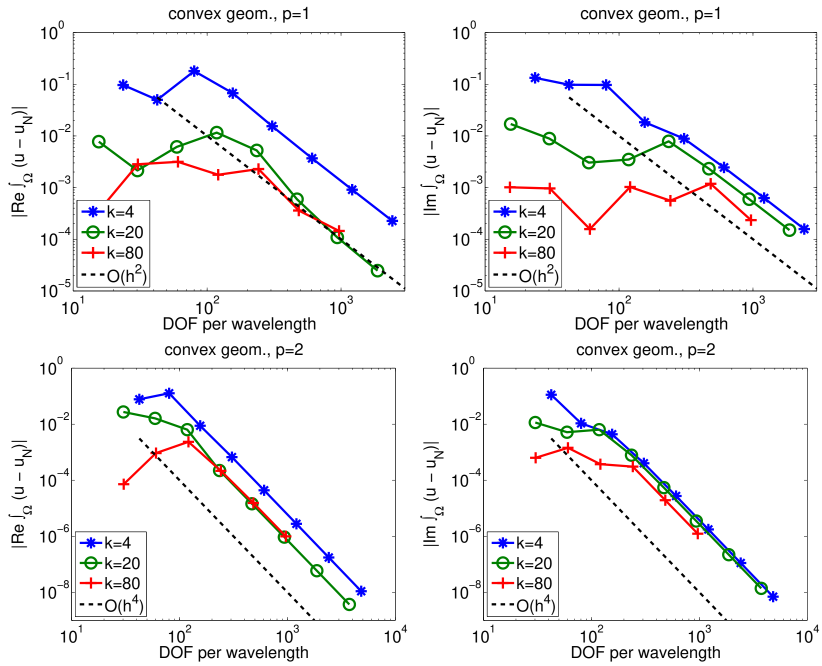

Figure 9: (cf. Example 5.3). h-FEM with $p = 1$ (top) and $p = 2$ (bottom) for convex geometry. Left: $|\operatorname{Re} \int_\Omega (u - u_N)|$. Right: $|\operatorname{Im} \int_\Omega (u - u_N)|$

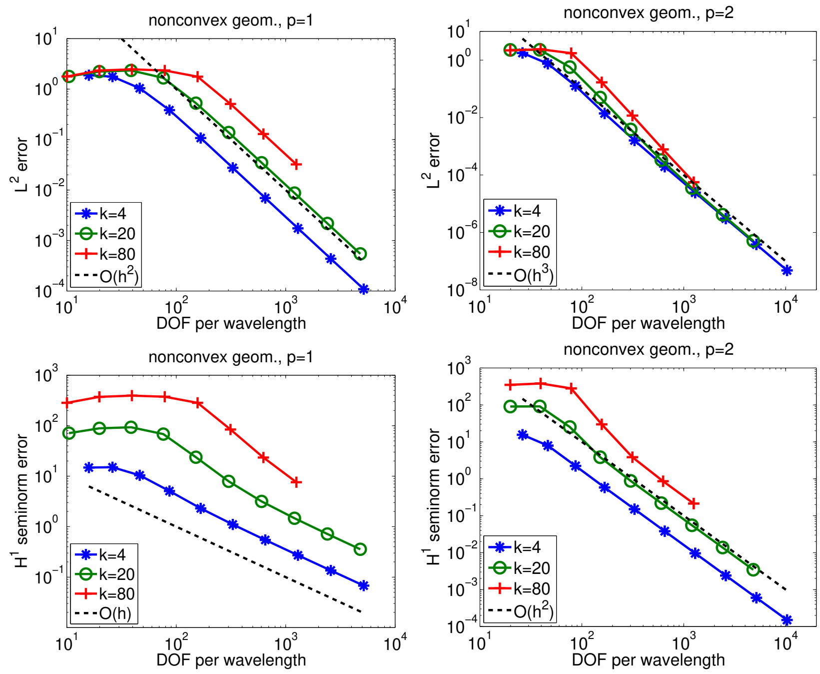

Figure 10: (cf. Example 5.4) h-FEM with $p = 1$ (left) and $p = 2$ (right) for nonconvex domain. Top: L^2-error. Bottom: H^1-seminorm error.

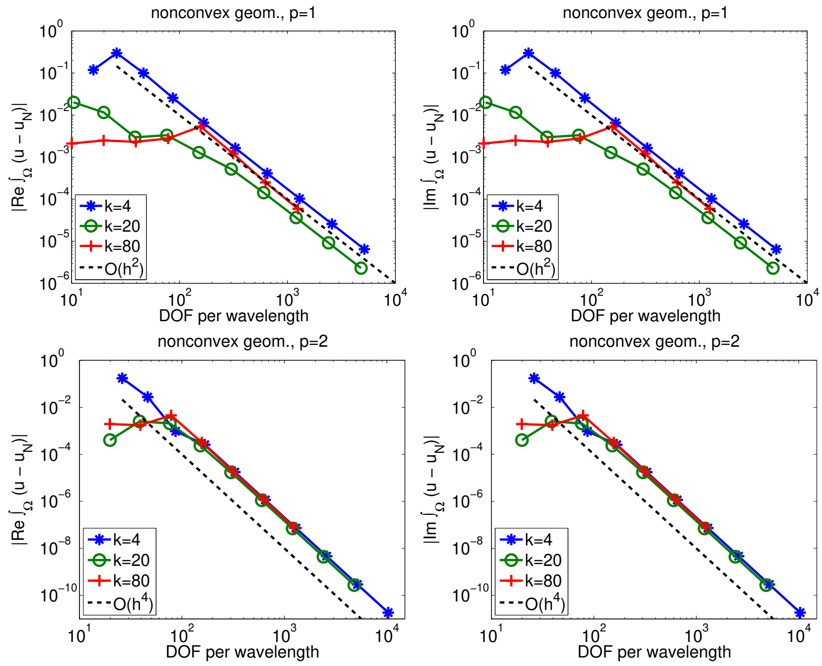

Figure 11: (cf. Example 5.4). h-FEM with $p = 1$ (top) and $p = 2$ (bottom) on nonconvex geometry. Left: $|\operatorname{Re}\int_\Omega (u - u_N)|$. Right: $|\operatorname{Im}\int_\Omega (u - u_N)|$.

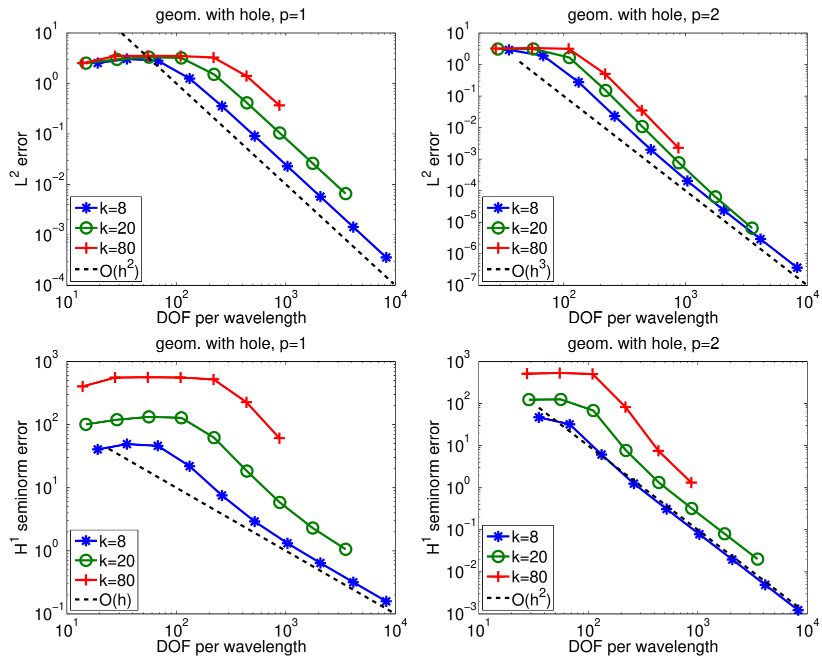

Figure 12: (cf. Example 5.5) h-FEM with $p = 1$ (left) and $p = 2$ (right) for domain with hole. Top: L^2-error. Bottom: H^1-seminorm error.

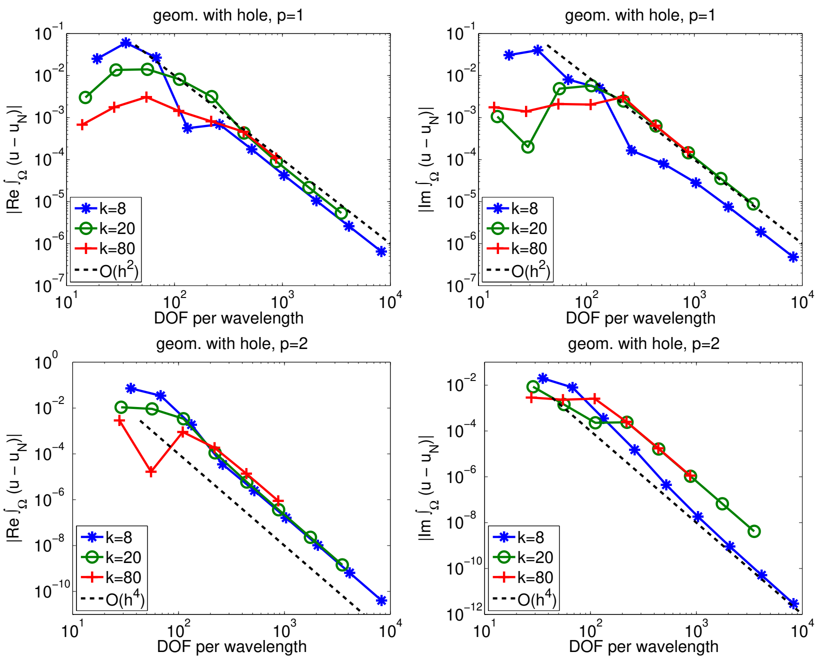

Figure 13: (cf. Example 5.5). h-FEM with $p = 1$ (top) and $p = 2$ (bottom) on geometry with hole. Left: $|\operatorname{Re}\int_\Omega (u - u_N)|$. Right: $|\operatorname{Im}\int_\Omega (u - u_N)|$.

6. The optimally blended FE-SE scheme

On regular, translation-invariant meshes, it is possible to analyze the dispersive properties of a numerical scheme with tools such as Fourier analysis and Bloch waves. Such a fine analysis is performed, for example, in [13, 14, 12, 10] in an h-FEM context and in [1, 3, 4] in a p-FEM and in a spectral element context; various DG-methods are analyzed in [2] regarding their dispersion errors. A key idea of the recent work [4] is to exploit the difference in the dispersive behavior of two different schemes in order to design a new scheme with less pollution error. Specifically, [4] proposes to use a linear combination of the Galerkin method (i.e., all bilinear forms are evaluated exactly) with the spectral element method (here: all bilinear forms are evaluated with the Gauß-Lobatto rule), giving the two terms the relative weight $1 : p$. That is, the bilinear form of the so-called "optimally blended scheme" is given by

$$B_{FE-SE}(u,v) = \frac{1}{p+1} B_{FEM}(u,v) + \left(1 - \frac{1}{p+1}\right) B_{SEM}(u,v),$$

where p is the polynomial degree employed and $B_{FEM}(\cdot,\cdot)$ and $B_{SEM}(\cdot,\cdot)$ are bilinear forms of the Galerkin method and the spectral element method respectively. On regular (infinite) grids, one can associate a discrete wavenumber $\tilde{k}$ with the numerical scheme and correspondingly measure the dispersion error by relating the discrete wavenumber $\tilde{k}$ to the exact wavenumber k. It is shown in [1, 3, 4] that

$$\left.\begin{array}{rcll} |k-\tilde{k}| &=& kO((kh)^{2p}) & \text{for the Galerkin method,} \\ |k-\tilde{k}| &=& kO((kh)^{2p}) & \text{for the spectral element method,} \\ |k-\tilde{k}| &=& kO((kh)^{2p+2}) & \text{for the optimally blended spectral element method.} \end{array}\right\} \tag{6.1}$$

6.1. Error analysis of the lowest-order optimally blended scheme

The dispersion errors given in (6.1) focus on the discrepancy between the exact wavenumber and the discrete wavenumber. In Theorem 6.1 below, we will show that these bounds for the dispersion error translate into actually error bounds. We will do this specifically for the lowest order case $p = 1$ and errors in the $L^2(I)$-norm for the 1D model problem (3.1). One motivation for us to study the lowest order case $p = 1$ and the $L^2(I)$-norm arises from the fact that, as we have seen earlier, low order Galerkin methods are particularly prone to pollution and that the k-dependence of the Galerkin method for $p = 1$ is very pronounced.

Let $V_N \subset \{v \in H^1(I) \,|\, v(0) = 0\}$ consist of the classical piecewise linear functions on a regular mesh with mesh size h. Since we will analyze the classical Galerkin method, the spectral method, and the optimally blended method, we may assume that the discretization has the following form: Find $u_h^\alpha \in V_N$ such that

$$B_h^\alpha(u_h^\alpha, v) = l(v) := \int_I f\varphi \qquad \forall \varphi \in V_N, \tag{6.2}$$

where the parameter α in the bilinear form B_h^α reflects the dispersive properties of the method studied. The analysis assumes that the stiffness matrix corresponding to the method is tridiagonal and that the regular structure of the mesh allows one to introduce the notion of a discrete wavenumber $\widetilde{k}$ and a discrete Green's function as it is done, for example, in [13, 14, 12]. The parameter α indicates the dispersion error, i.e., we assume

$$|\tilde{k} - k| = kO((hk)^{2\alpha}), \quad \alpha \geq 1. \tag{6.3}$$

This assumption covers the classical Galerkin method with $\alpha = 1$ (this case has been analyzed previously in [12, Sec. 4.6.4]), the classical lowest order spectal method (again $\alpha = 1$), and the optimally blended scheme with $\alpha = 2$. In this setting, we have the following result:

Theorem 6.1. *Let u be the exact solution of the 1D-Helmholtz problem (3.1) with $g = 0$. Let u_h^α be the piecewise linear function on a regular mesh solving (6.2). Then, for sufficiently smooth f and $kh = O(1)$ the error $u - u_h^\alpha$ can be estimated by*

$$\|u - u_h^\alpha\|_{L^2} \lesssim h^2\big(1 + k(hk)^{2(\alpha-1)}\big)C_f,$$

where C_f depends only on the data f. In particular, the Galerkin method and the lowest order spectral method (i.e., the integrals are evaluated with the trapezoidal rule) are covered with $\alpha = 1$ and the optimally blended scheme of [4] is covered, where $\alpha = 2$.

Remark 6.2. We note the marked difference between the cases $\alpha = 1$ (covering the lowest order Galerkin and spectral element method) and $\alpha \geq 2$ (which includes the optimally blended scheme). If $\alpha = 1$, then $\|u - u_h\|_{L^2} \lesssim kh^2 C_f$. Assuming that the solution behaves like $\|u\|_{L^2} \sim k^{-2}$ (as can be ascertained for smooth f using the solution formula) this leads to a relative error

$$\frac{\|u - u_h\|_{L^2}}{\|u\|_{L^2}} \lesssim k(hk)^2. \tag{6.4}$$

Thus, the FEM converges at the optimal rate as measured in relative error versus N_λ, the number of degrees of freedom per wavelength, but the constant is $O(k)$. The case $\alpha = 2$ representing the optimally blended scheme gives

$$\|u - u_h\|_{L^2} \lesssim h^2(1 + k(hk)^2)C_f.$$

Thus in this case we arrive at

$$\frac{\|u - u_h\|_{L^2}}{\|u\|_{L^2}} \lesssim (hk)^2, \tag{6.5}$$

where the constant in front of N_λ^{-2} is bounded uniformly in k. ■

The observation of Remark 6.2 is illustrated in the following numerical example.

Example 6.3. We consider (3.1) with $f = 1$ and $g = 0$. The exact solution u is given by

$$u(x) = \frac{1}{k^2}(e^{\mathbf{i}kx} - \mathbf{i}e^{\mathbf{i}k}\sin(kx) - 1). \tag{6.6}$$

The top leftmost plot in Fig. 14 shows the performance of the optimally blended scheme. The relative error in L^2 is plotted versus N_λ. We note the good agreement with the *a priori* estimate (6.5). The performance of the classical Galerkin FEM is shown in Fig. 2, which clearly shows the k-dependence predicted in (6.4). The remaining plots in Fig. 14 show the performance of the optimally blended scheme on non-uniform meshes. The mesh points of a regular mesh were randomly perturbed by n percent, where $n \in \{10, 20, 30, 40, 50\}$. Although the favorable properties of the optimally blended scheme are not proved under these circumstances, the numerical results indicate a certain robustness of the method under mesh perturbation. ■

Example 6.4. We consider (3.1) with $f = x^\alpha$ and $g = 0$. For the case $\alpha = -1/2$ we present the relative error in L^2 versus N_λ. We compare for $p = 1$ and $p = 2$ the Galerkin method with the optimally blended scheme. Fig. 15. We remark in passing that the L^2-norm of the exact solution is observed numerically to scale like $O(k^{-3/2})$. Although this examples is not covered by Theorem 6.1, the optimally blended scheme is, in particular for the lowest order case, superior to the Galerkin method. ■

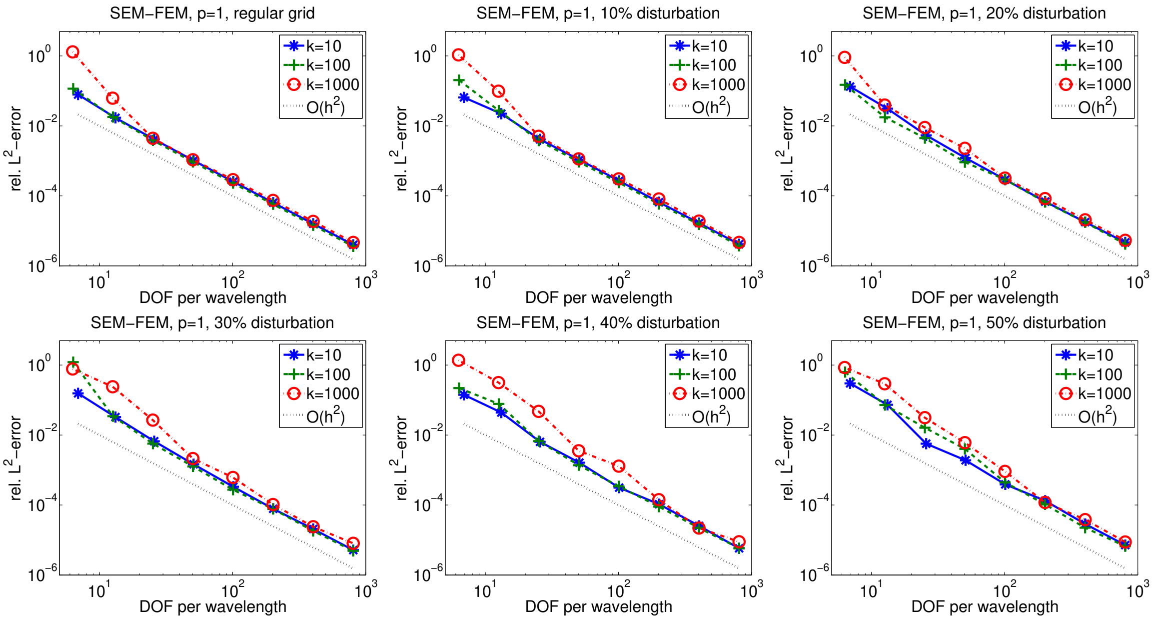

Figure 14: (cf. Example 6.3) h-method for the 1D blended SEM-FEM on uniform and randomly perturbed meshes (mesh points of regular mesh perturbed by $n\%$ for $n \in \{0, 10, 20, 30, 40, 50\}$).

6.2. Key steps of the proof of Theorem 6.1

Sketch of the proof of Theorem 6.1: As mentioned before the solution can be written in the form

$$u(x) = \int_\Omega G(x,y) f(y)\, dy,$$

where the Green's function is defined in (3.2). Likewise, as described, for example, in [12], the nodal values $u_h^\alpha(x_i)$ of the discrete solution u_h^α can be expressed by means of a discrete Green's function G_h^α in terms of the discrete wavenumber $\tilde{k}$:

$$\begin{aligned}
u_h^\alpha(x_i) &= h \sum_{j=1}^{N} G_h^\alpha(x_i, x_j) r_h(x_j), \\
G_h^\alpha(x,y) &= \frac{1}{h \sin(h\tilde{k})} \begin{cases} \sin(\tilde{k}x)\big(A \sin(\tilde{k}y) + \cos(\tilde{k}y)\big), & 0 \le x \le y \le 1 \\ \sin(\tilde{k}y)\big(A \sin(\tilde{k}x) + \cos(\tilde{k}x)\big), & 0 \le y \le x \le 1, \end{cases} \\
A &:= A(k, \tilde{k}) = \frac{(hk)^2 \sin(\tilde{k}) \cos(\tilde{k}) + \mathbf{i}\sqrt{12}\sqrt{12 - (hk)^2}}{12 - (hk)^2 \cos^2(\tilde{k})}, \\
r_h(x_j) &= h \int_\Omega f(y) \varphi_j(y) dy.
\end{aligned}$$

Here, the nodes $x_i = ih$, $i = 0, \dots, N$, represent the mesh, and the functions φ_i, $i = 0, \dots, N$ are the classical hat functions associated with the nodes x_i. In particular we see via Taylor expansion at $hk = 0$ that $A = \mathbf{i} + O(hk)^2$.

Let u_I be the piecewise linear interpolatant of the solution u. From the triangle inequality $\|u - u_h^\alpha\|_{L^2(\Omega)} \le \|u - u_I\|_{L^2(\Omega)} + \|u_I - u_h^\alpha\|_{L^2(\Omega)}$ and the standard polynomial interpolation estimate

$$\|u - u_I\|_{L^2(\Omega)} \le C h^2 \big(\|f\|_\infty + \|f'\|_\infty\big) \lesssim h^2 C_f$$

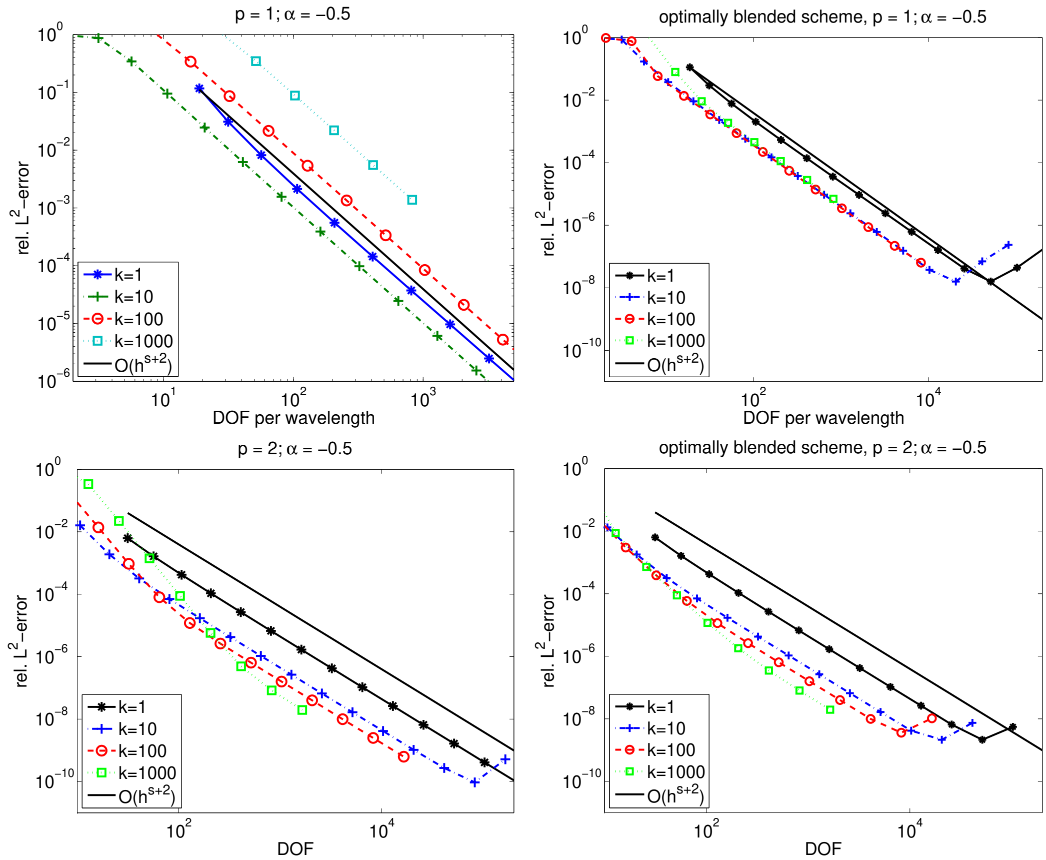

Figure 15: (cf. Example 6.4) Galerkin FEM and optimally blended scheme for non-smooth right-hand side. Top: $p = 1$ (left: Galerkin, right: optimally blended), bottom: $p = 2$ (left: Galerkin, right: optimally blended).

we see that we have to estimate

$$
\begin{aligned}
\|u_I - u_h^\alpha\|^2_{L^2(\Omega)} &= \int_\Omega |(u_I - u_h^\alpha)(x)|^2 dx \le h \sum_i |u(x_i) - u_h^\alpha(x_i)|^2 \qquad (6.7)\\
&\lesssim h \sum_i \Big| \int_\Omega G(x_i,y) f(y) dy - h \sum_j G_h^\alpha(x_i,x_j) r_h(x_j) \Big|^2 \\
&\lesssim h \sum_i \Big| \underbrace{\int_0^{x_i} G(x_i,y) f(y) dy - \Big(h \sum_{j=0}^{i-1} G_h^\alpha(x_i,x_j) r_h(x_j) + \frac{h}{2} G_h^\alpha(x_i,x_i) r_h(x_i) \Big)}_{=:A_i} + \\
&\qquad + \underbrace{\int_{x_i}^1 G(x_i,y) f(y) dy - \Big(h \sum_{j=i+1}^{N} G_h^\alpha(x_i,x_j) r_h(x_j) + \frac{h}{2} G_h^\alpha(x_i,x_i) r_h(x_i) \Big)}_{=:Bi} \Big|^2.
\end{aligned}
$$

We are thus left with bounding the sums $\sum_i |A_i|^2$ and $\sum_i |B_i|^2$. This is achieved using integration by parts and summation by parts, thereby exploiting regularity of the right-hand side f. Here, we give merely some key steps and refer to Appendix A for more details.

We will need the following observation:

Lemma 6.5. *With the abbreviation $x_{j+1/2} = (j+1/2)h$, we have*

$$
\begin{aligned}
r_h(0) &= 0, \\
r_h(x_N) &= \frac{h^2}{2} f(x_N) - \frac{h^3}{6} f'(x_N) + O(h^4 \|f''\|_\infty), \\
r_h(j) &= h^2 f(x_j) + O(h^4 \|f''\|_\infty) \quad \textit{for } 0 < i < N, \\
r_h(x_1) - r_h(0) &= r_h(x_1), \\
r_h(x_N) - r_h(x_{N-1}) &= -\frac{h^2}{2} f(x_{N-1/2}) + f'(x_{N-1/2}) \frac{7h^3}{12} + O(h^4 \|f''\|_\infty), \\
r_h(x_{j+1}) - r_h(x_j) &= h^3 f'(x_{j+1/2}) + O(h^5 \|f'''\|_\infty) \quad \textit{for } 0 < j < N-2.
\end{aligned}
$$

We abbreviate a term that arises in the definition of G_h^α:

$$
\alpha_i := A \sin(\tilde{k} x_i) + \cos(\tilde{k} x_i) = e^{\mathbf{i}\tilde{k} x_i} + (A - \mathbf{i}) \sin(\tilde{k} x_i) = e^{\mathbf{i}\tilde{k} x_i} + O((kh)^2). \qquad (6.8)
$$

We recall the summation by parts rule:

$$
\sum_{j=0}^{N} x_j y_j = y_N \sum_{j=0}^{N} x_j - \sum_{j=0}^{N-1} \sum_{l=0}^{j} x_l \big(y_{j+1} - y_j \big). \qquad (6.9)
$$

Using summation by parts, integration by parts, and properties of the right-hand side f we get (after a lengthy calculation) for the first term, A_i:

$$
\begin{aligned}
A_i &= \frac{1}{k^2} e^{\mathbf{i}k x_i} f(0) - \frac{\tilde{\alpha}_i h^2}{4 \sin^2(\frac{h\tilde{k}}{2})} \big(f(0) + O(h^2 \|f''\|_\infty) \big) \\
&\quad - \Big[\frac{1}{k^2} e^{\mathbf{i}k x_i} \cos(k x_i) f(x_i) - \frac{\tilde{\alpha}_i h^2}{4 \sin^2(\frac{h\tilde{k}}{2})} \cos(\tilde{k} x_i) \big(f(x_i) + O(h^2 \|f''\|_\infty) \big) \Big] \\
&\quad + \frac{1}{k^2} e^{\mathbf{i}k x_i} \int_0^{x_i} \cos(ky) f'(y) dy - \frac{\tilde{\alpha}_i h^3}{2 \sin(h\tilde{k}) \sin(\frac{h\tilde{k}}{2})} \sum_{j=0}^{i-1} \cos(\tilde{k} x_{j+1/2}) \big(f'(x_{j+1/2}) + O(h^2 \|f'''\|_\infty) \big) \\
&=: ⓐ + ⓑ + ⓒ.
\end{aligned}
$$

Inserting the definition of $\tilde{\alpha}_i$ given in (6.8) and writing the discrete wavenumber $\tilde{k}$ in the form $\tilde{k} = k(1+\varepsilon)$ with small $\varepsilon = (hk)^{2\alpha}$, we get

$$\begin{aligned}
ⓐ &= \frac{1}{k^2} e^{\mathbf{i}kx_i} f(0) - \frac{h^2}{4\sin(\frac{h\tilde{k}}{2})^2}\big(e^{\mathbf{i}\tilde{k}x_i} + O(hk)^2\big)\big(f(0) + O(h^2\|f''\|_\infty)\big) \\
&= \frac{1}{k^2} e^{\mathbf{i}kx_i}\Big(1 - \frac{(hk)^2}{4\sin(\frac{h\tilde{k}}{2})^2} e^{\mathbf{i}(\tilde{k}-k)x_i}\Big) f(0) + O(h^2 f(0)) + O(h^2 k^{-2}\|f''\|_\infty) \\
&= O\big((h^2 + k^{-1}\varepsilon)\|f\|_\infty\big) + O(h^2 k^{-2}\|f''\|_\infty).
\end{aligned}$$

For ⓑ we get by inserting the asymptotics of $\tilde{\alpha}_i$ given in (6.8) and using $\tilde{k} - k = k\varepsilon$ for small ε:

$$\begin{aligned}
ⓑ &= -\frac{1}{k^2} e^{\mathbf{i}kx_i}\cos(kx_i) f(x_i) + \frac{h^2}{4\sin\big(\frac{h\tilde{k}}{2}\big)^2}\big(e^{\mathbf{i}\tilde{k}x_i} + O(hk)^2\big)\cos(\tilde{k}x_i)\Big[f(x_i) + O(h^2\|f''\|_\infty)\Big] \\
&= -\frac{1}{k^2} e^{\mathbf{i}kx_i}\Big(\cos(kx_i) - \frac{(hk)^2}{4\sin\big(\frac{h\tilde{k}}{2}\big)^2} e^{\mathbf{i}(\tilde{k}-k)x_i}\cos(\tilde{k}x_i)\Big) f(x_i) + O(h^2\|f\|_\infty) + O(h^2k^{-2}\|f''\|_\infty) \\
&= O\big(h^2 + k^{-1}\varepsilon)\|f\|_\infty\big) + O(h^2k^{-2}\|f''\|_\infty).
\end{aligned}$$

The treatment of the term ⓒ is more involved since is requires as a first step the discretization of the integral by the midpoint rule:

$$\frac{1}{k^2} e^{\mathbf{i}kx_i}\int_0^{x_i}\cos(ky) f'(y)\,dy = h\sum_{j=0}^{i-1}\cos(kx_{j+1/2}) f'(x_{j+1/2}) + h^2 O(k^2\|f'\|_\infty + k\|f''\|_\infty + \|f'''\|_\infty).$$

Inserting this result in the definition of ⓒ, we get after some calculations

$$ⓒ \lesssim (h^2 + k^{-1}\varepsilon)\|f'\|_\infty + h^2(k^{-1}\|f''\|_\infty + k^{-2}\|f'''\|_\infty).$$

Thus we obtain

$$|A_i| = ⓐ + ⓑ + ⓒ \lesssim \big(h^2 + k^{-1}\varepsilon\big)\big(\|f\|_\infty + \|f'\|_\infty\big) + h^2\big(k^{-1}\|f''\|_\infty + k^{-2}\|f'''\|_\infty\big).$$

For the second term we proceed similarly: Summation by parts and use of the properties stated in Lemma 6.5 yields

$$\begin{aligned}
B_i &= \Big\{\frac{1}{\mathbf{i}k^2}\sin(kx_i)e^{\mathbf{i}k} f(1) + \frac{h^2(1+e^{\mathbf{i}\tilde{k}h})}{2\sin(h\tilde{k})(1-e^{\mathbf{i}\tilde{k}h})}\sin(\tilde{k}x_i)e^{\mathbf{i}\tilde{k}} f(1)\Big\} \\
&\quad + \Big\{\frac{h^2}{4\sin^2(\frac{\tilde{k}h}{2})}\sin(\tilde{k}x_i)\cos(\tilde{k}) f(1)(A - \mathbf{i}) \\
&\quad - \frac{1}{\mathbf{i}k^2}\sin(kx_i)e^{\mathbf{i}kx_i} f(x_i) - \frac{h^2(1+e^{\mathbf{i}\tilde{k}h})}{2\sin(h\tilde{k})(1-e^{\mathbf{i}\tilde{k}h})}\sin(\tilde{k}x_i)e^{\mathbf{i}\tilde{k}x_i} f(x_i)\Big\} \\
&\quad \Big\{-\frac{h^2}{4\sin^2(\frac{\tilde{k}h}{2})}\sin(\tilde{k}x_i)\cos(\tilde{k}x_i) f(x_i)(A - \mathbf{i}) \\
&\quad -\frac{1}{\mathbf{i}k^2}\sin(kx_i)\int_{x_i}^1 e^{\mathbf{i}ky} f'(y)dy - \frac{h^2 e^{\frac{\mathbf{i}\tilde{k}h}{2}}}{\sin(h\tilde{k})(1-e^{\mathbf{i}\tilde{k}h})}\sin(\tilde{k}x_i) h\sum_{j=i}^{N-1} e^{\mathbf{i}\tilde{k}x_{j+1/2}}\big(f'(x_{j+1/2}) + O(h^2\|f'''\|_\infty)\big) \\
&\quad + \frac{h^2}{2\sin(\frac{h\tilde{k}}{2})} h\sum_{j=i}^{N-1}\cos(\tilde{k}x_{j+1/2})\big(f'(x_{j+1/2}) + O(h^2\|f'''\|_\infty)\big)(A - \mathbf{i})\Big\} \\
&=: ⓓ + ⓔ + ⓕ.
\end{aligned}$$

By similar arguments as in the case of the term A_i, one can show

$$\begin{array}{lcl} ⓓ & \lesssim & |f(1)|(h^2+k^{-1}\varepsilon), \\ ⓔ & \lesssim & (h^2+k^{-1}\varepsilon)\|f\|_\infty, \\ ⓕ & \lesssim & h^2(\|f\|_\infty+\|f'\|_\infty+h^2\|f'''\|_\infty)+(h^2+k^{-1}\varepsilon)\|f'\|_\infty+h^2(k^{-1}\|f''\|_\infty+k^{-2}\|f'''\|_\infty). \end{array}$$

This leads us again to

$$|B_i| = ⓓ + ⓔ + ⓕ \lesssim \big(h^2+k^{-1}\varepsilon\big)\big(\|f\|_\infty+\|f'\|_\infty\big)+h^2\big(k^{-1}\|f''\|_\infty+k^{-2}\|f'''\|_\infty\big),$$

and we end up with

$$\|u_I-u_h^\alpha\|_{L^2}^2 \lesssim \sqrt{h\sum_i |A_i+B_i|^2} \lesssim \big(h^2+k^{-1}\varepsilon\big)\big(\|f\|_\infty+\|f'\|_\infty\big)+h^2\big(k^{-1}\|f''\|_\infty+k^{-2}\|f'''\|_\infty\big).$$

Since we assumed $\varepsilon=(hk)^{2\alpha}, \alpha\geq 1$, we conclude for smooth f

$$\|u-u_h\|_{L^2} \lesssim \big(h^2+k^{-1}(hk)^{2\alpha}\big)C_f \lesssim h^2\big(1+k(hk)^{2(\alpha-1)}\big)C_f.$$

For more details about estimating $|A_i|$ and $|B_i|$ see Appendix A. $\square$

Acknowledgements

Financial support by the *Vienna Science and Technology Fund* (WWTF) through project No. MA09-030 is gratefully acknowledged.

References

[1] M. Ainsworth, Discrete dispersion relation for *hp*-version finite element approximation at high wave number, SIAM J. Numer. Anal. 42 (2) (2004) 553–575.

[2] M. Ainsworth, P. Monk, W. Muniz, Dispersive and dissipative properties of discontinuous Galerkin finite element methods for the second-order wave equation, J. Sci. Comput. 27 (1-3) (2006) 5–40.
URL `http://dx.doi.org/10.1007/s10915-005-9044-x`

[3] M. Ainsworth, H. A. Wajid, Dispersive and dissipative behavior of the spectral element method, SIAM J. Numer. Anal. 47 (5) (2009) 3910–3937.
URL `http://dx.doi.org/10.1137/080724976`

[4] M. Ainsworth, H. A. Wajid, Optimally blended spectral-finite element scheme for wave propagation and non-standard reduced integration, SIAM J. Numer. Anal. 48 (1) (2010) 346–371.
URL `http://dx.doi.org/10.1137/090754017`

[5] I. Babuška, J. Osborn, Eigenvalue problems, in: Handbook of Numerical Analysis, Vol. II, North Holland, 1991, pp. 641–789.

[6] A. Bayliss, C. Goldstein, E. Turkel, On accuracy conditions for the numerical computation of waves, J. Comput. Physics 59 (1985) 396–404.

[7] J. Bramble, R. Scott, Simultaneous approximation in scales of Banach spaces, Math. Comp. 32 (1978) 947–954.

[8] S. C. Brenner, L. R. Scott, The mathematical theory of finite element methods, vol. 15 of Texts in Applied Mathematics, 3rd ed., Springer, New York, 2008.
URL `http://dx.doi.org/10.1007/978-0-387-75934-0`

[9] P. Cummings, X. Feng, Sharp regularity coefficient estimates for complex-valued acoustic and elastic Helmholtz equations, Math. Models Methods Appl. Sci. 16 (1) (2006) 139–160.
URL `http://dx.doi.org/10.1142/S021820250600108X`

[10] A. Deraemaeker, I. Babuška, P. Bouillard, Dispersion and pollution of the FEM solution for the Helmholtz equation in one, two and three dimensions, Int. J. Numer. Meth. Eng. 46 (4) (1999) 471–499.

[11] S. Esterhazy, J. Melenk, On stability of discretizations of the Helmholtz equation, in: I. Graham, T. Hou, O. Lakkis, R. Scheichl (eds.), Numerical Analysis of Multiscale Problems, vol. 83 of Lecture Notes in Computational Science and Engineering, Springer Verlag, 2012, pp. 285–324, iSBN 978-3-642-22060-9.

[12] F. Ihlenburg, Finite Element Analysis of Acoustic Scattering, vol. 132 of Applied Mathematical Sciences, Springer Verlag, 1998.

[13] F. Ihlenburg, I. B. ska, Finite element solution to the Helmholtz equation with high wave number. Part I: The *h*-version of the FEM, Comput. Math. Appl. 30 (1995) 9–37.

[14] F. Ihlenburg, I. B. ska, Finite element solution to the Helmholtz equation with high wave number. Part II: The *hp*-version of the FEM, SIAM J. Numer. Anal. 34 (1997) 315–358.

[15] H. Li, H. Ma, W. Sun, Legendre Spectral Galerkin Method for Electromagnetic Scattering from Large Cavities, SIAM J. Numer. Anal. 51 (1) (2013) 353–376.
URL `http://dx.doi.org/10.1137/110833853`

[16] J. Melenk, *hp* finite element methods for singular perturbations, vol. 1796 of Lecture Notes in Mathematics, Springer Verlag, 2002.

[17] J. Melenk, A. Parsania, S. Sauter, General DG-methods for highly indefinite Helmholtz problems, J. Sci. Comp. ((in press)).

[18] J. Melenk, S. Sauter, Convergence analysis for finite element discretizations of the Helmholtz equation with Dirichlet-to-Neumann boundary conditions, Math. Comp. 79 (2010) 1871–1914.

[19] J. Melenk, S. Sauter, Wavenumber explicit convergence analysis for finite element discretizations of the Helmholtz equation, SIAM J. Numer. Anal. 49 (2011) 1210–1243.

[20] J. M. Melenk, On generalized finite element methods, Ph.D. thesis, University of Maryland, available at `http://www.math.tuwien.ac.at/~melenk/publications` (1995).

[21] J. Schöberl, Finite Element Software Netgen/NGSolve version 4.13, http://sourceforge.net/projects/ngsolve/.
URL `http://sourceforge.net/projects/ngsolve/`

[22] J. Schöberl, NETGEN - an advancing front 2d/3d-mesh generator based on abstract rules, Computing and Visualization in Science 1 (1) (1997) 41–52.

[23] J. Shen, L.-L. Wang, Analysis of a spectral-Galerkin approximation to the Helmholtz equation in exterior domains, SIAM J. Numer. Anal. 45 (5) (2007) 1954–1978.
URL `http://dx.doi.org/10.1137/060665737`

[24] L. Tartar, An introduction to Sobolev spaces and interpolation spaces, vol. 3 of Lecture Notes of the Unione Matematica Italiana, Springer, Berlin, 2007.

[25] H. Triebel, Interpolation theory, function spaces, differential operators, 2nd ed., Johann Ambrosius Barth, Heidelberg, 1995.
[26] L. Wahlbin, Local behavior in finite element methods, in: P. Ciarlet, J. Lions (eds.), Handbook of numerical Analysis. Volume II: Finite element methods (Part 1), North Holland, 1991, pp. 353–522.

A. Proof of Theorem 6.1: detailed version

As discussed in Theorem 6.1 we need to estimate the pollution error $e_{poll} = u_I - u_h^\alpha$ in the L^2-norm. This will be done in (A.20).

In particular from (6.7) we have to estimate

$$\|u_I - u_h^\alpha\|_{L^2}^2 \lesssim h \sum_i |A_i + B_i|^2$$

where

$$A_i := \int_0^{x_i} G(x_i, y) f(y) dy - \Big(h \sum_{j=0}^{i-1} G_h^\alpha(x_i, x_j) r_h(x_j) + \frac{h}{2} G_h^\alpha(x_i, x_i) r_h(x_i) \Big)$$

and

$$B_i := \int_{x_i}^1 G(x_i, y) f(y) dy - \Big(h \sum_{j=i+1}^{N} G_h^\alpha(x_i, x_j) r_h(x_j) + \frac{h}{2} G_h^\alpha(x_i, x_i) r_h(x_i) \Big)$$

Our strategy now is to estimate both terms A_i and B_i by the same expression (independent of i).

A standing assumption will be that kh (and thus $\tilde{k}h$) is small. We will also use the abbreviation

$$\begin{aligned} \tilde{\alpha}_i &:= A(k, \tilde{k}) \sin(\tilde{k} x_i) + \cos(\tilde{k} x_i) \\ A(k, \tilde{k}) &:= \frac{(hk)^2 \sin(\tilde{k}) \cos(\tilde{k}) + \mathbf{i}\sqrt{12}\sqrt{12 - (hk)^2}}{12 - (hk)^2 \cos^2(\tilde{k})} \end{aligned} \tag{A.1}$$

This readily implies for $kh \to 0$ (which also implies $\tilde{k}h \to 0$) the relation

$$\tilde{\alpha}_i = e^{\mathbf{i}\tilde{k}x_i} + (A(k, \tilde{k}) - \mathbf{i}) \sin(\tilde{k} x_i) = e^{\mathbf{i}\tilde{k}x_i} + O(kh)^2 = e^{\mathbf{i}\tilde{k}x_i}(1 + O((kh)^2)) \tag{A.2}$$

The basic mechanism to obtain additional powers of k^{-1} on the continuous level is an integration by parts. On the discrete level, this role is taken by the summation by parts formula:

$$\sum_{j=0}^{N} x_j y_j = y_N \sum_{j=0}^{N} x_j - \sum_{j=0}^{N-1} \sum_{l=0}^{j} x_l \big(y_{j+1} - y_j\big) \tag{A.3}$$

We will also require the identity

$$\sum_{l=0}^{j} \sin \tilde{k} x_l = \frac{\sin \frac{j\tilde{k}h}{2} \sin(\frac{j+1}{2}\tilde{k}h)}{\sin \frac{\tilde{k}h}{2}} = \frac{\cos \frac{\tilde{k}h}{2} - \cos(j + \frac{1}{2})\tilde{k}h}{2 \sin \frac{\tilde{k}h}{2}} \tag{A.4}$$

We start by studying the discrete right-hand side defined by

$$r_h(x_j) = h \int_\Omega f(y) \varphi_j(y) dy$$

which has the following properties:

Lemma A.1. *(i)* $r_h(0) = 0$

(ii) $r_h(x_N) = \frac{h^2}{2} f(x_N) - \frac{h^3}{6} f'(x_N) + O(h^4 \|f''\|_\infty)$

(iii) $r_h(x_j) = h^2 f(x_j) + O(h^4 \|f''\|_\infty)$, *for* $0 < i < N$

(iv) $r_h(x_1) - r_h(0) = r_h(x_1)$

(v) $r_h(x_N) - r_h(x_{N-1}) = -\frac{h^2}{2} f(x_{N-1/2}) + f'(x_{N-1/2})\frac{7h^3}{12} + O(h^4\|f''\|_\infty)$

(vi) $r_h(x_{j+1}) - r_h(x_j) = h^3 f'(x_{j+1/2}) + \frac{h^5}{8} f'''(x_{j+1/2}) + O(h^6\|f^{(4)}\|_\infty)$ *for* $0 < j < N-2$

(vii) $r_h(x_{j+1}) - r_h(x_j) = h^3 f'(x_{j+1/2}) + O(h^4\|f''\|_\infty)$

(viii) $r_h(x_{j+1}) - r_h(x_j) = h^3 f'(x_{j+1/2}) + O(h^5\|f'''\|_\infty)$

Proof. In more detail, we have due to the Dirichlet boundary conditions on the left boundary that $r_h(0) = 0$. Further we can calculate

$$\begin{aligned}
r_h(N) &= h\int_0^1 f(y)\varphi_N(y)dy = h\int_{x_{N-1}}^{x_N} f(y)\frac{y-x_{N-1}}{h}dy \\
&= \int_{x_{N-1}}^{x_N} \big(f(x_N) + f'(x_N)(y-x_N) + f''(x_N)\frac{(y-x_N)^2}{2} + O((y-x_N)^3)\big)(y-x_{N-1})dy \\
&= f(x_N)\int_{x_{N-1}}^{x_N}(y-x_{N-1})dy + f'(x_N)\int_{x_{N-1}}^{x_N}(y-x_N)(y-x_{N-1})dy \\
&\quad + f''(x_N)\int_{x_{N-1}}^{x_N}\frac{(y-x_N)^2}{2}(y-x_{N-1}) + \int_{x_{N-1}}^{x_N} O((y-x_N)^3)(y-x_{N-1})dy \\
&= f(x_N)\frac{h^2}{2} - \frac{h^3}{6}f'(x_N) + O(h^4)
\end{aligned}$$

and

$$\begin{aligned}
r_h(j) &= h\int_0^1 f(y)\varphi_i(y)dy = h\int_{x_{j-1}}^{x_j} f(y)\frac{y-x_{j-1}}{h}dy + h\int_{x_j}^{x_{j+1}} f(y)\frac{x_{i+1}-y}{h}dy \\
&= \int_{x_{j-1}}^{x_j}\big(f(x_j) + f'(x_j)(y-x_j) + f''(x_j)\frac{(y-x_j)^2}{2} + O((y-x_j)^3)\big)(y-x_{j-1})dy \\
&\quad + \int_{x_j}^{x_{j+1}}\big(f(x_j) + f'(x_j)(y-x_j) + f''(x_j)\frac{(y-x_j)^2}{2} + O((y-x_j)^3)\big)(x_{j+1}-y)dy \\
&= f(x_j)\Big(\int_{x_{j-1}}^{x_j}(y-x_{j-1})dy + \int_{x_j}^{x_{j+1}}(x_{j+1}-y)dy\Big) \\
&\quad + f'(x_j)\Big(\int_{x_{j-1}}^{x_j}(y-x_j)(y-x_{j-1})dy + \int_{x_j}^{x_{j+1}}(y-x_j)(x_{j+1}-y)dy\Big) \\
&\quad + f''(x_j)/2\Big(\int_{x_{j-1}}^{x_j}(y-x_j)^2(y-x_{j-1})dy + \int_{x_j}^{x_{j+1}}(y-x_j)^2(x_{j+1}-y)dy\Big) + \dots \\
&= f(x_j)h^2 + O(h^4),
\end{aligned}$$

for $0 < i < N$. Property (iv) follows obviously from (i). Next,

$$\begin{aligned}
&r_h(x_N) - r_h(x_{N-1}) = \\
&= h\int_0^1 f(y)\varphi_N(y)dy - h\int_0^1 f(y)\varphi_{N-1}(y)dy \\
&= -h\int_{x_{N-2}}^{x_{N-1}} f(y)\varphi_{N-1}(y)dy + h\int_{x_{N-1}}^{x_N} f(y)\big(\varphi_N(y) - \varphi_{N-1}(y)\big)dy \\
&= -\int_{x_{N-2}}^{x_{N-1}}\big(f(x_{N-1/2}) + f'(x_{N-1/2})(y-x_{N-1/2}) + O((y-x_{N-1/2})^2)\big)(y-x_{N-2})dy
\end{aligned}$$

$$
\begin{aligned}
& +\int_{x_{N-1}}^{x_N} \big(f(x_{N-1/2})+f'(x_{N-1/2})(y-x_{N-1/2})+O((y-x_{N-1/2})^2)\big)(2y-(x_N+x_{N-1}))dy \\
= \;& f(x_{N-1/2})\Big(-\int_{x_{N-2}}^{x_{N-1}}(y-x_{N-2})dy+\int_{x_{N-1}}^{x_N}(2y-(x_N+x_{N-1}))dy\Big) \\
& +f'(x_{N-1/2})\Big(-\int_{x_{N-2}}^{x_{N-1}}(y-x_{N-1/2})(y-x_{N-2})dy+\int_{x_{N-1}}^{x_N}(y-x_{N-1/2})(2y-(x_N+x_{N-1}))dy\Big) \\
& +\Big(\int_{x_{N-2}}^{x_{N-1}} O((y-x_{N-1/2})^2)(y-x_{N-2})dy+\int_{x_{N-1}}^{x_N} O((y-x_{N-1/2})^2)(2y-(x_N+x_{N-1}))dy\Big) \\
= \;& -f(x_{N-1/2})\frac{h^2}{2}+f'(x_{N-1/2})\frac{7h^3}{12}+O(h^4).
\end{aligned}
$$

Finally

$$
\begin{aligned}
r_h(x_{j+1})-r_h(x_j) \;&=\; h\int_0^1 f(y)\varphi_{j+1}(y)dy-h\int_0^1 f(y)\varphi_j(y)dy=h\int_0^1 f(y)\left(\varphi_{j+1}(y)-\varphi_j(y)\right)dy \\
&=\; h\int_0^1 \Big(f(x_{j+1/2})+f'(x_{j+1/2})(y-x_{j+1/2})+f''(x_{j+1/2})\;\frac{(y-x_{j+1/2})^2}{2} \\
&\qquad +f'''(x_{j+1/2})\;\frac{(y-x_{j+1/2})^3}{6}+O((y-x_{j+1/2})^4)\Big)\big(\varphi_{j+1}(y)-\varphi_j(y)\big)dy \\
&=\; hf(x_{j+1/2})\int_0^1 \varphi_{j+1}(y)-\varphi_j(y)dy \\
&\quad +hf'(x_{j+1/2})\int_0^1 (y-x_{j+1/2})(\varphi_{j+1}(y)-\varphi_j(y))dy \\
&\quad +hf''(x_{j+1/2})\int_0^1 \frac{(y-x_{j+1/2})^2}{2}(\varphi_{j+1}(y)-\varphi_j(y))dy \\
&\quad +hf'''(x_{j+1/2})\int_0^1 \frac{(y-x_{j+1/2})^3}{6}(\varphi_{j+1}(y)-\varphi_j(y))dy \\
&\quad +h\int_0^1 O((y-x_{j+1/2})^4)(\varphi_{j+1}(y)-\varphi_j(y))dy \\
&=\; h^3f'(x_{j+1/2})+\frac{h^5}{8}f'''(x_{j+1/2})+h\int_0^1 O((y-x_{j+1/2})^4)(\varphi_{j+1}(y)-\varphi_j(y))dy \\
&=\; h^3f'(x_{j+1/2})+\frac{h^5}{8}f'''(x_{j+1/2})+O(h^6)
\end{aligned}
$$

for $0<j<N-2$. □

A.1. The term A_i

In order to estimate the term A_i, we will need the following result:

Lemma A.2.

$$
\begin{aligned}
&\sum_{j=0}^{i-1}\sin(\tilde{k}x_j)r_h(x_j)+\frac{1}{2}\sin(\tilde{k}x_i)r_h(x_i)= \\
&= \frac{h^2\cos(\frac{h\tilde{k}}{2})}{2\sin(\frac{h\tilde{k}}{2})}\big[f(0)+\cos(\tilde{k}x_i)f(x_i)+O(h^2\|f''\|_\infty)\big]+\frac{h^2}{2\sin(\frac{h\tilde{k}}{2})}\sum_{j=0}^{i-1}\cos(\tilde{k}x_{j+1/2})\big(hf'(x_{j+1/2})+O(h^3\|f'''\|_\infty)\big)
\end{aligned}
$$

Proof. The essential ingredient of the proof is a summation by parts given by (A.3). Together with (A.4) we get

$$\sum_{j=0}^{i-1}\sin(\tilde{k}x_j)r_h(x_j)+\frac{1}{2}\sin(\tilde{k}x_i)r_h(x_i)=$$

$$\begin{aligned}
&= \left(\sum_{j=0}^{i-1}\sin(\tilde{k}x_j)\right)r_h(x_{i-1})-\sum_{j=0}^{i-2}\left(\sum_{l=0}^{j}\sin(\tilde{k}x_l)\right)\big(r_h(x_{j+1})-r_h(x_j)\big)+\frac{1}{2}\sin(\tilde{k}x_i)r_h(x_i)\\
&= \frac{1}{2\sin(\frac{h\tilde{k}}{2})}\big(\cos(\frac{h\tilde{k}}{2})-\cos(\tilde{k}x_i-\frac{h\tilde{k}}{2})\big)r_h(x_{i-1})\\
&\quad -\frac{1}{2\sin(\frac{h\tilde{k}}{2})}\sum_{j=0}^{i-2}\big(\cos(\frac{h\tilde{k}}{2})-\cos(\tilde{k}x_j+\frac{h\tilde{k}}{2})\big)\big(r_h(x_{j+1})-r_h(x_j)\big)+\frac{1}{2}\sin(\tilde{k}x_i)r_h(x_i)\\
&= \frac{1}{2\sin(\frac{h\tilde{k}}{2})}\Big[\big(\cos(\frac{h\tilde{k}}{2})-\cos(\tilde{k}x_i-\frac{h\tilde{k}}{2})\big)r_h(x_{i-1})-\cos(\frac{h\tilde{k}}{2})\sum_{j=0}^{i-2}\big(r_h(x_{j+1})-r_h(x_j)\big)\\
&\quad +\sum_{j=0}^{i-2}\cos(\tilde{k}x_j+\frac{h\tilde{k}}{2})\big(r_h(x_{j+1})-r_h(x_j)\big)+\sin(\frac{h\tilde{k}}{2})\sin(\tilde{k}x_i)r_h(x_i)\Big]\\
&= \frac{1}{2\sin(\frac{h\tilde{k}}{2})}\Big[\big(\cos(\frac{h\tilde{k}}{2})-\cos(\tilde{k}x_i-\frac{h\tilde{k}}{2})\big)r_h(x_{i-1})-\cos(\frac{h\tilde{k}}{2})\big(r_h(x_{i-1})-r_h(0)\big)\\
&\quad +\sum_{j=1}^{i-1}\cos(\tilde{k}x_j+\frac{h\tilde{k}}{2})\big(r_h(x_{j+1})-r_h(x_j)\big)-\cos(\tilde{k}x_i-\frac{h\tilde{k}}{2})\big(r_h(x_i)-r_h(x_{i-1})\big)\\
&\quad +\cos(\frac{h\tilde{k}}{2})\big(r_h(x_1)-r_h(0)+\sin(\frac{h\tilde{k}}{2})\sin(\tilde{k}x_i)r_h(x_i)\Big]\\
&= \frac{\cos(\frac{h\tilde{k}}{2})}{2\sin(\frac{h\tilde{k}}{2})}r_h(x_1)+\frac{\cos(\frac{h\tilde{k}}{2})}{2\sin(\frac{h\tilde{k}}{2})}\cos(\tilde{k}x_i)r_h(x_i)+\frac{1}{2\sin(\frac{h\tilde{k}}{2})}\sum_{j=1}^{i-1}\cos(\tilde{k}x_j+\frac{h\tilde{k}}{2})\big(r_h(x_{j+1})-r_h(x_j)\big)
\end{aligned}$$

Then, after applying the properties of the discrete right-hand side given in Lemma A.1, we get

$$\sum_{j=0}^{i-1}\sin(\tilde{k}x_j)r_h(x_j)+\frac{1}{2}\sin(\tilde{k}x_i)r_h(x_i)=$$

$$\begin{aligned}
&= \frac{h^2\cos(\frac{h\tilde{k}}{2})}{2\sin(\frac{h\tilde{k}}{2})}\big(f(x_1)+O(h^2\|f''\|_\infty)\big)+\frac{h^2\cos(\frac{h\tilde{k}}{2})}{2\sin(\frac{h\tilde{k}}{2})}\cos(\tilde{k}x_i)\big(f(x_i)+O(h^2\|f''\|_\infty)\big)\\
&\quad +\frac{1}{2\sin(\frac{h\tilde{k}}{2})}\sum_{j=1}^{i-1}\cos(\tilde{k}x_j+\frac{h\tilde{k}}{2})\big(h^3f'(x_{j+1/2})+O(h^5\|f'''\|_\infty)\big)\\
&= \frac{h^2\cos(\frac{h\tilde{k}}{2})}{2\sin(\frac{h\tilde{k}}{2})}\big(f(x_1)+O(h^2\|f''\|_\infty)-hf'(x_{1/2})+O(h^3\|f'''\|_\infty)\big)+\frac{h^2\cos(\frac{h\tilde{k}}{2})}{2\sin(\frac{h\tilde{k}}{2})}\cos(\tilde{k}x_i)\big(f(x_i)+O(h^2\|f''\|_\infty)\big)\\
&\quad +\frac{h^2}{2\sin(\frac{h\tilde{k}}{2})}\sum_{j=0}^{i-1}\cos(\tilde{k}x_j+\frac{h\tilde{k}}{2})\big(hf'(x_{j+1/2})+O(h^3\|f'''\|_\infty)\big)\\
&= \frac{h^2\cos(\frac{h\tilde{k}}{2})}{2\sin(\frac{h\tilde{k}}{2})}\big(f(0)+hf'(0)+O(h^2\|f''\|_\infty)-h(f'(0)+\frac{h}{2}f''(0)+O(h^2\|f'''\|_\infty)\big)
\end{aligned}$$

$$
\begin{aligned}
& +\frac{h^2\cos(\frac{h\tilde{k}}{2})}{2\sin(\frac{h\tilde{k}}{2})}\cos(\tilde{k}x_i)\big(f(x_i)+O(h^2\|f''\|_\infty)\big) \\
& +\frac{h^2}{2\sin(\frac{h\tilde{k}}{2})}\sum_{j=0}^{i-1}\cos(\tilde{k}x_j+\frac{h\tilde{k}}{2})\big(hf'(x_{j+1/2})+O(h^3\|f'''\|_\infty)\big) \\
= \quad & \frac{h^2\cos(\frac{h\tilde{k}}{2})}{2\sin(\frac{h\tilde{k}}{2})}\big(f(0)+O(h^2\|f''\|_\infty)\big)+\frac{h^2\cos(\frac{h\tilde{k}}{2})}{2\sin(\frac{h\tilde{k}}{2})}\cos(\tilde{k}x_i)\big(f(x_i)+O(h^2\|f''\|_\infty)\big) \\
& +\frac{h^2}{2\sin(\frac{h\tilde{k}}{2})}\sum_{j=0}^{i-1}\cos(\tilde{k}x_j+\frac{h\tilde{k}}{2})\big(hf'(x_{j+1/2})+O(h^3\|f'''\|_\infty)\big)
\end{aligned}
$$

□

Using Lemma A.2, we obtain with the definition of $\tilde{\alpha}_i$ in (A.1):

$$
\begin{aligned}
A_i := & \int_0^{x_i} G(x_i,y)f(y)dy-\Big(h\sum_{j=0}^{i-1}G_h^\alpha(x_i,x_j)r_h(x_j)+\frac{1}{2}hG_h^\alpha(x_i,x_i)r_h(x_i)\Big) \\
= & \frac{1}{k}e^{\mathbf{i}kx_i}\int_0^{x_i}\sin(ky)f(y)dy \\
& -\Big(h\frac{1}{h\sin(h\tilde{k})}\tilde{\alpha}_i\sum_{j=0}^{i-1}\sin(\tilde{k}x_j)r_h(x_j)+\frac{h}{2h\sin(h\tilde{k})}\tilde{\alpha}_i\sin(\tilde{k}x_i)r_h(x_i)\Big) \\
= & \frac{1}{k}e^{\mathbf{i}kx_i}\Big[-\frac{1}{k}\cos(ky)f(y)\Big|_0^{x_i}+\frac{1}{k}\int_0^{x_i}\cos(ky)f'(y)dy\Big] \\
& -\frac{\tilde{\alpha}_i}{\sin(h\tilde{k})}\Big[\sum_{j=0}^{i-1}\sin(\tilde{k}x_j)r_h(x_j)+\frac{1}{2}\sin(\tilde{k}x_i)r_h(x_i)\Big] \\
= & \frac{1}{k^2}e^{\mathbf{i}kx_i}\Big[f(0)-\cos(kx_i)f(x_i)+\int_0^{x_i}\cos(ky)f'(y)dy\Big] \\
& -\frac{\tilde{\alpha}_i}{\sin(h\tilde{k})}\Big[\frac{h^2\cos(\frac{h\tilde{k}}{2})}{2\sin(\frac{h\tilde{k}}{2})}\{f(0)+\cos(\tilde{k}x_i)f(x_i)+O(h^2\|f''\|_\infty)\}+ \\
& \frac{h^2}{2\sin(\frac{h\tilde{k}}{2})}\sum_{j=0}^{i-1}\cos(\tilde{k}x_{j+1/2})\{hf'(x_{j+1/2})+O(h^3\|f'''\|_\infty)\}\Big] \\
= & \left\{\frac{1}{k^2}e^{\mathbf{i}kx_i}f(0)-\frac{h^2}{4\sin^2(\frac{h\tilde{k}}{2})}\tilde{\alpha}_i\big(f(0)+O(h^2\|f''\|_\infty)\big)\right\} \qquad ⓐ \\
& \left\{-\Big[\frac{1}{k^2}e^{\mathbf{i}kx_i}\cos(kx_i)f(x_i)-\frac{h^2}{4\sin^2(\frac{h\tilde{k}}{2})}\tilde{\alpha}_i\cos(\tilde{k}x_i)\big(f(x_i)+O(h^2\|f''\|_\infty)\big)\Big]\right\} \qquad ⓑ \\
& \left\{+\frac{1}{k^2}e^{\mathbf{i}kx_i}\int_0^{x_i}\cos(ky)f'(y)dy-\frac{h^2}{2\sin(h\tilde{k})\sin(\frac{h\tilde{k}}{2})}\tilde{\alpha}_ih\sum_{j=0}^{i-1}\cos(\tilde{k}x_j+\frac{h\tilde{k}}{2})\big(f'(x_{j+1/2})+O(h^2\|f'''\|_\infty)\big)\right\} ⓒ
\end{aligned}
$$

Next, we aim to estimate each of the terms ⓐ, ⓑ, and ⓒ. Therefore we will need the following estimates:

Lemma A.3. *As $kh \to 0$ (and thus $\varepsilon \to 0$) we have (uniformly in x_i, x_j, x, $y \in [0,1]$)*

$$\frac{1}{k^2}\left|e^{\mathbf{i}kx_i} - \frac{(kh)^2}{4\sin^2(\frac{h\tilde{k}}{2})}\tilde{\alpha}_i\right| = O(h^2) + O(k^{-1}\varepsilon) \tag{A.5}$$

$$\frac{1}{k^2}\left|e^{\mathbf{i}kx_i}\cos(kx_j) - \frac{(kh)^2}{4\sin^2(\frac{h\tilde{k}}{2})}\tilde{\alpha}_i\cos(\tilde{k}x_j)\right| = O(h^2) + O(k^{-1}\varepsilon) \tag{A.6}$$

$$e^{\mathbf{i}\tilde{k}x} - e^{\mathbf{i}kx} = O(k\varepsilon) \tag{A.7}$$

$$e^{\mathbf{i}\tilde{k}x}\cos(\tilde{k}y) - e^{\mathbf{i}kx}\cos(ky) = O(k\varepsilon) \tag{A.8}$$

$$\frac{(hk)^2}{4\sin^2(\frac{h\tilde{k}}{2})}e^{\mathbf{i}(\tilde{k}-k)x_i} = (1 + O((kh)^2) + O(\varepsilon))(1 + O(k\varepsilon)). \tag{A.9}$$

Proof. We start with the proof of (A.7):

$$e^{\mathbf{i}\tilde{k}x} - e^{\mathbf{i}kx} = e^{\mathbf{i}kx}\left(e^{\mathbf{i}(\tilde{k}-k)x} - 1\right) = e^{\mathbf{i}kx}\left(e^{\mathbf{i}k\varepsilon x} - 1\right) = O(k\varepsilon), \qquad \forall \varepsilon \to 0. \tag{A.10}$$

(If $k\varepsilon$ is small, then the statement is shown by Taylor expansion; if $k\varepsilon$ is *not* small, then $e^{\mathbf{i}k\varepsilon x} - 1$ is $O(1)$ since k, ε, x are real).

Next, we observe that (A.10) implies

$$\cos(kx) - \cos(\tilde{k}x) = \frac{1}{2}\left(e^{\mathbf{i}kx} - e^{\mathbf{i}\tilde{k}x} + e^{-\mathbf{i}kx} - e^{\mathbf{i}\tilde{k}x}\right) = O(k\varepsilon). \tag{A.11}$$

The bounds (A.8) is shown similarly using (A.7), (A.11):

$$\begin{aligned}
e^{\mathbf{i}\tilde{k}x}\cos(ky) - e^{\mathbf{i}\tilde{k}x}\cos(\tilde{k}y) &= e^{\mathbf{i}\tilde{k}x}\left[\cos(ky) - e^{\mathbf{i}(\tilde{k}-k)x}\left(\cos(\tilde{k}y) - \cos(ky) + \cos(ky)\right)\right] \\
&= e^{\mathbf{i}\tilde{k}x}\left[\cos(ky) - (1 + O(k\varepsilon))(\cos(ky) + O(k\varepsilon))\right] \\
&= O(k\varepsilon).
\end{aligned}$$

(Here, we ignore the term $O(k^2\varepsilon^2)$ that would formally arise since if $k\varepsilon = O(1)$, then the left-hand side is also $O(1)$).

Next, we show (A.9):

$$\begin{aligned}
\frac{(hk)^2}{4\sin^2(\frac{h\tilde{k}}{2})}e^{\mathbf{i}(\tilde{k}-k)x_i} &= \left(\frac{k}{\tilde{k}}\right)^2\frac{(h\tilde{k})^2}{4\sin^2(\frac{h\tilde{k}}{2})}e^{\mathbf{i}(\tilde{k}-k)x_i} = \left(\frac{1}{1+\varepsilon}\right)^2\frac{(h\tilde{k})^2}{4\sin^2(\frac{h\tilde{k}}{2})}e^{\mathbf{i}\varepsilon kx_i} \\
&= (1 + O(\varepsilon))\left(1 + O(h\tilde{k})^2\right)(1 + O(k\varepsilon)) \\
&= \left(1 + O((kh)^2) + O(\varepsilon)\right)(1 + O(k\varepsilon)).
\end{aligned}$$

Turning to the proof of (A.5), we get in view of (A.1) and (A.9) that (as $kh \to 0$)

$$\begin{aligned}
\left|\frac{1}{k^2}e^{\mathbf{i}kx_i} - \frac{(kh)^2}{4\sin^2(\frac{h\tilde{k}}{2})}\tilde{\alpha}_i\right| &= \frac{1}{k^2}\left|1 - \frac{(hk)^2}{4\sin^2(\frac{h\tilde{k}}{2})}e^{\mathbf{i}(\tilde{k}-k)x_i}(1 + O(kh)^2)\right| \\
&= \frac{1}{k^2}\left|1 - \frac{(hk)^2}{4\sin^2(\frac{h\tilde{k}}{2})}e^{\mathbf{i}(\tilde{k}-k)x_i}\right| + O(h^2) \\
&= k^{-2}\left\{O((kh)^2) + O(\varepsilon) + (1 + O((kh)^2) + O(\varepsilon))O(k\varepsilon)\right\} + k^2O(\varepsilon^2)\Big\} + O(h^2) \\
&= k^{-2}\left\{O((kh)^2) + O(k\varepsilon)\right\} + O(h^2) = O(h^2) + O(k^{-1}\varepsilon)
\end{aligned}$$

We finally show (A.6):

$$\frac{1}{k^2}\left|e^{\mathbf{i}kx_i}\cos(kx_j) - \frac{(kh)^2}{4\sin^2(\frac{h\tilde{k}}{2})}\tilde{\alpha}_i\cos(\tilde{k}x_j)\right| = \frac{1}{k^2}\left|e^{\mathbf{i}kx_i}\cos(kx_j) - \frac{(kh)^2}{4\sin^2(\frac{h\tilde{k}}{2})}(e^{\mathbf{i}\tilde{k}x_j} + O(kh)^2)\cos(\tilde{k}x_j)\right|$$
$$= \frac{1}{k^2}\left|e^{\mathbf{i}kx_i}\cos(kx_j) - \frac{(kh)^2}{4\sin^2(\frac{h\tilde{k}}{2})}e^{\mathbf{i}\tilde{k}x_j}\cos(\tilde{k}x_j)\right| + O(h^2)$$
$$= O(h^2) + O(k^{-1}\varepsilon).$$

□

With these estimates, we can analyze ⓐ, ⓑ, ⓒ. From (A.5) we get

$$\begin{aligned}
a &:= \frac{1}{k^2}e^{\mathbf{i}kx_i}f(0) - \frac{h^2}{4\sin(\frac{h\tilde{k}}{2})^2}\tilde{\alpha}_i\big(f(0) + O(h^2\|f''\|_\infty)\big) \\
&= \frac{1}{k^2}\left(e^{\mathbf{i}kx_i} - \frac{(kh)^2}{4\sin(\frac{h\tilde{k}}{2})^2}\tilde{\alpha}_i\right)f(0) + \frac{1}{k^2}\frac{(kh)^2}{4\sin^2(h\tilde{k}/2)}O(h^2\|f''\|_\infty) \\
&\lesssim (h^2 + k^{-1}\varepsilon)\|f\|_\infty + h^2k^{-2}\|f''\|_\infty.
\end{aligned}$$

Similarly we get with (A.6):

$$\begin{aligned}
b &:= -\frac{1}{k^2}e^{\mathbf{i}kx_i}\cos(kx_i)f(x_i) + \frac{h^2}{4\sin\left(\frac{h\tilde{k}}{2}\right)^2}\tilde{\alpha}_i\cos(\tilde{k}x_i)\Big[f(x_i) + O(h^2\|f''\|_\infty)\Big] \\
&= \left[-\frac{1}{k^2}e^{\mathbf{i}kx_i}\cos(kx_i) + \frac{h^2}{4\sin\left(\frac{h\tilde{k}}{2}\right)^2}\tilde{\alpha}_i\cos(\tilde{k}x_i)\right]f(x_i) + O(k^{-2}h^2\|f''\|_\infty) \\
&\lesssim (h^2 + k^{-1}\varepsilon)\|f\|_\infty + k^{-2}h^2\|f''\|_\infty.
\end{aligned}$$

For the third term, ⓒ, we start with the observation

$$\frac{1}{2\sin(h\tilde{k})\sin(\frac{h\tilde{k}}{2})} = \frac{1}{4\sin^2(\frac{h\tilde{k}}{2})}\frac{1}{\cos(\frac{h\tilde{k}}{2})} = \frac{1}{4\sin^2(\frac{h\tilde{k}}{2})}(1 + O(kh)^2), \qquad kh \to 0. \tag{A.12}$$

For the term ⓒ, we discretize the integral by the midpoint rule to get

$$\frac{1}{k^2}e^{\mathbf{i}kx_i}\int_0^{x_i}\cos(ky)f'(y)\,dy = \frac{1}{k^2}e^{\mathbf{i}kx_i}h\sum_{j=0}^{i-1}\cos(kx_{j+1/2})f'(x_{j+1/2}) + k^{-2}h^2O(k^2\|f'\|_\infty + k\|f''\|_\infty + \|f'''\|_\infty) \tag{A.13}$$

Using (A.12) and (A.13), (A.6) we get for the third term ⓒ:

$$\begin{aligned}
c &:= \frac{1}{k^2}e^{\mathbf{i}kx_i}\int_0^{x_i}\cos(ky)f'(y)dy - \Big(\frac{1}{2\sin(h\tilde{k})\sin(\frac{h\tilde{k}}{2})}\tilde{\alpha}_i\sum_{j=0}^{i-1}\cos(\tilde{k}x_{j+1/2})\big(h^3f'(x_{j+1/2}) + O(\frac{h^5}{8}\|f'''\|_\infty)\Big) \\
&= \frac{1}{k^2}e^{\mathbf{i}kx_i}h\sum_{j=0}^{i-1}\cos(kx_{j+1/2})f'(x_{j+1/2}) \quad + h^2O(\|f'\|_\infty + k^{-1}\|f''\|_\infty + k^{-2}\|f'''\|_\infty) \\
&\quad - \frac{h^2}{2\sin(h\tilde{k})\sin(\frac{h\tilde{k}}{2})}\tilde{\alpha}_ih\sum_{j=0}^{i-1}\cos(\tilde{k}x_{j+1/2})\big(f'(x_{j+1/2}) + O(\frac{h^2}{8}\|f'''\|_\infty)\big)) \\
&= \frac{1}{k^2}e^{\mathbf{i}kx_i}h\sum_{j=0}^{i-1}\cos(kx_{j+1/2})f'(x_{j+1/2}) - \frac{h^2}{2\sin(h\tilde{k})\sin(\frac{h\tilde{k}}{2})}\tilde{\alpha}_ih\sum_{j=0}^{i-1}\cos(\tilde{k}x_{j+1/2})f'(x_{j+1/2})
\end{aligned}$$

$$
\begin{aligned}
&+ h^2 O(\|f'\|_\infty + k^{-1}\|f''\|_\infty + k^{-2}\|f'''\|_\infty) \\
&= h\sum_{j=0}^{i-1}\Big[\frac{1}{k^2}e^{\mathbf{i}kx_i}\cos(kx_{j+1/2}) - \frac{h^2}{4\sin^2(\frac{h\tilde{k}}{2})}(1+O(kh)^2)\tilde{\alpha}_i\cos(\tilde{k}x_{j+1/2})\Big]f'(x_{j+1/2}) \\
&\quad + h^2 O(\|f'\|_\infty + k^{-1}\|f''\|_\infty + k^{-2}\|f'''\|_\infty) \\
&\lesssim (h^2 + k^{-1}\varepsilon)\|f'\|_\infty + h^2k^{-1}\|f''\|_\infty + h^2k^{-2}\|f'''\|_\infty
\end{aligned}
$$

This leads us to

$$
A_i = ⓐ + ⓑ + ⓒ \lesssim \big(h^2 + k^{-1}\varepsilon\big)\big(\|f\|_\infty + \|f'\|_\infty\big) + k^{-1}h^2\|f''\|_\infty + k^{-2}h^2\|f'''\|_\infty\big) \tag{A.14}
$$

A.2. The term B_i

For the second term B_i we will need

Lemma A.4. *For $kh \to 0$ (and thus $\tilde{k}h \to 0$) we have*

$$
\begin{aligned}
\sum_{j=i+1}^{N} e^{\mathbf{i}\tilde{k}x_j}r_h(x_j) + \frac{1}{2}e^{\mathbf{i}\tilde{k}x_i}r_h(x_i) = &-\frac{h^2(1+e^{\mathbf{i}\tilde{k}h})}{2(1-e^{\mathbf{i}\tilde{k}h})}e^{\mathbf{i}\tilde{k}}\big(f(1) + O(h^2\|f''\|_\infty)\big) \\
&+ \frac{h^2(1+e^{\mathbf{i}\tilde{k}h})}{2(1-e^{\mathbf{i}\tilde{k}h})}e^{\mathbf{i}\tilde{k}x_i}\big(f(x_i) + O(h^2\|f''\|_\infty)\big) \\
&+ \frac{h^2 e^{\frac{i\tilde{k}h}{2}}}{(1-e^{\mathbf{i}\tilde{k}h})}h\sum_{j=i}^{N-1} e^{\mathbf{i}\tilde{k}x_{j+1/2}}\big(f'(x_{j+1/2}) + O(h^2\|f'''\|_\infty)\big)
\end{aligned}
$$

$$
\begin{aligned}
\sum_{j=i+1}^{N}\sin(\tilde{k}x_j)r_h(x_j) + \frac{1}{2}\sin(\tilde{k}x_i)r_h(x_i) = &-\frac{h^2\cos(\frac{h\tilde{k}}{2})}{2\sin(\frac{h\tilde{k}}{2})}\cos(\tilde{k}x_N)f(1) + O(h^3\|f'\|_\infty + \tilde{k}^{-1}h^3\|f''\|_\infty) \\
&+ \frac{h^2\cos(\frac{h\tilde{k}}{2})}{2\sin(\frac{h\tilde{k}}{2})}\cos(\tilde{k}x_i)\big(f(x_i) + O(h^2\|f''\|_\infty)\big) \\
&+ \frac{h^2}{2\sin(\frac{h\tilde{k}}{2})}h\sum_{j=i}^{N-1}\cos(\tilde{k}x_{j+1/2})\big(f'(x_{j+1/2}) + O(h^2\|f'''\|_\infty)\big)
\end{aligned}
$$

Proof. These two identities are again shown via summation by parts:

$$
\begin{aligned}
&\sum_{j=i+1}^{N} e^{\mathbf{i}\tilde{k}x_j}r_h(x_j) + \frac{1}{2}e^{\mathbf{i}\tilde{k}x_i}r_h(x_i) = \\
&= \left(\sum_{j=i+1}^{N} e^{\mathbf{i}\tilde{k}x_j}\right)r_h(x_N) - \sum_{j=i+1}^{N-1}\left(\sum_{l=i+1}^{j} e^{\mathbf{i}\tilde{k}x_l}\right)\big(r_h(x_{j+1}) - r_h(x_j)\big) + \frac{1}{2}e^{\mathbf{i}\tilde{k}x_i}r_h(x_i) \\
&= \frac{e^{\mathbf{i}\tilde{k}x_{i+1}} - e^{\mathbf{i}\tilde{k}x_{N+1}}}{1-e^{\mathbf{i}\tilde{k}h}}r_h(x_N) - \sum_{j=i+1}^{N-1}\frac{e^{\mathbf{i}\tilde{k}x_{i+1}} - e^{\mathbf{i}\tilde{k}x_{j+1}}}{1-e^{\mathbf{i}\tilde{k}h}}\big(r_h(x_{j+1}) - r_h(x_j)\big) + \frac{1}{2}e^{\mathbf{i}\tilde{k}x_i}r_h(x_i) \\
&= \frac{1}{(1-e^{\mathbf{i}\tilde{k}h})}\Big[(e^{\mathbf{i}\tilde{k}x_{i+1}} - e^{\mathbf{i}\tilde{k}x_{N+1}})r_h(x_N) - e^{\mathbf{i}\tilde{k}x_{i+1}}\sum_{j=i+1}^{N-1}\big(r_h(x_{j+1}) - r_h(x_j)\big) \\
&+ \sum_{j=i+1}^{N-1} e^{\mathbf{i}\tilde{k}x_{j+1}}\big(r_h(x_{j+1}) - r_h(x_j)\big) + \frac{1}{2}(1-e^{\mathbf{i}\tilde{k}h})e^{\mathbf{i}\tilde{k}x_i}r_h(x_i)\Big]
\end{aligned}
$$

$$= \frac{1}{(1-e^{\mathbf{i}\tilde{k}h})}\Big[(e^{\mathbf{i}\tilde{k}x_{i+1}} - e^{\mathbf{i}\tilde{k}x_{N+1}})r_h(x_N) - e^{\mathbf{i}\tilde{k}x_{i+1}}\big(r_h(x_N) - r_h(x_{i+1})\big)$$

$$+ \sum_{j=i}^{N-1} e^{\mathbf{i}\tilde{k}x_{j+1}}\big(r_h(x_{j+1}) - r_h(x_j)\big) - e^{\mathbf{i}\tilde{k}x_{i+1}}\big(r_h(x_{i+1}) - r_h(x_i)\big) + \frac{1}{2}(1-e^{\mathbf{i}\tilde{k}h})e^{\mathbf{i}\tilde{k}x_i}r_h(x_i)\Big]$$

$$= \frac{1}{(1-e^{\mathbf{i}\tilde{k}h})}\Big[-e^{\mathbf{i}\tilde{k}x_{N+1}}r_h(x_N) + e^{\mathbf{i}\tilde{k}x_{i+1}}r_h(x_i) + \frac{1}{2}(1-e^{\mathbf{i}\tilde{k}h})e^{\mathbf{i}\tilde{k}x_i}r_h(x_i)$$

$$+ \sum_{j=i}^{N-2} e^{\mathbf{i}\tilde{k}x_{j+1}}\big(r_h(x_{j+1}) - r_h(x_j)\big) + e^{\mathbf{i}\tilde{k}x_N}\big(r_h(x_N) - r_h(x_{N-1})\big)\Big]$$

$$= \frac{1}{(1-e^{\mathbf{i}\tilde{k}h})}\Big[e^{\mathbf{i}\tilde{k}}\Big(\big(r_h(x_N) - r_h(x_{N-1})\big) - e^{\mathbf{i}\tilde{k}h}r_h(x_N)\Big) + \frac{1}{2}(1+e^{\mathbf{i}\tilde{k}h})e^{\mathbf{i}\tilde{k}x_i}r_h(x_i) + \sum_{j=i}^{N-2} e^{\mathbf{i}\tilde{k}x_{j+1}}\big(r_h(x_{j+1}) - r_h(x_j)\big)\Big]$$

Applying the properties of r_h shown in Lemma A.1 produces

$$\sum_{j=i+1}^{N} e^{\mathbf{i}\tilde{k}x_j}r_h(x_j) + \frac{1}{2}e^{\mathbf{i}\tilde{k}x_i}r_h(x_i) =$$

$$= \frac{1}{(1-e^{\mathbf{i}\tilde{k}h})}\Big[e^{\mathbf{i}\tilde{k}}\Big(\big(-f(x_{N-1/2})\frac{h^2}{2} + f'(x_{N-1/2})\frac{7h^3}{12} + O(h^4\|f''\|_\infty)\big) - e^{\mathbf{i}\tilde{k}h}\big(\frac{h^2}{2}f(x_N) - \frac{h^3}{6}f'(x_N) + O(h^4\|f''\|_\infty)\big)\Big)$$

$$+ \frac{1}{2}(1+e^{\mathbf{i}\tilde{k}h})e^{\mathbf{i}\tilde{k}x_i}\big(f(x_i)h^2 + O(h^4\|f''\|_\infty)\big) + \sum_{j=i}^{N-1} e^{\mathbf{i}\tilde{k}x_{j+1}}\big(h^3 f'(x_{j+1/2}) + O(h^5\|f'''\|_\infty)\big)$$

$$- e^{\mathbf{i}\tilde{k}}\big(h^3 f'(x_{N-1/2}) + O(h^5\|f'''\|_\infty)\big)\Big]$$

$$= \frac{e^{\mathbf{i}\tilde{k}}}{(1-e^{\mathbf{i}\tilde{k}h})}\Big[-\frac{h^2}{2}\Big(f(x_N) - \frac{h}{2}f'(x_N)\Big) + \frac{7h^3}{12}\Big(f'(x_N)\Big) + O(h^4\|f''\|_\infty)$$

$$- e^{\mathbf{i}\tilde{k}h}\big(\frac{h^2}{2}f(x_N) - \frac{h^3}{6}f'(x_N)\big) - h^3\Big(f'(x_N)\Big) + O(h^4\|f'''\|_\infty)\Big]$$

$$+ \frac{1+e^{\mathbf{i}\tilde{k}h}}{2(1-e^{\mathbf{i}\tilde{k}h})}e^{\mathbf{i}\tilde{k}x_i}\big(f(x_i)h^2 + O(h^4\|f''\|_\infty)\big) + \frac{1}{(1-e^{\mathbf{i}\tilde{k}h})}\sum_{j=i}^{N-1} e^{\mathbf{i}\tilde{k}x_{j+1}}\big(h^3 f'(x_{j+1/2}) + O(h^5\|f'''\|_\infty)\big)$$

$$= \frac{e^{\mathbf{i}\tilde{k}}}{(1-e^{\mathbf{i}\tilde{k}h})}\Big[-\frac{h^2}{2}(1+e^{\mathbf{i}\tilde{k}h})f(x_N) - \frac{h^3}{6}(1-e^{\mathbf{i}\tilde{k}h})f'(x_N) + O(h^4\|f''\|_\infty)\Big]$$

$$+ \frac{1+e^{\mathbf{i}\tilde{k}h}}{2(1-e^{\mathbf{i}\tilde{k}h})}e^{\mathbf{i}\tilde{k}x_i}\big(f(x_i)h^2 + O(h^4\|f''\|_\infty)\big) + \frac{1}{(1-e^{\mathbf{i}\tilde{k}h})}\sum_{j=i}^{N-1} e^{\mathbf{i}\tilde{k}x_{j+1}}\big(h^3 f'(x_{j+1/2}) + O(h^5\|f'''\|_\infty)\big)$$

$$= -\frac{h^2(1+e^{\mathbf{i}\tilde{k}h})}{2(1-e^{\mathbf{i}\tilde{k}h})}e^{\mathbf{i}\tilde{k}}\left(f(1) + O(h^2\|f''\|_\infty)\right) - \frac{h^3}{6}f'(1)e^{\mathbf{i}\tilde{k}} + \frac{h^2(1+e^{\mathbf{i}\tilde{k}h})}{2(1-e^{\mathbf{i}\tilde{k}h})}e^{\mathbf{i}\tilde{k}x_i}\big(f(x_i) + O(h^2\|f''\|_\infty)\big)$$

$$+ \frac{e^{\frac{i\tilde{k}h}{2}}}{(1-e^{\mathbf{i}\tilde{k}h})}\sum_{j=i}^{N-1} e^{\mathbf{i}\tilde{k}x_{j+1/2}}\big(h^3 f'(x_{j+1/2}) + O(h^5\|f'''\|_\infty)\big)$$

$$= -\frac{h^2(1+e^{\mathbf{i}\tilde{k}h})}{2(1-e^{\mathbf{i}\tilde{k}h})}e^{\mathbf{i}\tilde{k}}\big(f(1) + O(h^2\|f''\|_\infty)\big) + \frac{h^2(1+e^{\mathbf{i}\tilde{k}h})}{2(1-e^{\mathbf{i}\tilde{k}h})}e^{\mathbf{i}\tilde{k}x_i}\big(f(x_i) + O(h^2\|f''\|_\infty)\big)$$

$$+ \frac{h^2 e^{\frac{i\tilde{k}h}{2}}}{(1-e^{\mathbf{i}\tilde{k}h})}h\sum_{j=i}^{N-1} e^{\mathbf{i}\tilde{k}x_{j+1/2}}\big(f'(x_{j+1/2}) + O(h^2\|f''\|_\infty)\big)$$

For the second identity of the lemma, we calculate with the summation by parts formula (A.3) and the trigonometric identity (A.4):

$$
\begin{aligned}
&\sum_{j=i+1}^{N} \sin(\tilde{k}x_j) r_h(x_j) + \frac{1}{2}\sin(\tilde{k}x_i) r_h(x_i) = \\
&= \left(\sum_{j=i+1}^{N} \sin(\tilde{k}x_j)\right) r_h(x_N) - \sum_{j=i+1}^{N-1}\left(\sum_{l=i+1}^{j} \sin(\tilde{k}x_l)\right)\big(r_h(x_{j+1}) - r_h(x_j)\big) + \frac{1}{2}\sin(\tilde{k}x_i) r_h(x_i) \\
&= \frac{1}{2\sin(\frac{h\tilde{k}}{2})}\big(\cos(\tilde{k}x_{i+1/2}) - \cos(\tilde{k}x_{N+1/2})\big) r_h(x_N) \\
&- \frac{1}{2\sin(\frac{h\tilde{k}}{2})}\sum_{j=i+1}^{N-1}\big(\cos(\tilde{k}x_{i+1/2}) - \cos(\tilde{k}x_{j+1/2})\big)\big(r_h(x_{j+1}) - r_h(x_j)\big) + \frac{1}{2}\sin(\tilde{k}x_i) r_h(x_i) \\
&= \frac{1}{2\sin(\frac{h\tilde{k}}{2})}\Big[\big(\cos(\tilde{k}x_{i+1/2}) - \cos(\tilde{k}x_{N+1/2})\big) r_h(x_N) - \cos(\tilde{k}x_{i+1/2})\sum_{j=i+1}^{N-1}\big(r_h(x_{j+1}) - r_h(x_j)\big) \\
&+ \sum_{j=i+1}^{N-1}\cos(\tilde{k}x_{j+1/2})\big(r_h(x_{j+1}) - r_h(x_j)\big) + \sin(\frac{h\tilde{k}}{2})\sin(\tilde{k}x_i) r_h(x_i)\Big] \\
&= \frac{1}{2\sin(\frac{h\tilde{k}}{2})}\Big[\big(\cos(\tilde{k}x_{i+1/2}) - \cos(\tilde{k}x_{N+1/2})\big) r_h(x_N) - \cos(\tilde{k}x_{i+1/2})\big(r_h(x_N) - r_h(x_{i+1})\big) \\
&+ \sum_{j=i}^{N-2}\cos(\tilde{k}x_{j+1/2})\big(r_h(x_{j+1}) - r_h(x_j)\big) - \cos(\tilde{k}x_{i+1/2})\big(r_h(x_{i+1}) - r_h(x_i)\big) \\
&+ \cos(\tilde{k}x_{N-1/2})\big(r_h(x_N) - r_h(x_{N-1})\big) + \sin(\frac{h\tilde{k}}{2})\sin(\tilde{k}x_i) r_h(x_i)\Big] \\
&= \frac{1}{2\sin(\frac{h\tilde{k}}{2})}\Big[\big(\cos(\tilde{k}x_{N-1/2}) - \cos(\tilde{k}x_{N+1/2})\big) r_h(x_N) - \cos(\tilde{k}x_{N-1/2}) r_h(x_{N-1})\big) \\
&+ \sum_{j=i}^{N-2}\cos(\tilde{k}x_{j+1/2})\big(r_h(x_{j+1}) - r_h(x_j)\big) + \Big(\cos(\tilde{k}x_{i+1/2}) + \sin(\frac{h\tilde{k}}{2})\sin(\tilde{k}x_i)\Big) r_h(x_i)\Big] \\
&= \sin(\tilde{k}x_N) r_h(x_N) - \frac{1}{2\sin(\frac{h\tilde{k}}{2})}\cos(\tilde{k}x_{N-1/2}) r_h(x_{N-1}) + \frac{\cos(\frac{h\tilde{k}}{2})}{2\sin(\frac{h\tilde{k}}{2})}\cos(\tilde{k}x_i) r_h(x_i) \\
&+ \frac{1}{2\sin(\frac{h\tilde{k}}{2})}\sum_{j=i}^{N-2}\cos(\tilde{k}x_{j+1/2})\big(r_h(x_{j+1}) - r_h(x_j)\big) \\
&= \sin(\tilde{k}x_N)\big(\frac{h^2}{2} f(x_N) - \frac{h^3}{6} f'(x_N) + O(h^4\|f''\|_\infty)\big) - \frac{1}{2\sin(\frac{h\tilde{k}}{2})}\cos(\tilde{k}x_{N-1/2})\big(h^2 f(x_{N-1}) + O(h^4\|f''\|_\infty)\big) \\
&+ \frac{\cos(\frac{h\tilde{k}}{2})}{2\sin(\frac{h\tilde{k}}{2})}\cos(\tilde{k}x_i)\big(h^2 f(x_i) + O(h^4\|f''\|_\infty)\big) + \frac{1}{2\sin(\frac{h\tilde{k}}{2})}\sum_{j=i}^{N-1}\cos(\tilde{k}x_{j+1/2})\big(h^3 f'(x_{j+1/2}) + O(h^5\|f'''\|_\infty)\big) \\
&- \frac{1}{2\sin(\frac{h\tilde{k}}{2})}\cos(\tilde{k}x_{N-1/2})\big(h^3 f'(x_{N-1/2}) + O(h^5\|f'''\|_\infty)\big) \\
&= \sin(\tilde{k}x_N)\big(\frac{h^2}{2} f(x_N) - \frac{h^3}{6} f'(x_N) + O(h^4\|f''\|_\infty)\big)
\end{aligned}
$$

$$
\begin{aligned}
&-\frac{1}{2\sin(\frac{h\tilde{k}}{2})}\cos(\tilde{k}x_{N-1/2})\big(h^2(f(x_N)-hf'(x_N)+O(h^2\|f''\|_\infty))+O(h^4\|f''\|_\infty)\big)\\
&+\frac{\cos(\frac{h\tilde{k}}{2})}{2\sin(\frac{h\tilde{k}}{2})}\cos(\tilde{k}x_i)\big(h^2 f(x_i)+O(h^4\|f''\|_\infty)\big)+\frac{1}{2\sin(\frac{h\tilde{k}}{2})}\sum_{j=i}^{N-1}\cos(\tilde{k}x_{j+1/2})\big(h^3 f'(x_{j+1/2})+O(h^5\|f'''\|_\infty)\big)\\
&-\frac{1}{2\sin(\frac{h\tilde{k}}{2})}\cos(\tilde{k}x_{N-1/2})\big(h^3(f'(x_N)-\frac{h}{2}f''(x_N)+O(h^2\|f'''\|_\infty))+O(h^5\|f'''\|_\infty)\big)\\
&=-\frac{h^2\cos(\frac{h\tilde{k}}{2})}{2\sin(\frac{h\tilde{k}}{2})}\cos(\tilde{k}x_N)f(x_N)-\frac{h^3}{6}f'(1)\sin(\tilde{k})+\sin(\tilde{k})O(\tilde{k}^{-1}h^3\|f''\|_\infty)+\frac{h^2\cos(\frac{h\tilde{k}}{2})}{2\sin(\frac{h\tilde{k}}{2})}\cos(\tilde{k}x_i)\big(f(x_i)+O(h^2\|f''\|_\infty)\big)\\
&+\frac{1}{2\sin(\frac{h\tilde{k}}{2})}\sum_{j=i}^{N-1}\cos(\tilde{k}x_{j+1/2})\big(h^3 f'(x_{j+1/2})+O(h^5\|f'''\|_\infty)\big)\\
&=-\frac{h^2\cos(\frac{h\tilde{k}}{2})}{2\sin(\frac{h\tilde{k}}{2})}\cos(\tilde{k}x_N)f(x_N)+O(h^3\|f'\|_\infty+\tilde{k}^{-1}h^3\|f''\|_\infty)+\frac{h^2\cos(\frac{h\tilde{k}}{2})}{2\sin(\frac{h\tilde{k}}{2})}\cos(\tilde{k}x_i)\big(f(x_i)+O(h^2\|f''\|_\infty)\big)\\
&+\frac{h^2}{2\sin(\frac{h\tilde{k}}{2})}h\sum_{j=i}^{N-1}\cos(\tilde{k}x_{j+1/2})\big(f'(x_{j+1/2})+O(h^2\|f'''\|_\infty)\big)
\end{aligned}
$$

$\square$

Thus, using the structure of $\tilde{\alpha}_j$ given in (A.1) and Lemma A.4

$$
\begin{aligned}
B_i &:= \int_{x_i}^1 G(x_i,y)f(y)dy-\Big(h\sum_{j=i+1}^{N}G_h^\alpha(x_i,x_j)r_h(x_j)+\frac{h}{2}G_h^\alpha(x_i,x_i)r_h(x_i)\Big)\\
&=\frac{1}{k}\sin(kx_i)\int_{x_i}^1 e^{\mathbf{i}ky}f(y)dy-\Big(\frac{h}{h\sin(h\tilde{k})}\sin(\tilde{k}x_i)\sum_{j=i+1}^{N}\tilde{\alpha}_j r_h(x_j)+\frac{h}{2h\sin(h\tilde{k})}\sin(\tilde{k}x_i)\tilde{\alpha}_i r_h(x_i)\Big)\\
&=\frac{1}{k}\sin(kx_i)\Big[\frac{1}{\mathbf{i}k}e^{\mathbf{i}ky}f(y)\Big|_{x_i}^1-\frac{1}{\mathbf{i}k}\int_{x_i}^1 e^{\mathbf{i}ky}f'(y)dy\Big]\\
&\quad-\frac{1}{\sin(h\tilde{k})}\sin(\tilde{k}x_i)\Big[\sum_{j=i+1}^{N}\big(e^{\mathbf{i}\tilde{k}x_j}+\sin(\tilde{k}x_j)(A(k,\tilde{k})-\mathbf{i})\big)r_h(x_j)+\frac{1}{2}\big(e^{\mathbf{i}\tilde{k}x_i}+\sin(\tilde{k}x_i)(A(k,\tilde{k})-\mathbf{i})\big)r_h(x_i)\Big]\\
&=\frac{1}{\mathbf{i}k^2}\sin(kx_i)\Big[e^{\mathbf{i}k}f(1)-e^{\mathbf{i}kx_i}f(x_i)-\int_{x_i}^1 e^{\mathbf{i}ky}f'(y)dy\Big]\\
&\quad-\frac{1}{\sin(h\tilde{k})}\sin(\tilde{k}x_i)\Big[\sum_{j=i+1}^{N}e^{\mathbf{i}\tilde{k}x_j}r_h(x_j)+\frac{1}{2}e^{\mathbf{i}\tilde{k}x_i}r_h(x_i)+\Big(\sum_{j=i+1}^{N}\sin(\tilde{k}x_j)r_h(x_j)+\frac{1}{2}\sin(\tilde{k}x_i)r_h(x_i)\Big)(A(k,\tilde{k})-\mathbf{i})\Big]\\
&=\frac{1}{\mathbf{i}k^2}\sin(kx_i)\Big[e^{\mathbf{i}k}f(1)-e^{\mathbf{i}kx_i}f(x_i)-\int_{x_i}^1 e^{\mathbf{i}ky}f'(y)dy\Big]\\
&\quad-\frac{1}{\sin(h\tilde{k})}\sin(\tilde{k}x_i)\Big(-\frac{h^2(1+e^{\mathbf{i}\tilde{k}h})}{2(1-e^{\mathbf{i}\tilde{k}h})}\big(e^{\mathbf{i}\tilde{k}}f(1)-e^{\mathbf{i}\tilde{k}x_i}f(x_i)+O(h^2\|f''\|_\infty)\big)\\
&\quad+\frac{h^2e^{\frac{\mathbf{i}\tilde{k}h}{2}}}{(1-e^{\mathbf{i}\tilde{k}h})}h\sum_{j=i}^{N-1}e^{\mathbf{i}\tilde{k}x_{j+1/2}}\big(f'(x_{j+1/2})+O(h^2\|f''\|_\infty)\big)\Big)\\
&\quad-\frac{1}{\sin(h\tilde{k})}\sin(\tilde{k}x_i)(A(k,\tilde{k})-\mathbf{i})\Big\{-\frac{h^2\cos(\frac{h\tilde{k}}{2})}{2\sin(\frac{h\tilde{k}}{2})}\big(\cos(\tilde{k})f(1)-\cos(\tilde{k}x_i)f(x_i)\big)+O(h^3\|f'\|_\infty+\tilde{k}^{-1}h^3\|f''\|_\infty)
\end{aligned}
$$

$$+\frac{h^2}{2\sin(\frac{h\tilde{k}}{2})}h\sum_{j=i}^{N-1}\cos(\tilde{k}x_{j+1/2})\big(f'(x_{j+1/2})+O(h^2\|f'''\|_\infty)\big)\Big\}$$

$$=\Big\{\frac{1}{\mathbf{i}k^2}\sin(kx_i)e^{\mathbf{i}k}f(1)+\frac{h^2(1+e^{\mathbf{i}\tilde{k}h})}{2\sin(h\tilde{k})(1-e^{\mathbf{i}\tilde{k}h})}\sin(\tilde{k}x_i)e^{\mathbf{i}\tilde{k}}f(1)\Big\} \qquad \text{ⓓ}$$

$$+\Big\{\frac{h^2}{4\sin^2(\frac{\tilde{k}h}{2})}\sin(\tilde{k}x_i)\cos(\tilde{k})f(1)(A(k,\tilde{k})-\mathbf{i})$$

$$-\frac{1}{\mathbf{i}k^2}\sin(kx_i)e^{\mathbf{i}kx_i}f(x_i)-\frac{h^2(1+e^{\mathbf{i}\tilde{k}h})}{2\sin(h\tilde{k})(1-e^{\mathbf{i}\tilde{k}h})}\sin(\tilde{k}x_i)e^{\mathbf{i}\tilde{k}x_i}f(x_i)\Big\} \qquad \text{ⓔ}$$

$$\Big\{-\frac{h^2}{4\sin^2(\frac{\tilde{k}h}{2})}\sin(\tilde{k}x_i)\cos(\tilde{k}x_i)f(x_i)(A(k,\tilde{k})-\mathbf{i})$$

$$-\frac{1}{\mathbf{i}k^2}\sin(kx_i)\int_{x_i}^1 e^{\mathbf{i}ky}f'(y)dy-\frac{h^2e^{\frac{\mathbf{i}\tilde{k}h}{2}}}{\sin(h\tilde{k})(1-e^{\mathbf{i}\tilde{k}h})}\sin(\tilde{k}x_i)h\sum_{j=i}^{N-1}e^{\mathbf{i}\tilde{k}x_{j+1/2}}\big(f'(x_{j+1/2})+O(h^2\|f'''\|_\infty)\big)$$

$$+\frac{h^2}{2\sin(\frac{h\tilde{k}}{2})}h\sum_{j=i}^{N-1}\cos(\tilde{k}x_{j+1/2})\big(f'(x_{j+1/2})+O(h^2\|f'''\|_\infty)\big)(A(k,\tilde{k})-\mathbf{i})\Big\} \qquad \text{ⓕ}$$

In order to simplify these three terms, we need a lemma:

Lemma A.5. *For $kh \to 0$ (and thus $\tilde{k}h \to 0$)*

$$A(k,\tilde{k})-\mathbf{i}=O((kh)^2) \tag{A.15}$$

$$\frac{1}{\mathbf{i}k^2}\sin(kx_i)e^{\mathbf{i}k}+\frac{h^2(1+e^{\mathbf{i}\tilde{k}h})}{2\sin(h\tilde{k})(1-e^{\mathbf{i}\tilde{k}h})}\sin(\tilde{k}x_i)e^{\mathbf{i}\tilde{k}}=O(k\varepsilon)+O(h^2) \tag{A.16}$$

$$\frac{1}{\mathbf{i}k^2}\sin(kx_i)e^{\mathbf{i}ky}+\frac{h^2e^{\mathbf{i}\tilde{k}h/2}}{\sin(h\tilde{k})(1-e^{\mathbf{i}h\tilde{k}})}\sin(\tilde{k}x_i)e^{\mathbf{i}\tilde{k}y}=O(h^2)+O(k^{-1}\varepsilon). \tag{A.17}$$

Proof. (A.15) follows from the definition of $A(k,\tilde{k})$ and a straight forward Taylor expansion.

For (A.16), we first note that the estimate is trivial if $k\varepsilon=O(1)$ (and kh is small). We may therefore assume that additionally $k\varepsilon$ is small. With $\tilde{k}=k(1+\varepsilon)$ we then have

$$\frac{1}{\mathbf{i}k^2}\sin(kx_i)e^{\mathbf{i}k}+\frac{h^2(1+e^{\mathbf{i}\tilde{k}h})}{2\sin(h\tilde{k})(1-e^{\mathbf{i}\tilde{k}h})}\sin(\tilde{k}x_i)e^{\mathbf{i}\tilde{k}}=$$
$$\frac{1}{\mathbf{i}k^2}e^{\mathbf{i}k}\left(\sin(kx_i)+\mathbf{i}\frac{(kh)^2(1+e^{\mathbf{i}kh(1+\varepsilon)})}{2\sin(kh(1+\varepsilon))(1-e^{\mathbf{i}kh(1+\varepsilon)})}\sin(k(1+\varepsilon)x_i)e^{\mathbf{i}k\varepsilon)}\right)$$

We set $\delta=kh$ and perform a Taylor expansions (assuming δ and ε to be small) to get

$$\begin{aligned}
\frac{(kh)^2(1+e^{\mathbf{i}kh(1+\varepsilon)})}{2\sin(kh(1+\varepsilon))(1-e^{\mathbf{i}kh(1+\varepsilon)})}&=\frac{\delta^2(2+\mathbf{i}\delta(1+\varepsilon)+O(\delta^2))}{2(\delta(1+\varepsilon)+O(\delta^3))(1-(1+\mathbf{i}\delta(1+\varepsilon)-\frac{1}{2}(\delta(1+\varepsilon))^2+O(\delta^3))}\\
&=\frac{1+\frac{\mathbf{i}\delta(1+\varepsilon)}{2}+O(\delta^2)}{(1+\varepsilon+O(\delta^2))(-\mathbf{i}(1+\varepsilon)+\frac{1}{2}\delta(1+\varepsilon)^2+O(\delta^2))}\\
&=\frac{1}{-\mathbf{i}(1+\varepsilon)}\frac{1+\frac{\mathbf{i}\delta(1+\varepsilon)}{2}+O(\delta^2)}{(1+\varepsilon+O(\delta^2))(1+\mathbf{i}\frac{1}{2}\delta(1+\varepsilon)+O(\delta^2))}\\
&=\frac{1}{-\mathbf{i}(1+\varepsilon)^2}(1+O(\delta^2))=\frac{1}{-\mathbf{i}}(1+O(\delta^2)+O(\varepsilon))
\end{aligned}$$

Therefore, we get

$$
\begin{aligned}
&\frac{1}{\mathbf{i}k^2}e^{\mathbf{i}k}\left(\sin(kx_i)+\mathbf{i}\frac{(kh)^2(1+e^{\mathbf{i}kh(1+\varepsilon)})}{2\sin(kh(1+\varepsilon))(1-e^{\mathbf{i}kh(1+\varepsilon)})}\sin(k(1+\varepsilon)x_i)e^{\mathbf{i}k\varepsilon)}\right)\\
&=\frac{1}{\mathbf{i}k^2}e^{\mathbf{i}k}\left(\sin(kx_i)-(1+O(\delta^2)+O(\varepsilon))\sin(kx_i(1+\varepsilon))e^{\mathbf{i}k\varepsilon}\right)\\
&=\frac{1}{\mathbf{i}k^2}e^{\mathbf{i}k}\left(\sin(kx_i)-(1+O(\delta^2)+O(\varepsilon))(\sin(kx_i)+O(k\varepsilon))(1+O(k\varepsilon))\right)\\
&k^{-2}\left(O(\delta^2)+O(k\varepsilon)\right)
\end{aligned}
$$

Recalling that $\delta = kh$ finishes the proof of (A.16).

We now show (A.17). Taylor expansion gives (for small δ and ε)

$$
\frac{\delta^2 e^{\mathbf{i}\delta(1+\varepsilon)/2}}{\sin(\delta(1+\varepsilon))(1-e^{\mathbf{i}\delta(1+\varepsilon)})}=-1+O(\delta^2)+O(\varepsilon)
$$

Hence, we get with the notation $\delta = kh$

$$
\begin{aligned}
&\frac{1}{\mathbf{i}k^2}\sin(kx_i)e^{\mathbf{i}ky}+\frac{h^2e^{\mathbf{i}\tilde{k}h/2}}{\sin(h\tilde{k})(1-e^{\mathbf{i}h\tilde{k}})}\sin(\tilde{k}x_i)e^{\mathbf{i}\tilde{k}y}\\
&=\frac{1}{\mathbf{i}k^2}e^{\mathbf{i}ky}\left(\sin(kx_i)+(-1+O(\delta^2)+O(\varepsilon))\sin(k(1+\varepsilon)x_i)e^{\mathbf{i}k\varepsilon y}\right)\\
&=\frac{1}{\mathbf{i}k^2}e^{\mathbf{i}ky}\left(\sin(kx_i)+(-1+O(\delta^2)+O(\varepsilon))(\sin(kx_i)+O(k\varepsilon))(1+O(k\varepsilon))\right)\\
&=k^{-2}\left(O(\delta^2)+O(k\varepsilon)\right),
\end{aligned}
$$

which concludes the proof of (A.17). □

With Lemma A.5 in hand, we can bounds the terms ⓓ, ⓔ, and ⓕ.

From (A.16), we get

$$
|ⓓ|\le C|f(1)|\left(h^2+k^{-1}\varepsilon\right).
$$

Combining (A.15) and (A.16) yields

$$
|ⓔ|\le C|f(x_i)|\left(h^2+k^{-1}\varepsilon\right)+Ch^2|f(1)|.
$$

The term ⓕ consists of three terms

$$
ⓕ = ⓕ_1 + ⓕ_2 + ⓕ_3.
$$

The terms $ⓕ_1$ and $ⓕ_2$ can be estimated using (A.15) by

$$
|ⓕ_1|+|ⓕ_3|\le Ch^2|f(x_i)|+Ch^2\left(\|f'\|_\infty+h^2\|f'''\|_\infty\right).
$$

The term $ⓕ_2$ requires more care. Discretizing the integral in the term $ⓕ_2$ with the midpoint rule we get

$$
-\frac{1}{\mathbf{i}k^2}\sin(kx_i)\int_{x_i}^1 e^{\mathbf{i}ky}f'(y)\,dy=-\frac{1}{\mathbf{i}k^2}\sin(kx_i)h\sum_{j=i}^{N-1}e^{\mathbf{i}kx_{j+1/2}}f'(x_{j+1/2})+h^2O(k^2\|f'\|_\infty+k\|f''\|_\infty+\|f'''\|_\infty). \tag{A.18}
$$

With the aid of (A.17) and (A.18) we get for ⓒ:

$$
ⓕ:=-\frac{1}{\mathbf{i}k^2}\sin(kx_i)\int_{x_i}^1 e^{\mathbf{i}ky}f'(y)dy-\frac{h^2e^{\frac{i\tilde{k}h}{2}}}{\sin(h\tilde{k})(1-e^{\mathbf{i}\tilde{k}h})}\sin(\tilde{k}x_i)h\sum_{j=i}^{N-1}e^{\mathbf{i}\tilde{k}x_{j+1/2}}\left(f'(x_{j+1/2})+O(h^2\|f'''\|_\infty)\right)
$$

$$
\begin{aligned}
&= -\frac{1}{\mathbf{i}k^2}\sin(kx_i)h\sum_{j=i}^{N} e^{\mathbf{i}kx_{j+1/2}} f'(x_{j+1/2}) \quad + k^{-2}h^2 O(k^2\|f'\|_\infty + k\|f''\|_\infty + \|f'''\|_\infty) \\
&\quad -\frac{h^2 e^{\frac{\mathbf{i}\tilde{k}h}{2}}}{\sin(h\tilde{k})(1-e^{\mathbf{i}\tilde{k}h})}\sin(\tilde{k}x_i)h\sum_{j=i}^{N-1} e^{\mathbf{i}\tilde{k}x_{j+1/2}}\big(f'(x_{j+1/2}) + O(h^2\|f'''\|_\infty)\big) \\
&= -h\sum_{j=i}^{N-1}\Big[\frac{1}{\mathbf{i}k^2}\sin(kx_i)e^{\mathbf{i}kx_{j+1/2}} + \frac{h^2 e^{\frac{\mathbf{i}\tilde{k}h}{2}}}{\sin(h\tilde{k})(1-e^{\mathbf{i}\tilde{k}h})}\sin(\tilde{k}x_i)e^{\mathbf{i}\tilde{k}x_{j+1/2}}\Big] f'(x_{j+1/2}) \\
&\quad + k^{-2}h^2 O(k^2\|f'\|_\infty + k\|f''\|_\infty + \|f'''\|_\infty) \\
&= (O(h^2) + O(k^{-1}\varepsilon))\|f'\|_\infty + k^{-2}h^2 O(k^2\|f'\|_\infty + k\|f''\|_\infty + \|f'''\|_\infty).
\end{aligned}
$$

This leads us to

$$
B_i = ⓓ + ⓔ + ⓕ \lesssim \big(h^2 + k^{-1}\varepsilon\big)\big(\|f\|_\infty + \|f'\|_\infty\big) + h^2(k^{-1}\|f''\|_\infty + k^{-2}\|f'''\|_\infty). \tag{A.19}
$$

A.3. The final estimate

Combining (A.14) and (A.19) we arrive at

$$
\|e_{poll}\|_{L^2} \lesssim \sqrt{h\sum_i |A_i + B_i|^2} \lesssim \big(h^2 + k^{-1}\varepsilon\big)\big(\|f\|_\infty + \|f'\|_\infty\big) + h^2k^{-1}\|f''\|_\infty + h^2k^{-2}\|f'''\|_\infty \tag{A.20}
$$

B. Duality arguments for specific right-hand sides

For simplicity of exposition, we do not work out the k-dependence explicitly. Our arguments here follow standard lines as illustrated, for example, in [26, Sec. 1.5]. We start with the nodal error:

Lemma B.1. *Consider (3.1) and let V_N be the conforming subspace of piecewise polynomials of degree p. Let $u \in H^{p+1}(I)$ and $u_N \in V_N$ be the Galerkin approximation. Then for all mesh points x_i:*

$$|u(x_i) - u_N(x_i)| \leq C_{p,k} h^{2p} \|u^{(p+1)}\|_{L^\infty},$$

where the constant $C_{p,k}$ is independent of h (but may depend on p and k).

Proof. Let G be the Green's function and $IG(x, \cdot) \in V_N$ be a piecewise polynomial approximation to it. Then by the piecewise smoothness of $G(x_i, \cdot)$

$$\|G(x_i, \cdot) - IG(x_i, \cdot)\|_{\mathcal{H}} \leq Ch^p.$$

$$\begin{aligned} |u(x_i) - u_N(x_i)| &= B(u - u_N, G(x_i, \cdot)) = |B(u - u_N, G(x_i, \cdot) - IG(x_i, \cdot))| \\ &\leq \|u - u_N\|_{\mathcal{H}} \|G(x_i, \cdot) - IG(x_i, \cdot)\|_{\mathcal{H}} \leq C_{k,p} h^{2p}. \end{aligned}$$

∎

For quasi-uniform meshes, we also have L^∞-bounds for the derivative:

Lemma B.2. *Assume the hypotheses of Lemma B.1. Assume additionally that the mesh is quasi-uniform. Then*

$$\|(u - u_N)'\|_{L^\infty(I)} \leq Ch^p \|u^{(p+1)}\|_{L^\infty(I)}.$$

Proof. The proof follows [26, Thm. 1.5.1]. Fix an interval K of the mesh. Let $L_0, \dots, L_{p-1}$ be the Legendre polynomials scaled to the interval $K = (x_i, x_{i+1})$. Write, on the interval K, the error $e'(x) = u'(x) - u_N'(x)$ as

$$e'(x) = \sum_{j=0}^{p-1} c_j L_j(x) + O(h^p),$$

where the $O(h^p)$-term involves only $\|u^{(p)}\|_{L^\infty(K)}$. We next show that the coefficients $c_j = O(h^p)$. To that end, we denote by χ_K the characteristic function of K and let

$$\mathcal{E}g := \int_0^x \chi_K(t) g(t)\, dt.$$

We note that if g is a polynomial of degree $p-1$, then $\mathcal{E}g \in V_N$. Hence, the Galerkin orthogonality gives us

$$\int_K e' g\, dt = k^2 \int_I e \mathcal{E}g\, dt$$

In particular, therefore,

$$\left| \int_K e' g\, dt \right| \leq Ck^2 \|e\|_{L^2(I)} \|g\|_{L^2(K)}$$

Using the orthogonality of the Legendre polynomials, we get with $h_K \sim h$:

$$c_j \sim h_K^{-1} \int_K (e' + O(h^p)) L_j\, dt \lesssim h^{-1} \left(O(h^{p+1}) + k^2 \|e\|_{L^2(I)} \|L_j\|_{L^2(K)} \right) = O(h^p) + k^2 h^{p+1} h^{-1/2} = O(h^p).$$

∎

We now turn to the evaluation of linear functionals:

Theorem B.3. *Let V_N consist of piecewise polynomials on a quasi-uniform mesh with mesh size h. Let u and u_N be the exact solution of (3.1) and its Galerkin approximation. Assume that $u \in W^{t,1}(I)$ with $t \geq 1$. Let ψ be smooth and ψ_N be its Galerkin approximation. Then*

$$|B(u - u_N, \psi)| \leq C_{p,k} h^{\min\{t-1,p\}+p}.$$

Proof. By Galerkin orthogonality, we have

$$|B(u-u_N,\psi)| = |B(u-u_N,\psi-\psi_N)| = |B(u-Iu,\psi-\psi_N)| \leq C_k \|u - Iu\|_{W^{1,1}(I)} \|\psi - \psi_N\|_{W^{1,\infty}(I)},$$

where Iu is an arbitrary interpolant of u. Inserting now the approximation properties for the interpolant Iu and using Lemma B.2 concludes the proof. $\square$

Theorem B.3 may be applied as follows:

Lemma B.4. *Let u be of the form*

$$u(x) = x^{\alpha+2} + \tilde{u},$$

where $\tilde{u}$ is smooth. Then $u \in W^{t,1}(I)$ for any $0 < t < \alpha + 3$.

Proof. The proof follows standard lines as worked out, for example, in [5]. We just consider the case $\tilde{u} \equiv 0$. Let $\chi \in C^\infty(\mathbb{R})$ with $\operatorname{supp} \chi \subset [-1,1]$ and $\chi \equiv 1$ on $[-1/2, 1/2]$. For $\delta > 0$ define χ_δ by $\chi_\delta(x) := \chi(x/\delta)$. Consider the decomposition

$$u = \chi_\delta x^{\alpha+2} + (1-\chi_\delta) x^{\alpha+2} =: u_1 + u_2,$$

where the parameter δ will be chosen later. Then for any integer $k > \alpha + 3$

$$\|(u_2)^{(k)}\|_{L^1(I)} \leq \int_{\delta/2}^{\delta} x^{(\alpha+2-k)}\, dx + \sum_{j=0}^{k} \delta^{-(k-j)} \int_{\delta/2}^{\delta} x^{\alpha+2-j}\, dx + \int_{\delta}^{1} x^{\alpha+2-k}\, dx \sim \delta^{\alpha+3-k}$$

Hence, for $k > \alpha + 3$

$$\|u_1\|_{W^{k,1}(I)} \leq C\delta^{\alpha+3-k}$$

Next, for u_2 we have

$$\|u_1\|_{L^1(I)} \leq \int_0^\delta x^{\alpha+2}\, dx \sim \delta^{\alpha+3}$$

This implies for the K-functional:

$$K(u,t) \leq \|u_2\|_{L^1(I)} + t\|u_1\|_{W^{k,1}(I)} \leq C\delta^{\alpha+3}(1 + t\delta^{-k}).$$

Upon selecting $\delta = t^{1/k}$, we get

$$K(u,t) \leq Ct^{(\alpha+3)/k}.$$

We calculate

$$\int_{t=0}^{1} t^{-\sigma} K(u,t) \frac{dt}{t} \leq C \int_{t=0}^{1} t^{-1-\sigma+(\alpha+3)k)}\, dt < \infty$$

if

$$\sigma < (\alpha+3)/k$$

Given that $W^{t,1}(I) = (W^{t_1,1}(I), W^{t_2,1}(I))_{\theta,1}$ with $t = \theta t_1 + (1-\theta)t_2$ for integer t_1, t_2, we conclude that

$$u \in W^{\sigma,1}(I), \qquad \sigma < (\alpha+3)/k \cdot k = (\alpha+3).$$

$\square$

Corollary B.5. *Let V_N consist of piecewise polynomials of degree p on a quasi-uniform mesh of mesh size h. Let u be solution of (3.1) with $f(x) = x^\alpha$. Then, for smooth z, the error in the linear functional given by (2.11) is expected to be*

$$|L(u) - L(u_N)| \leq Ch^{p+\min\{\alpha+2,p\}}$$

Proof. This follows by combining Theorem B.3 with Lemma B.4. Strictly speaking, this procedure only yields convergence $O(h^{p+\min\{\alpha+3,p\}-\varepsilon}$ for all $\varepsilon > 0$ but the proof shows that ε can be removed. $\square$

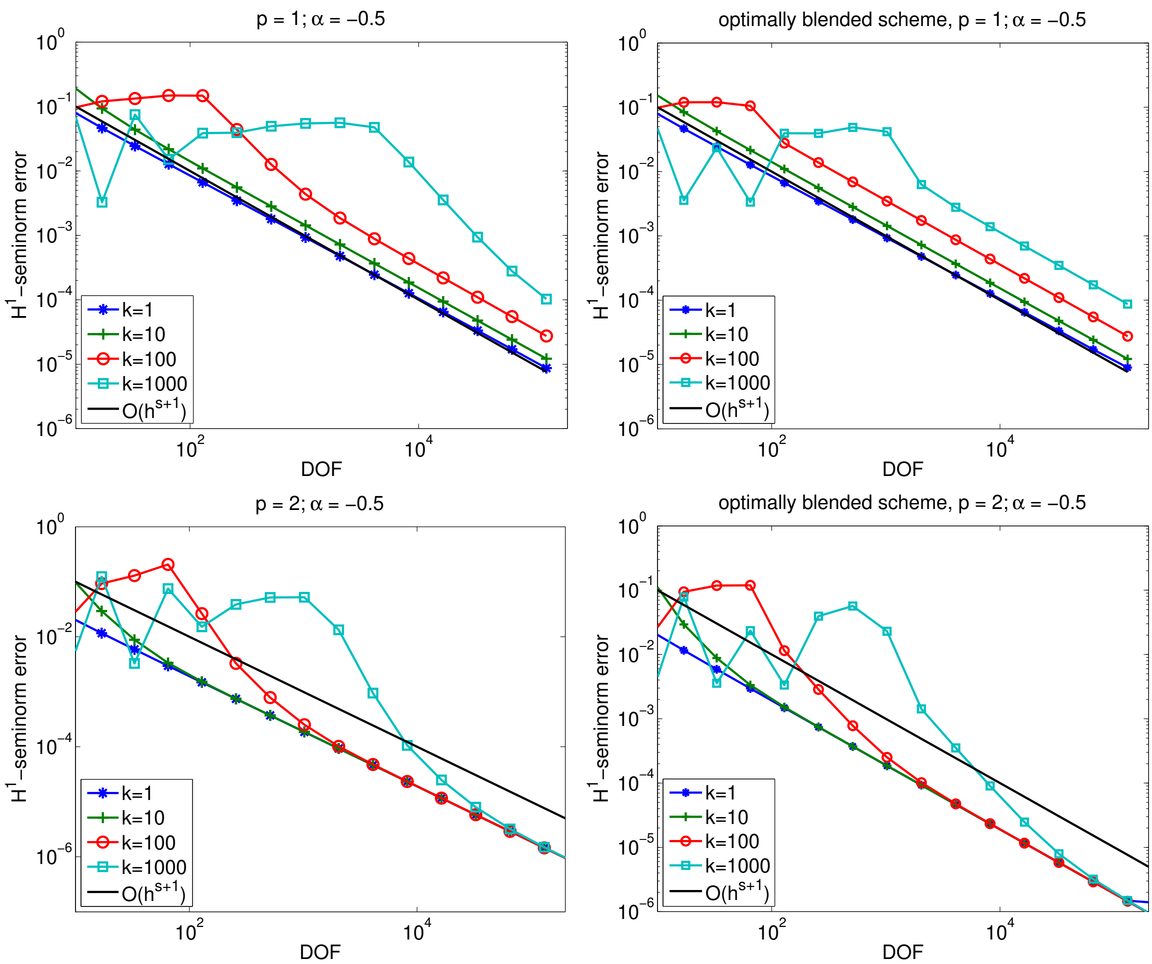

Figure C.1: Galerkin FEM and optimally blended scheme for non-smooth right-hand side. top: $p = 1$ (left: Galerkin, right: optimally blended), bottom: $p = 2$ (left: Galerkin, right: optimally blended).

C. Further numerical examples

We collect additional numerical examples in this section.

Example C.1. We continue Example 6.4 for the case $\alpha = -1/2$ and compare the H^1-performance of the Galerkin method with the optimally blended scheme. We observe in Fig. C.1 that both methods have the same asymptotic behavior but that the optimally blended scheme is much more efficient at suppressing pollution, i.e., it reduces the preasymptotic regime.

Fig. C.2 presents a comparison of the Galerkin method with the optimally blended scheme for the evaluation of the average (i.e., the linear functional is given by (2.11) with $z = 1$). ∎

Example C.2. We continue Example 6.4 for the case $\alpha = +1/2$. In Fig. C.3 and compare the relative L^2-performance of the Galerkin method with the optimally blended scheme for the cases $\alpha = 1/2$ (which corresponds to $s = 1$) and $p = 2$ as well as $p = 3$. We mention that the numerics suggest an $O(k^{-2})$-behavior for the L^2-norm of the exact solution.

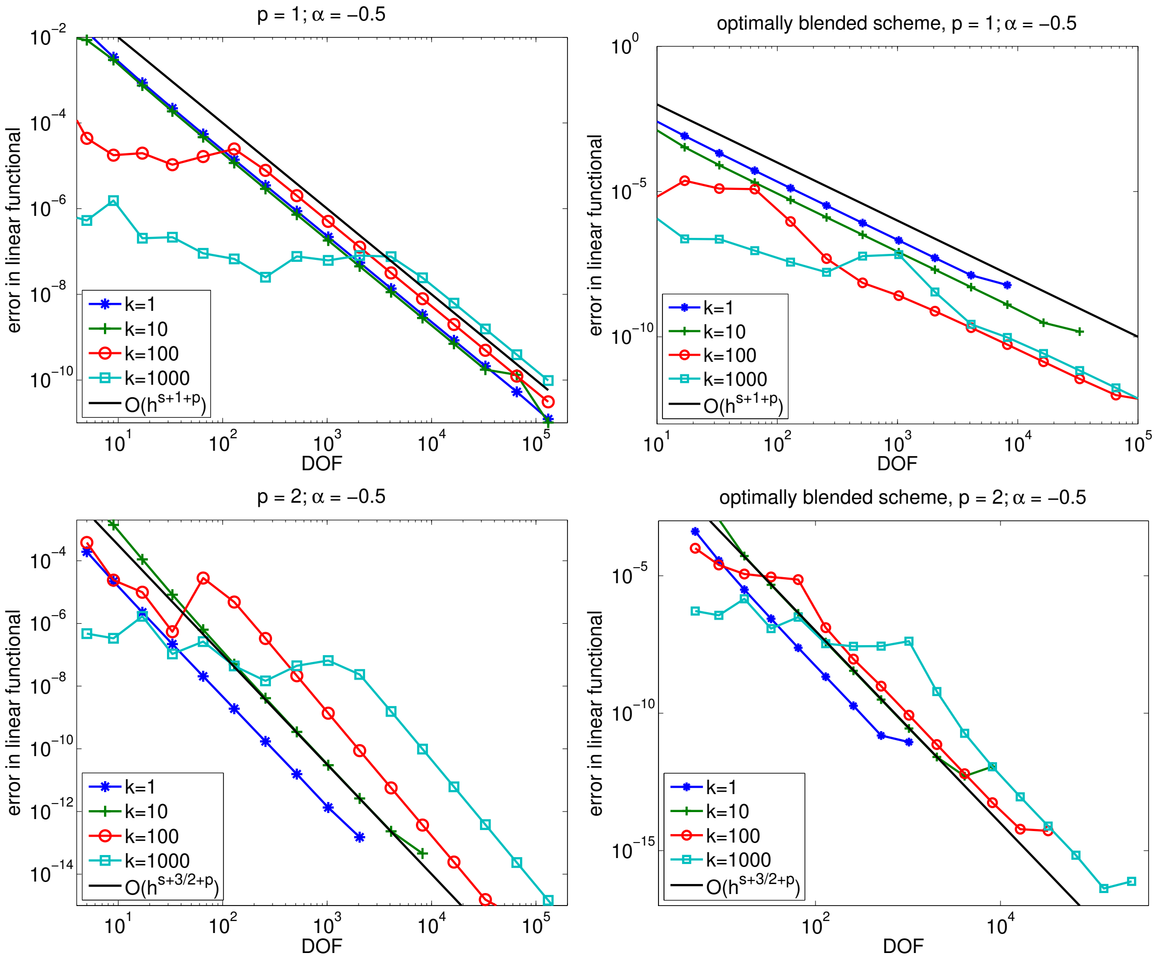

Figure C.2: Galerkin FEM and optimally blended scheme for non-smooth right-hand side. top: $p = 1$ (left: Galerkin, right: optimally blended), bottom: $p = 2$ (left: Galerkin, right: optimally blended).

Fig. C.4 presents the comparison of the Galerkin method with the optimally blended scheme for the cases $p = 2$ and $p = 3$ as measured in the H^1-seminorm and Fig. C.5 the comparison for the evalulation of a linear functional given by (2.11) with $z = 1$. ∎

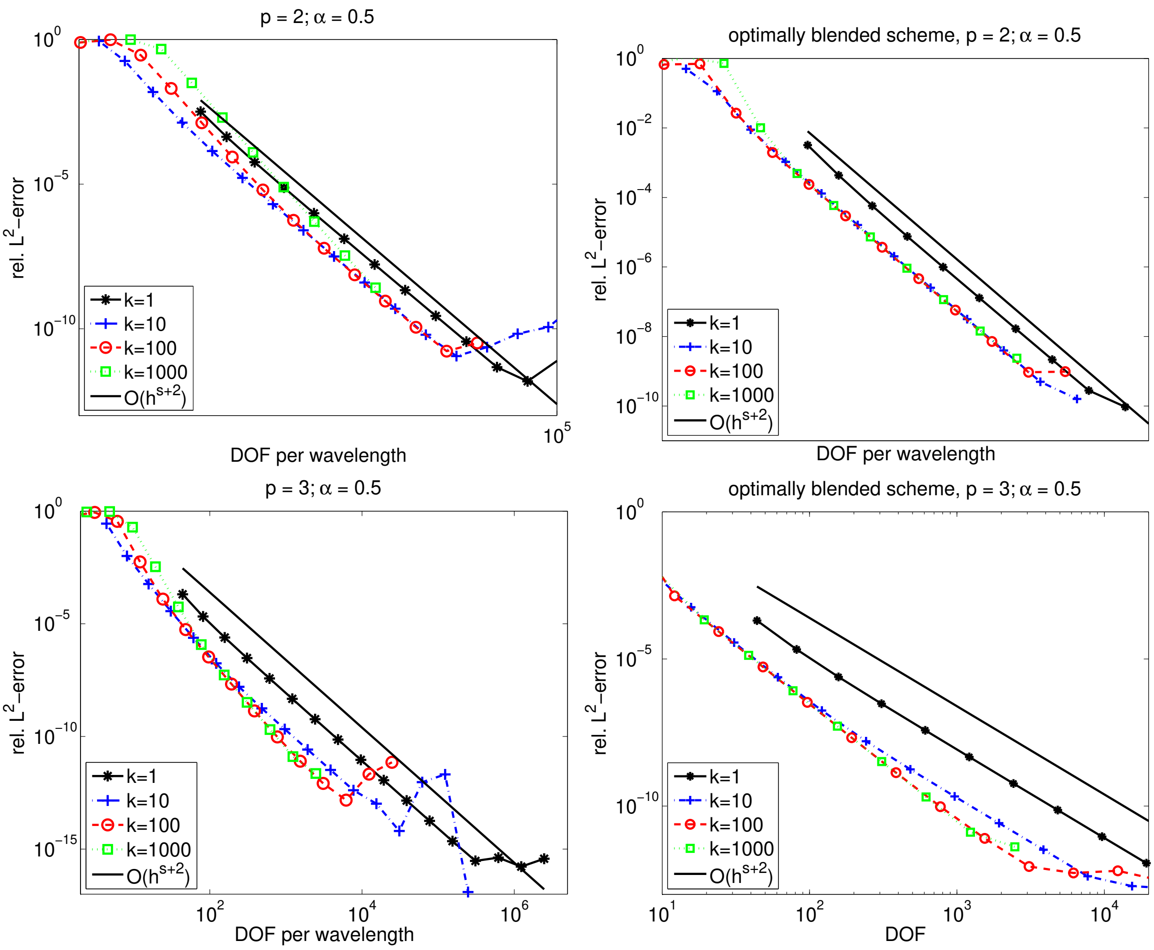

Figure C.3: Galerkin FEM and optimally blended scheme for non-smooth right-hand side. top: $p = 2$ (left: Galerkin, right: optimally blended), bottom: $p = 3$ (left: Galerkin, right: optimally blended) for $\alpha = 1/2$.

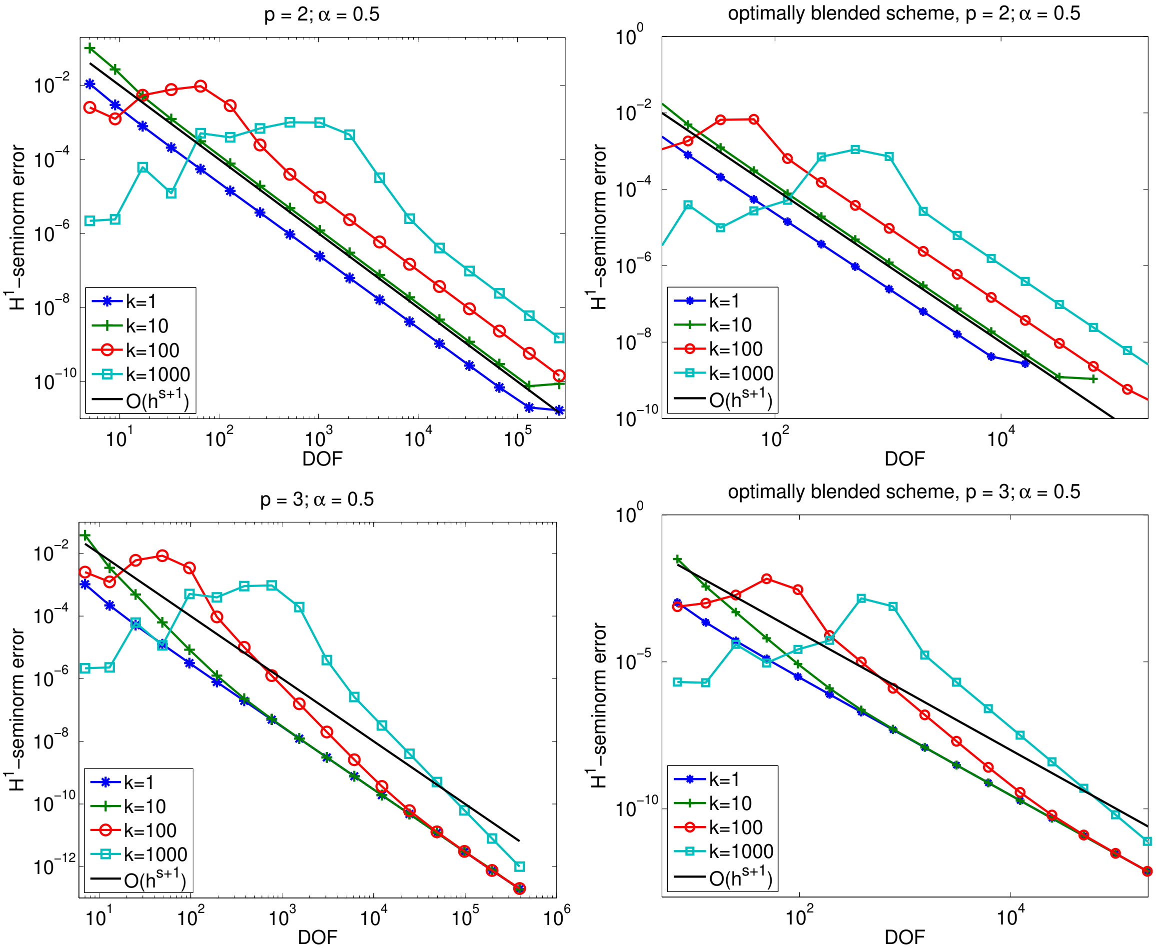

Figure C.4: Galerkin FEM and optimally blended scheme for non-smooth right-hand side. top: $p = 2$ (left: Galerkin, right: optimally blended), bottom: $p = 3$ (left: Galerkin, right: optimally blended) for $\alpha = 1/2$.

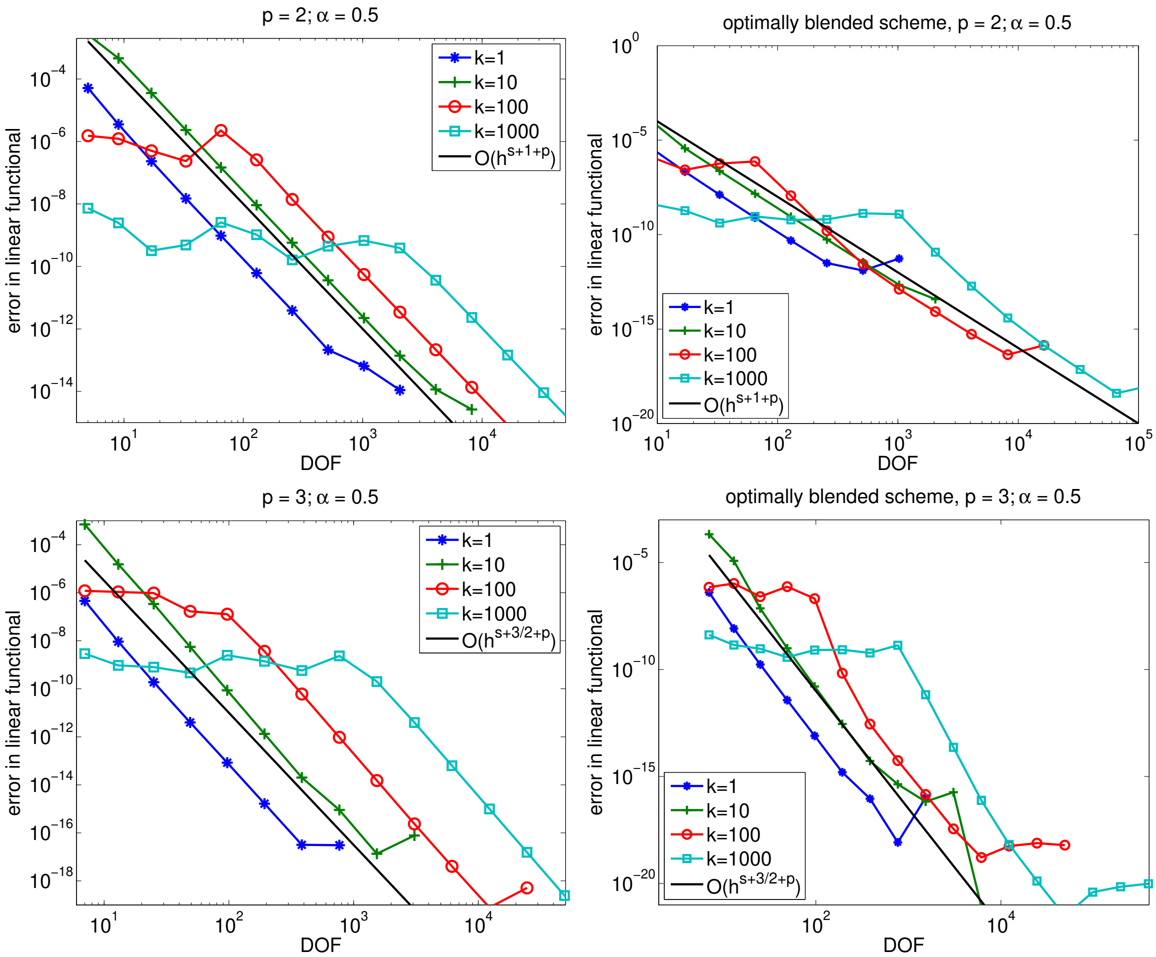

Figure C.5: Galerkin FEM and optimally blended scheme for non-smooth right-hand side. top: $p = 2$ (left: Galerkin, right: optimally blended), bottom: $p = 3$ (left: Galerkin, right: optimally blended) for $\alpha = 1/2$.